UNIVERSIDADE FEDERAL DE VIÇOSA

LILLIAN MATIAS DE OLIVEIRA

ETHYLENE AND NICKEL IN THE RESISTANCE OF MAIZE AGAINST THE INFECTION BY *Exserohilum turcicum*

VIÇOSA - MINAS GERAIS
2020

LILLIAN MATIAS DE OLIVEIRA

ETHYLENE AND NICKEL IN THE RESISTANCE OF MAIZE AGAINST THE INFECTION BY *Exserohilum turcicum*

Thesis presented to the Universidade Federal de Viçosa, as part of the requirements of the Plant Physiology Graduate Program, to obtain the title of Doctor Scientiae.

Advisor: Fabrício Ávila Rodrigues
Co-advisor: Patrícia Ricardino da Silveira

VIÇOSA - MINAS GERAIS
2020

Ficha catalográfica elaborada pela Biblioteca Central da Universidade Federal de Viçosa - Campus Viçosa

T

O48e
2020

Oliveira, Lillian Matias de, 1989-
Ethylene and nickel in the resistance of maize against the infection by *Exserohilum turcicum* / Lillian Matias de Oliveira. - Viçosa, MG, 2020.
115 f. : il. (algumas color.) ; 29 cm.

Orientador: Fabrício de Ávila Rodrigues.
Tese (doutorado) - Universidade Federal de Viçosa.
Inclui bibliografia.

1. Milho - Doenças e pragas. 2. Metabolismo. 3. Hormônios vegetais. 4. Plantas - Nutrição. 5. Fotossíntese. I. Universidade Federal de Viçosa. Departamento de Biologia Vegetal. Programa de Pós-Graduação em Fisiologia Vegetal. II. Título.

CDD 22. ed. 633.1594

LILLIAN MATIAS DE OLIVEIRA

ETHYLENE AND NICKEL IN THE RESISTANCE OF MAIZE AGAINST THE INFECTION BY *Exserohilum turcicum*

Thesis presented to the Universidade Federal de Viçosa, as part of the requirements of the Plant Physiology Graduate Program, to obtain the title of *Doctor Scientiae*.

APPROVED: November 27, 2020.

Assent:

Lillian Matias de Oliveira
Author

Fabrício Ávila Rodrigues
Advisor

Ask the Lord to bless your plans, and you will be successful in carrying them out.

Proverbs 16:3

I dedicate to my parents, José Maria Oliveira and Luiza Oliveira, and my brothers, Thais Oliveira, and Willian Oliveira, for the love and unconditional support in all stages of this achievement.

ACKNOWLEDGMENTS

I thank God for FAITH and for blessing all my achievements.

I am immensely grateful to:

My parents and siblings for their trust and love, and they did not know how to measure efforts so that another stage in my life was completed.

To all my family for their support, love, words of encouragement, and understanding of my absence during family moments.

Professor Fabrício Ávila Rodrigues for his guidance, understanding, patience, and encouragement to complete this study.

Federal University of Viçosa and the Graduate Program in Plant Physiology for all the support and infrastructure.

Coordenação de Aperfeiçoamento de Pessoal de Nível Superior (CAPES) for its financial support.

To the employees of the Departments of Plant Biology and Plant Pathology.

To my friends at the Laboratory of Host-Pathogen Interaction, completing this step would be much more difficult without your help and affection.

To the gifts I received in Viçosa: Aline Batista, Aline Paixão, Emanuel Naves, Gélia Viana, Greice Leal, Guilherme Oliveira, Mariana Silva, and Neuza Rodrigues.

My friends, particularly Ariele Andrade, Carla Coelho, Jaomara da Silva, Myriam Neves, and Pablo Coutinho, even from afar, were present with words and gestures of encouragement and affection, demonstrating that true friendships overcome long distances.

To all of you who have contributed to this stage in some way, my sincere thanks.

BIOGRAPHY

LILLIAN MATIAS DE OLIVEIRA, daughter of José Maria Araújo de Oliveira and Luiza Matias de Oliveira, was born on September 25, 1989, in Capitão Poço, Pará, Brazil. In 2014, she graduated in Agronomy at Universidade Federal Rural da Amazônia (UFRA), Capitão Poço-PA. In February 2016, she obtained the Master Scientiae in Agronomy at Universidade Federal de Santa Maria (UFSM), Santa Maria-RS, Brazil. In August 2016, she started the doctoral degree in the Plant Physiology Program at Universidade Federal de Viçosa (UFV) under the guidance of Professor Fabrício Ávila Rodrigues defending her thesis on November 27, 2020.

ABSTRACT

OLIVEIRA, Lillian Matias de, D.Sc., Universidade Federal de Viçosa, November, 2020. **Ethylene and nickel in the resistance of maize against the infection by Exserohilum turcicum**. Advisor: Fabrício Ávila Rodrigues. Co-advisor: Patrícia Ricardino da Silveira.

Diseases cause a negative impact on maize yield worldwide, and the northern leaf blight (NLB), caused by the hemibiotrophic fungus Exserohilum turcicum, is one of the most important. Considering the harmful effects of E. turcicum infection in the leaves of maize plants, the objectives of this study were to investigate the alterations in the photosynthesis (parameters related to leaf gas exchange and chlorophyll a fluorescence), the foliar concentration of micronutrients, and reactive oxygen species (ROS), production of ethylene, activities of both defense and antioxidant enzymes, and the expression of the genes related to the production of hormones. The first study investigated the role of ethylene (ET) in increasing the resistance of maize plants against NLB at physiological, biochemical, and molecular levels. Maize plants were sprayed with ET, aminooxyacetic acid (AOA) (an ET inhibitor), and water (control). The ET application increased its concentration in the leaf tissues and contributed to the expansion of NLB lesions. Also, high NLB severity resulted in lower values for net carbon assimilation rate, stomatal conductance, transpiration rate, and maximum quantum yield of photosystem II (F_v/F_m) at advanced stages of fungal infection. Lower concentration of pigments and higher concentrations of malonaldehyde (MDA) and hydrogen peroxide (H_2O_2) were noticed for ET-sprayed plants infected by E. turcicum. Great NLB development in the leaves of ET-sprayed plants can probably be attributed to the lower activities of antioxidative (ascorbate peroxidase, glutathione reductase, and superoxide dismutase) and defense (chitinase, β-1,3-glucanase, lipoxygenase, and phenylalanine ammonia-lyase) enzymes. The second study was carried out to investigate the effect of foliar nickel (Ni) spray on the potentiation of maize resistance against E. turcicum infection by examining alterations at biochemical and physiological levels. In the in vitro assay, Ni efficiently inhibited the mycelial growth of E. turcicum. For Ni-sprayed and inoculated plants, there were higher foliar concentrations of manganese and Ni. These plants exhibited significant decreases of 33 and 24%, respectively, for NLB severity at 12 and 16 days after inoculation. There were lower MDA and H_2O_2 concentrations in the leaves of +Ni inoculated plants. The decrease in NLB severity for Ni-sprayed plants was related to its direct effect against E. turcicum infection or through the potentiation of host defense responses such

as high lipoxygenase and polyphenoloxidase activities as well as great production of phenolics and lignin.

Keywords: Antioxidative metabolism. Host defense responses. Northern leaf blight. Plant nutrition. Plant hormone. Photosynthesis.

RESUMO

OLIVEIRA, Lillian Matias de, D.Sc., Universidade Federal de Viçosa, novembro de 2020. **Etileno e níquel na resistência do milho à infecção por Exserohilum turcicum**. Orientador: Fabrício Ávila Rodrigues. Coorientadora: Patrícia Ricardino da Silveira.

Doenças causam impacto negativo na produção de milho em todo o mundo, sendo a queima foliar, causada pelo fungo hemibiotrófico Exserohilum turcicum, uma das mais importantes. Considerando os efeitos deletérios da infecção por E. turcicum nas folhas de plantas de milho, os objetivos deste estudo foram investigar as alterações na fotossíntese (parâmetros relacionados às trocas gasosas e fluorescência da clorofila a), concentrações foliares de micronutrientes, espécies reativas de oxigênio (EROS), produção de etileno, atividades de enzimas de defesa e antioxidantes e a expressão de genes relacionados à produção de hormônios. O primeiro estudo investigou o papel do etileno (ET) no aumento da resistência das plantas de milho contra a queima foliar em níveis fisiológicos, bioquímicos e moleculares. Plantas de milho foram pulverizadas com ET, ácido aminooxiacético (AOA) (um inibidor de ET) e água (controle). A aplicação do ET aumentou sua concentração nos tecidos foliares e contribuiu para a expansão das lesões da queima foliar. Além disso, a severidade da queima foliar alta resultou em valores mais baixos para a taxa líquida de assimilação de carbono, condutância estomática, taxa de transpiração e rendimento quântico máximo do fotossistema II (F_v/F_m) em estágios avançados da infecção fúngica. Menor concentração de pigmentos e maiores concentrações de malonaldeído (MDA) e peróxido de hidrogênio (H_2O_2) foram observadas para plantas pulverizadas com ET infectadas por E. turcicum. Grande desenvolvimento da queima foliar nas folhas de plantas pulverizadas com ET pode provavelmente ser atribuído às atividades mais baixas de enzimas antioxidantes (ascorbato peroxidase, glutationa redutase e superóxido dismutase) e de defesa (quitinase, β-1,3-glucanase, lipoxigenase e fenilalanina amônia-lyase). O segundo estudo foi realizado para investigar o efeito da pulverização foliar de níquel (Ni) na potenciação da resistência do milho à infecção por E. turcicum, examinando alterações em níveis bioquímicos e fisiológicos. No ensaio in vitro, o Ni inibiu de forma eficiente o crescimento micelial de E. turcicum. Para as plantas pulverizadas com Ni e inoculadas, houve maiores concentrações foliares de manganês e Ni. Essas plantas exibiram reduções significativas de 33 e 24%, respectivamente, para a severidade da queima foliar aos 12 e 16 dias após a inoculação. Houve menores concentrações de MDA e H_2O_2 nas folhas das plantas inoculadas com +Ni. A diminuição da severidade da queima foliar

para plantas pulverizadas com Ni foi relacionada ao seu efeito direto contra a infecção por E. turcicum ou através da potencialização de respostas de defesa do hospedeiro, como alta atividade da lipoxigenase e polifenoloxidase, bem como grande produção de fenólicos e lignina.

Palavras-chave: Fotossíntese. Hormônio vegetal. Metabolismo antioxidativo. Nutrição de plantas. Queima foliar. Respostas de defesa do hospedeiro.

SUMMARY

Chapter I

Involvement of Ethylene in the Infection Process of Exserohilum turcicum in Maize Leaves

Abstract

Even though ethylene (ET) plays diverse roles in plant growth and development, its involvement in the maize-Exserohilum turcicum interaction remains undetermined. Therefore, parameters related to leaf gas exchange and chlorophyll a fluorescence, concentrations of photosynthetic pigments as well as the activities of defense and antioxidant enzymes in maize plants sprayed with ET, aminooxyacetic acid (AOA) (an ET inhibitor), and water (control) and challenged or not with E. turcicum were investigated. The ET was produced in the infected leaves of plants from the control, AOA treatment, or sprayed with ET. However, the northern leaf blight (NLB) symptoms were more developed on the leaves of plants sprayed with ET. The harmful effect of E. turcicum was confirmed by decreases in the values of net carbon assimilation rate, stomatal conductance, transpiration rate, and maximal photosystem II quantum yield (F_v/F_m) at advanced stages of fungal infection. Furthermore, the concentrations of malondialdehyde and hydrogen peroxide were higher at the advanced fungal infection stage, especially for ET-sprayed plants due to great disease severity. The activities of defense enzymes increased in response to fungal infection regardless of the treatments. Taken together, it can be concluded that the exogenous supply of ET to the leaves of maize plants played a negative role in the infection process of E. turcicum besides modulating fungal-induced reactive oxygen species formation. The ET biosynthesis in the infected leaves was closely associated with NLB development. The increase in NLB symptoms can probably be attributed to the lower activities of defense (chitinase, β-1,3-glucanase, lipoxygenase, and phenylalanine ammonia-lyase) and antioxidative (ascorbate peroxidase, glutathione reductase, and superoxide dismutase) enzymes.

Keywords: Zea mays. Antioxidant metabolism. Chlorophyll a fluorescence. Host defense responses. Photosynthesis. Plant hormone.

Resumo

Embora o etileno (ET) desempenhe papéis diversos no crescimento e desenvolvimento das plantas, seu envolvimento na interação milho-Exserohilum turcicum permanece indeterminado. Portanto, parâmetros relacionados às trocas gasosas e fluorescência da clorofila a, concentrações de pigmentos fotossintéticos, bem como as atividades de enzimas de defesa e antioxidantes em plantas de milho pulverizadas com ET, ácido aminooxiacético (AOA) (um inibidor de ET) e água (controle) e inoculadas ou não com E. turcicum foram investigados. O ET foi produzido nas folhas infectadas de plantas do tratamento controle, AOA ou pulverizado com ET. No entanto, os sintomas da queima foliar foram mais desenvolvidos nas folhas das plantas pulverizadas com ET. O efeito prejudicial de E. turcicum foi confirmado por diminuições nos valores da taxa líquida de assimilação de carbono, condutância estomática, taxa de transpiração e rendimento quântico máximo do fotossistema II (F_v/F_m) em estágios avançados de infecção fúngica. Além disso, as concentrações de malonaldeído e peróxido de hidrogênio foram maiores no estágio de infecção fúngica avançada, especialmente para plantas pulverizadas com ET devido à grande severidade da doença. As atividades das enzimas de defesa aumentaram em resposta à infecção fúngica, independentemente dos tratamentos. Em conjunto, pode-se concluir que o fornecimento exógeno de ET às folhas de plantas de milho teve um papel negativo no processo de infecção de E. turcicum, além de modular a formação de espécies reativas de oxigênio induzidas por fungos. A biossíntese de ET nas folhas infectadas foi intimamente associada ao desenvolvimento da queima foliar. O aumento nos sintomas da queima foliar pode provavelmente ser atribuído às atividades mais baixas das enzimas de defesa (quitinase, β-1,3-glucanase, lipoxigenase e fenilalanina amônia-liase) e antioxidantes (ascorbato peroxidase, glutationa redutase e superóxido dismutase).

Palavras-chave: Zea mays. Fotossíntese. Fluorescência da clorofila a. Hormônio vegetal. Metabolismo antioxidativo. Respostas de defesa da planta.

Introduction

Northern leaf blight (NLB), caused by the fungus Exserohilum turcicum (Pass.) Leonard and Suggs (anamorph) (Setosphaeria turcica (Luttrell) Leonard and Suggs (teleomorph)) (Leonard and Suggs 1974; Luttrell and Bacon 1977; Sivanesan 1984), is one of the major diseases contributing to decreasing maize yield in all growing regions worldwide (Zhang et al. 2020). In the tropical regions, high humidity, overhead sprinkler irrigation, and cloudy weather periods favor NLB epidemics (Hennessy et al. 1990; Hooda et al. 2017). The major symptoms of NLB are elliptical lesions with necrotic centers and chlorotic halos on leaves, especially on the older ones (Munkvold and White 2016; Silveira et al. 2019). These chlorotic and necrotic areas reduce the leaf area photosynthetically active that will impact yield (Berger et al. 2007; Sibiya et al. 2013; Hurni et al. 2015).

In general, plants infected by pathogens of different lifestyles such as Ustilago maydis and Stenocarpella macrospora on maize (Horst et al. 2008; Bermúdez-Cardona et al. 2015b), Monographella albescens on rice (Tatagiba et al. 2015), and Phakopsora pachyrhizi on soybean (Rios et al. 2018) experience drastic reductions in the values of initial fluorescence, maximal fluorescence, maximal photosystem II quantum efficiency, effective photosystem II quantum yield, quantum yield of regulated energy dissipation, but a sharp increase in the values of quantum yield of non-regulated energy dissipation. Lower values for the parameters related to leaf gas exchange (e.g., net carbon assimilation rate, stomatal conductance to water vapor, and transpiration rate) have been reported for the maize-S. macrospora (Bermúdez-Cardona et al. 2015b), soybean-P. pachyrhizi (Rios et al. 2018), and rice-M. albescens (Tatagiba et al. 2015) interactions.

Fungal pathogens can manipulate the hormonal pathways of their hosts to ensure successful infections (Rodriguez-Moreno et al. 2018). Hormones such as abscisic acid, auxin, brassinosteroids, cytokinins, ethylene (ET), gibberellins, jasmonic acid, and salicylic acid play

important roles in many physiological processes during plant development (Shigenaga and Argueso 2016; Berens et al. 2017). The ET, in particular, is of detrimental importance for plant growth and development and better performance when exposed to abiotic and biotic stresses (Hao et al. 2017). However, the involvement of ET in the resistance of plants against diseases still controversial. In some cases, ET seems to increase the basal level of resistance of some crops against the infection by pathogens (Helliwell et al. 2013). On the other hand, pathogens such as Botrytis cinerea and Alternaria alternata infecting tomatoes and grapes, respectively, can produce ET to favor diseases symptoms' development (Cristescu et al. 2002; Zhu et al. 2017). The ET was important to increase rice and tomatoes susceptibilities to brown spot and Fusarium wilt, respectively (Van Bockhaven et al. 2015; Di et al. 2017).

The ET was linked with rice plants' resistance, which became susceptible to blast after being sprayed with an ET inhibitor (Yang et al. 2017). The ET was also positively involved with the resistance of rice to blast and sheath blight (Helliwell et al. 2013). Mutants of Arabidopsis plants deficient in ET biosynthesis were more susceptible to infection by Pseudomonas syringae pv. tomato (Guan et al. 2015). The ET-sprayed wheat plants showed less number of blast lesions in the leaves and lower disease severity due to an increase in the activities of chitinase, β-1,3-glucanase, peroxidase, and polyphenoloxidase (Rios et al. 2014). The response to ET is dependent on the host-pathogen interaction. An interesting case occurs for Bipolaris oryzae in rice, where the number of brown spot lesions increased due to a stimulation of the ET signaling pathway (De Vleesschauwer et al. 2010) while infection of Arabidopsis plants by B. oryzae was suppressed (Völz et al. 2020).

The ET concentration increased in maize seeds infected with Aspergillus flavus, stimulating its growth and conidia production (Wang et al. 2017). In addition, maize seedlings exhibiting lower expression of the ZmEIN2 gene or exposed to 1-methylcyclopropene (1-MCP) became resistant to infection by Fusarium graminearum (Zhou et al. 2018). The infection by

F. graminearum induced both ET biosynthetic and responsive genes in maize seedlings' roots (Ye et al. 2013). Several ET-responsive transcription factors were highly expressed in maize plants of cultivars susceptible to Cercospora zeina (Meyer et al. 2017). Shi et al. (2018) reported that at the beginning of S. turcica infection process in the leaves of maize plants, a total of 61 over 5903 differentially expressed genes were involved with the hormonal metabolism and about almost 7% with the ET biosynthesis.

Considering the controversial involvement of ET in the host-pathogen interactions, this study aimed to investigate the possible role of this hormone in increasing maize resistance against infection by E. turcicum by manipulating its accumulation through an exogenous application.

Material and Methods

Plant growth

Seeds of the maize cultivar P-1630 Hx (susceptible to E. turcicum) (Silveira et al. 2019) were sown in plastic pots containing 2 kg of a substrate (1:1:1 mixture of pine bark, peat, and expanded vermiculite) amended with 1.63 g of calcium phosphate monobasic. Plants were kept in a greenhouse (temperature of 25 ± 3°C (day) and 21 ± 2°C (night) and relative humidity of 75 ± 5%). Plants in each pot were fertilized, weekly, with 50 mL of a nutrient solution composed, in mg/L, of 192 KCl, 104.52 K_2SO_4, 150.37 $MgSO_4$, 61 CH_4N_2O, 100 NH_4NO_3, 0.27 $(NH_4)_6MO_7O_{24}$, 1.61 H_3BO_3, 6.67 $ZnSO_4$, 1.74 $CuSO_4$, 4.10 $MnCl_2$, 4.08 $FeSO_4$, and 5.58 ethylenediaminetetraacetic acid (EDTA).

Inoculum production, plant inoculation, and treatments

Plants were inoculated with the monosporic UFV-DFP Et22 isolate of E. turcicum. The fungus was grown in Petri dishes containing lactose casein hydrolysate (LCH) medium (Malca and

Ullstrup 1962) kept in an incubator (25°C and photoperiod of 16 hours light and 8 hours dark) for ten days. Plants were inoculated with a conidial suspension (1×10^4 conidia/ml) of E. turcicum at 20 days after emergence (plants with five fully expanded leaves) using a VL Airbrush atomizer (Paasche Airbrush Co., Chicago, IL). Gelatin (0.5% w/v) was added to the conidial suspension to aid conidia adhesion to the leaves. At eight days after inoculation, leaf fragments containing necrotic lesions were collected, disinfected in solutions of 70% (v/v) aqueous alcohol and 2% sodium hypochlorite (v/v), and transferred to Petri dishes (three-leaf fragments per dish) containing LCH medium. Petri dishes were transferred to an incubator (25°C and photoperiod of 16 hours of light and 8 hours of dark) for ten days. After this period, a total of 1 ml of sterile distilled water was added to each Petri dish, and fungal mycelia were carefully disrupted using a camel hair brush within a laminar flow chamber to induce fungal sporulation. After this procedure, Petri dishes were transferred to an incubator (25°C and photoperiod of 12 h with blacklight lamps emitting light near-ultraviolet (320-400 nm) and 12 h dark) for five days. Plants with five fully expanded leaves were inoculated with a conidial suspension of E. turcicum as described above and kept in a growth chamber (temperature of 25 ± 2°C and relative humidity of 90 ± 5%) under dark for the first 12 h to allow conidia germination and fungal penetration. After that, plants were transferred to a greenhouse (25 ± 2°C, the relative humidity of 75 ± 5%, and natural photon flux density) for the experiments' duration. Plants were sprayed with ET (Ethrel®, 100 µM; Sigma-Aldrich, São Paulo, Brazil) and with aminooxyacetic acid (AOA, 50 µM; Sigma-Aldrich, São Paulo, Brazil) at 24 and 48 h, respectively, before being inoculated with E. turcicum by using a VL Airbrush atomizer. Plants sprayed with water served as the control treatment.

Assessment of NLB severity

The NLB severity was evaluated on the fifth fully expanded leaf, from basis to top, of each plant per replication of each treatment at 4, 8, 12, and 16 days after inoculation (dai). The leaves were scanned at 600 dpi resolution, and the images were processed using the QUANT software (Vale et al. 2003) to obtain the severity values. The area under the disease progress curve (AUDPC) was calculated using the trapezoidal integration of NLB progress curves over time, according to Shaner and Finney (1977).

Determination of ET concentration

The ET was measured on the fourth fully expanded leaf, from basis to top, of each plant per replication of each treatment at 4, 8, 12, and 16 dai. The leaves were weighed to obtain their fresh weight and placed in Erlenmeyer flasks hermetically sealed. After an incubation of 12 h, an air sample of 1 mL was taken from the flask headspace and injected into a gas chromatograph (Hewlett-Packard 5890, series II) following the procedures described by Silva et al. (2014).

Determination of leaf gas exchange parameters

A portable open-system infrared gas analyzer (LI-6400XT, LI-COR, Lincoln, NE, USA) was used to obtain the values of net carbon assimilation rate (A), stomatal conductance to water vapor (g_s), internal CO_2 concentration (C_i), and transpiration rate (E) on the fifth fully expanded leaf, from basis to top, of each plant per replication of each treatment at 4, 12, and 16 dai. Evaluations were performed from 10:00 to 12:00 a.m. under artificial and saturating photon irradiance (1200 µmol m^{-2} s^{-1}) and CO_2 concentration of ± 400 ppm.

Determination of chlorophyll (Chl) a fluorescence

The images and fluorescence parameters of Chl a were obtained at 4, 8, 12, and 16 dai using an IMAGING-PAM fluorometer (Maxi version) and the Imaging Win software (Heinz Walz GmbH, Effeltrich, Germany). The images were obtained with a resolution of 640 × 480 pixels in the fifth fully expanded leaf, from basis to top, of each replication per treatment. The Chl a fluorescence emission transients were captured by a CCD (charge-coupled device) camera with a resolution of 640 × 480 pixels in a visible sample area of 24 × 32 mm on each leaf. The leaves were then exposed to a weak and modulated measuring beam (0.5 μmol m^{-2} s^{-1}, 100 μs, 1 Hz) to determine the initial fluorescence (F_0) when all the PSII reaction centers were open. Next, a saturating white light pulse of 2.400 μmol m^{-2} s^{-1} (10 Hz) was applied for 0.8 s to ensure maximum fluorescence emission (F_m) when all the PSII reaction centers are expected to be closed. The leaves were initially adapted to darkness for 30 min, after which they were carefully and individually fixed in support at a distance of 18.5 cm from the CCD camera. From these initial measurements, the maximum PSII photochemical efficiency of the dark-adapted leaves was estimated through the variable-to-maximum Chl fluorescence ratio as follows: $F_v/F_m = [(F_m - F_0)/F_m)]$. Following the calculations proposed by Kramer et al. (2004), the energy absorbed by the PSII for the following two yield components for dissipative processes was determined: the yield of photochemistry [(YII = F'_m - F/F'_m], the yield for dissipation by downregulation [$Y(NPQ) = (F_s/F'_m) - (F_s/F_m)$], and the yield for other non-photochemical (non-regulated) losses [$Y(NO) = F_s/F_m$]. These parameters were calculated using the Imaging Win software (Kramer et al. 2004).

Determination of the concentration of photosynthetic pigments

Five leaf discs (8 mm in diameter) obtained from the fifth fully expanded leaf, from basis to top, of each plant per replication, were placed in glass vials with 5 ml of dimethylsulfoxide (DMSO). The absorbances of the extracts were read at 480, 649, and 665 nm using DMSO as a blank after 24 h at 25°C (Wellburn 1994, Santos et al. 2008).

Biochemical assays

The fourth and fifth fully expanded leaves, from basis to top, of each plant per replication of each treatment were collected at 4, 8, 12, and 16 dai. Leaves were kept in liquid nitrogen during sampling and stored at -80°C thereafter.

Determination of superoxide anion radical (O_2^-) concentration

A total of 0.2 g of leaf tissue was ground into a fine powder with liquid nitrogen using a vibration ball mill and homogenized in 2 ml of a solution containing 100 mM sodium phosphate buffer (pH 7.2) and 1 mM sodium diethyldithiocarbamate (SDD). The homogenate was centrifuged at 22.000 g for 20 min at 4°C. After centrifugation, an aliquot of the supernatant was placed to react with a solution containing 100 mM sodium phosphate buffer (pH 7.2), 1 mM SDD, and 0.25 mM nitroblue tetrazolium (NBT). The O_2^- concentration was determined by subtracting the absorbance of the final product from the initial absorbance at 540 nm (Chaitanya and Naithani 1994).

Determination of hydrogen peroxide (H_2O_2) concentration

A total of 0.1 g of leaf tissue was ground into a fine powder with liquid nitrogen using a vibration ball mill and homogenized in 2 ml of 0.1% (w/v) of trichloroacetic acid (TCA). The homogenate was centrifuged at 12.000 g for 15 min at 4°C, and an aliquot of the supernatant

reacted with a mixture containing 10 mM potassium phosphate buffer (pH 7.0) and potassium iodide solution and incubated for 5 min. Absorbance was determined at 390 nm. The H_2O_2 concentration was determined based on a standard curve made with known concentrations of H_2O_2 (Sergiev et al. 1997).

Determination of malondialdehyde (MDA) concentration

A total of 0.1 g of leaf tissue was ground into a fine powder with liquid nitrogen using a vibration ball mill and homogenized and homogenized in 2 ml of a solution of TCA 0.1% (w/v). The homogenate was centrifuged at 12.000 g for 15 min at 4°C. An aliquot of the supernatant was mixed with 0.75 ml of 0.5% thiobarbituric acid (TBA) solution (w/v) (prepared in 20% (w/v) TCA) and incubated in a water bath at 95°C for 60 min. Thereafter, the reaction was quenched in an ice bath following centrifugation at 10.000 g for 10 min. The specific absorbance of the supernatant was determined at 532 nm. Non-specific absorbance was measured at 600 nm and subtracted from the value of the specific absorbance. The extinction coefficient of 155 mM^{-1} cm^{-1} was used to calculate the MDA concentration (Hodges et al. 1999).

Determination of total soluble phenolics (TSP) and lignin-thioglycolic acid (LTGA) derivatives concentrations

A total of 0.1 g of leaf tissue was ground into a fine powder with liquid nitrogen using a vibration ball mill and homogenized in 1.5 ml of 80% (v/v) methanol solution. The crude extract was shaken at 300 rpm at 25°C for 12 h, and the mixture was centrifuged at 13.000 g for 30 min. The TSP concentration was determined in the methanolic extract, and the pellet was kept at 20°C to determine the LTGA derivatives concentration, according to Fortunato et al. (2015).

Determination of antioxidant enzymes activities

A total of 0.2 g of leaf tissue was macerated in a vibration ball mill with liquid nitrogen to obtain a fine powder, which was homogenized in 2 ml of potassium phosphate buffer 100 mM (pH 6.8) containing 0.1 mM EDTA, 1 mM phenylmethyl-sulphonyl fluoride (PMSF), and 0.5% (w/v) polyvinylpolypyrrolidone (PVPP). The homogenate was centrifuged at 13.000 g for 15 min at 4°C, and the supernatant was divided into aliquots which were used as extracts for the determinations of superoxide dismutase (SOD, EC 1.15.1.1), catalase (CAT, EC 1.11.1.6), glutathione reductase (GR, EC 1.8.1.7), and ascorbate peroxidase (APX, EC 1.11.1.11) activities as previously described (Bermúdez-Cardona et al. 2015a, Tatagiba et al. 2015, Rios et al. 2017). Proteins concentration was measured using the Bradford assay with bovine serum albumin as a standard (Bradford 1976).

Determination of defense enzymes activities

A total of 0.2 g of leaf tissue was macerated in a vibration ball mill with liquid nitrogen to obtain a fine powder to determine the activities of chitinase (CHI) (EC 3.2.1.14), β-1,3-glucanase (GLU) (EC 3.2.1.39), peroxidase (POX) (EC 1.11.1.7), polyphenoloxidase (PPO), lipoxygenase (LOX) (EC 1.13.11.12), and phenylalanine ammonia-lyase (PAL) (EC 4.3.1.5). The fine powder was homogenized in 2 ml of a solution containing 50 mM potassium phosphate buffer (pH 6.8), 1 mM EDTA, 1 mM PMSF, and 0.5% (w/v) PVPP. The homogenate was centrifuged at 12.000 g for 15 min at 4 °C, and the supernatant was used to determine CHI, GLU, PAL, PPO, and LOX activities as previously described (Polanco et al. 2012; Fortunato et al. 2015; Fagundes-Nacarath et al. 2018). Proteins concentration was measured as described above.

Experimental design and statistical analysis

A 3 × 2 factorial experiment, consisting of plants sprayed with water (control), AOA, and ET, (referred to as treatments (T) thereafter) and plant inoculation (PI) (non-inoculated and inoculated plants), was arranged in a completely randomized design with eight replications. Each replication corresponded to a plastic pot containing two plants. The experiment was repeated once. All parameters and variables evaluated were subjected to analysis of variance, and means were compared by Tukey's test ($P \leq 0.05$). Data were analyzed using the Minitab software (version 18; Minitab Corporation).

Results

Analysis of variance

The factors foliar treatments (T) and plant inoculation (PI), as well as the T × PI interaction, were significant for most of the variables and parameters evaluated. The T × PI interaction was significant for the concentrations of H_2O_2, MDA, and LTGA derivatives, for the activities of CAT, GR, APX, CHI, POX, LOX, and PAL (Table 1).

Disease severity

The NLB severity progressed much faster on the leaves of ET-sprayed plants from 8 to 16 dai in comparison to plants sprayed with either water or AOA (Fig. 1A). The AUDPC was significantly lower by 27 and 31%, respectively, for plants from the control and AOA treatments in comparison to ET-sprayed plants (Fig. 1B).

ET production

The ET was not detected on the leaves of non-inoculated plants from the control and AOA treatments in comparison to the ET treatment, regardless of the evaluation time. By contrast, ET was produced by the leaves of ET-sprayed plants from 4 to 16 dai (Fig. 2A). Increases in ET production were 38-112% for inoculated ET-sprayed plants compared to the control and AOA treatments from 8 to 16 dai. The ET production significantly increased during the infection process of E. turcicum regardless of the treatments. For inoculated ET-sprayed plants, ET production increased by 37, 124, and 335%, respectively, at 8, 12, and 16 dai in comparison to non-inoculated ET-sprayed plants (Fig. 2B).

Leaf gas exchange parameters

For non-inoculated plants, there was no significant effect of the control, AOA, and ET treatments for A, g_s, C_i, and E regardless of the evaluation time (Fig. 3A, C, E, and G). For inoculated plants, there was no significant effect of the control, AOA, and ET treatments for g_s, C_i, and E regardless of the evaluation time and for A only at 12 dai (Fig. 3B, D, F, and H). For inoculated ET-sprayed plants, A significantly decreased by 31 and 27% in comparison to plants from the control and AOA treatments, respectively, at 12 dai (Fig. 3B). The deleterious effect of E. turcicum on leaf gas exchange was confirmed by significant decreases in A (12-15% for control and ET treatments at 4 dai as well as 36-70%, 46-71%, and 58-65%, respectively, for control, AOA, and ET treatments from 12 to 16 dai), g_s (39-52%, 50-61%, and 39-62% for control, AOA, and ET treatments, respectively, from 12 to 16 dai) and E (29% for ET treatment at 12 dai as well as 38, 36, and 53% for control, AOA, and ET treatments, respectively, at 16 dai) in comparison to non-inoculated plants (Fig. 3A-H). C_i significantly increased by 92, 52, and 84% for control, AOA, and ET treatments, respectively, at 16 dai in comparison to non-inoculated plants (Fig. 3E and F).

Chl a fluorescence parameters

There was no significant effect of the control, AOA, and ET treatments for F_v/F_m, Y(II), Y(NPQ), and Y(NO) regardless of plant inoculation during the time-course evaluated (Fig. 4A-H). For non-inoculated plants, the values for F_v/F_m (15-28, 14-24, and 14-21% for control, AOA, and ET treatments, respectively, from 12 to 16 dai), Y(II) (62, 31, and 39% for control, AOA, and ET treatments, respectively, at 16 dai), and Y(NO) (19-8, 9-21, and 17-9% for control, AOA, and ET treatments, respectively, from 12 to 16 dai) were significantly higher in comparison to inoculated ones (Fig. 4A-D and G-H). For inoculated plants, the values for Y(NPQ) (83-38, 66-70, and 76-82% for control, AOA, and ET treatments, respectively, from 12 to 16 dai) were significantly higher in comparison to the non-inoculated ones (Fig. 4E and F). The images of Chl a fluorescence parameters did not show any change among treatments for the non-inoculated plants. On the other hand, inoculated plants showed alterations in Chl a fluorescence, with progressive loss of photosynthetic capacity from 12 dai as indicated by the dark areas in the images (Fig. 5).

Photosynthetic pigments

There was a change in the concentrations of carotenoids and Chl a+b for plants sprayed with water, AOA, and ET regardless of plant inoculation. There were significant decreases in the concentrations of carotenoids (28-42%, 28-32%, and 29-35%, respectively, for control, AOA, and ET treatments) and Chl a+b (29-38%, 29-38%, and 30-43%, respectively, for control, AOA, and ET treatments) for inoculated in comparison to non-inoculated plants from 8 to 16 dai (Fig. 6A-D).

Concentrations of O_2^-, H_2O_2, MDA, TSP, and LTGA derivatives

For non-inoculated plants, there was no significant effect of the control, AOA, and ET treatments for the concentrations of O_2^-, H_2O_2, MDA, TSP, and LTGA derivatives regardless of the sampling time (Fig. 7A, C, E, G, and I). For inoculated plants, there was no significant effect of the control, AOA, and ET treatments for O_2^- and TSP concentrations regardless of the evaluation time (Fig. 7A-B and G-H). There was no significant effect of the control, AOA, and ET treatments for H_2O_2 and MDA concentrations at 4 and 8 dai and LTGA derivatives concentration at 4 dai (Fig. 7C-D, E-F, and I-J). The inoculated ET-sprayed plants displayed significant increases in H_2O_2 (20 and 38% at 12 and 16 dai, respectively), MDA concentration (60 and 32% at 12 and 16 dai, respectively), and significant decreases in LTGA derivatives concentration (23 and 13% at 8 and 16 dai, respectively) in comparison to the control treatment (Fig. 7D, F and J). The LTGA derivatives concentration was significantly lower by 23, 16, and 17%, respectively, at 8, 12, and 16 dai for ET-sprayed plants in comparison to AOA-sprayed ones. There were significant increases for O_2^-, H_2O_2, MDA, and TSP concentrations (34-52%, 52-55%, and 37-39%; 112-113%, 80-89%, and 158-178%; 125-250%, 53-291%, and 176-391%; and 57-126%, 25-169%, and 27-117%, respectively) for inoculated plants sprayed with water, AOA, and ET in comparison to their non-inoculated counterparts during the time-course evaluated (Fig. 7A-J).

Activities of antioxidant enzymes

For non-inoculated plants, SOD, CAT, GR, and APX activities were not significantly different among treatments regardless of the evaluation time (Fig. 8A, C, E, and G). For inoculated plants, there was no significant effect of the control, AOA, and ET treatments for the activities of SOD (8 and 16 dai), CAT (from 4 to 12 dai), GR (8 and 16 dai), and APX (4 dai) (Fig. 8B, D, F, and H). For inoculated AOA-sprayed plants, CAT and GR activities significantly

increased by 35 and 68% at 16 dai and by 51 and 59% at 4 dai in comparison, respectively, to the control and ET treatments. The inoculated ET-sprayed plants showed significant decreases in SOD (22 and 16% at 4 and 12 dai, respectively), GR (20% at 12 dai), and APX activities (33, 29, and 32% at 8, 12, and 16 dai, respectively) in comparison to the control treatment. The inoculated ET-sprayed plants showed significant decreases in SOD (17% at 12 dai), GR (37 and 36% at 4 and 12 dai, respectively), and APX activities (40, 35, and 41% at 8, 12, and 16 dai, respectively) in comparison to AOA-sprayed plants. There were significant increases for SOD, CAT, GR, and APX activities (31-54%, 33-64%, and 31-39%; 18-24%, 24-65%, and 8-26%; 253-413%, 67-440%, and 57-430%; and 40-193%, 60-169%, and 43-90%, respectively) for inoculated plants sprayed with water, AOA, and ET in comparison to their non-inoculated counterparts during the time-course evaluated (Fig. 8A-H).

Activities of defense enzymes

For non-inoculated plants, there was no significant effect of the control, AOA, and ET treatments for CHI, GLU, POX, PPO, LOX, and PAL activities regardless of the sampling time (Fig. 9A, C, E, G, I, and K). There was no significant effect of the control, AOA, and ET treatments for CHI (4 dai), GLU (16 dai), POX (4, 8, and 16 dai), PPO (12 and 16 dai), and LOX (4 dai). The CHI activity significantly decreased by 63 and 61% at 8 dai for AOA and ET treatments, respectively, in comparison to the control treatment. For the ET-sprayed plants, CHI activity was significantly lower by 54 and 62% at 12 dai and by 17 and 21% at 16 dai in comparison, respectively, to the control and AOA treatments (Fig. 9B). The GLU activity significantly increased by 340 and 247% at 4 dai for the control and AOA and treatments, respectively, in comparison to the ET treatment. For the AOA-sprayed plants, GLU activity was significantly lower by 21 and 72%, respectively, at 4 and 8 dai in comparison to the control treatment. The GLU activity significantly increased by 128 and 305% at 12 dai for AOA and

ET treatments, respectively, in comparison to the control treatment. For the ET-sprayed plants, GLU activity significantly increased by 78% at 12 dai in comparison to the AOA treatment (Fig. 9D). The POX activity significantly decreased by 29% at 12 dai for ET-sprayed plants in comparison to AOA-sprayed plants (Fig. 9F). The PPO activity significantly increased by 22% at 4 dai for ET-sprayed plants in comparison to AOA-sprayed plants. For AOA-sprayed plants, PPO activity significantly increased by 29 and 21% at 8 dai in comparison, respectively, to control and ET treatments (Fig. 9H). The LOX activity was significantly higher by 35, 26, and 41% at 8, 12, and 16 dai, respectively, for the AOA treatment in comparison to the control treatment. The LOX activity significantly decreased by 23, 35, and 48% at 8, 12, and 16 dai, respectively, for ET-sprayed plants in comparison to AOA-sprayed ones. The LOX activity was significantly lower by 18% at 12 dai for ET-sprayed plants in comparison to plants from the control treatment (Fig. 9J). The PAL activity significantly decreased by 48% at 4 dai for ET-sprayed plants in comparison to AOA-sprayed plants. At 8 dai, there were significant decreases of 33 and 38% on PAL activity for AOA and ET-sprayed plants, respectively, in comparison to plants from the control treatment. The PAL activity significantly decreased by 52 and 23% at 12 and 16 dai, respectively, for ET-sprayed plants in comparison to the control treatment. For ET-sprayed plants, PAL activity was significantly lower by 64 and 20% at 12 and 16 dai, respectively, in comparison to AOA-sprayed plants (Fig. 9L). There were significant increases for CHI, GLU, POX, PPO, LOX, and PAL activities (113-804%, 902-1352%, and 240-680%; 410-1099%, 486-2456%, and 194-3998%; 219-528%, 202-713%, and 239-471%; 78-118%, 72-167%, and 83-129%; 47%, 32-71%, and 13; and 43-160%, 103-159% and 130%, respectively) for inoculated plants sprayed with water, AOA, and ET in comparison to their non-inoculated counterparts during the time-course evaluated (Fig. 9A-L).

Discussion

The involvement of ET acting as either a positive or a negative mediator of host defense responses shows a great variation among the different host-pathogen interactions (Helliwell et al. 2013; Wang et al. 2017; Abdelsamad et al. 2019). The present study results bring new insights into the involvement of this hormone in maize plants' leaves in response to infection by E. turcicum. Our results showed that NLB symptoms were more expressive in the leaves of ET-sprayed plants.

The seq-RNA analysis for the maize-S. turcica interaction revealed that genes involved in the ET, JA, and SA biosynthesis pathways were differentially expressed in the first hours after fungal inoculation, and four ET-related pathway genes (6.56%) were identified (Shi et al. 2018). In the present study, ET was produced in maize leaves infected by E. turcicum. By contrast, in the leaves of non-inoculated plants, this hormone was not detected but was noticed only upon ET spray. Interestingly, the accumulation of ET was a general response of the leaves of maize plants against E. turcicum infection regardless of its application. For the rice-P. oryzae, ET was rapidly produced after fungal inoculation and dramatically increased as the lesions expanded (Helliewell et al. 2016). Other studies also confirmed the negative role played by ET on Arabidopsis-P. syringae and -Fusarium oxysporum (Chen et al. 2009a; Pantelides et al. 2013) and rice-B. oryzae (De Vleesschauwer et al. 2010) interactions. However, exogenous ET application increased the resistance of barrel clover plants against infection by Macrophomina phaseolina (Gaige et al. 2010) and soybean plants infected by Phytophthora sojae and Fusarium virguliforme (Sugano et al. 2013; Abdelsamad et al. 2019). Tomato mutant plants impaired in ET perception exhibited lower diseases symptoms in consequence of infections by Xanthomonas campestris pv. vesicatoria, P. syringae pv. tomato, and F. oxysporum f. sp. lycopersici compared to the wild-type plants (Lund et al. 1998). The ET application to rice plants increased their susceptibility to brown spot (De Vleesschauwer et al. 2010). Wang et al.

(2017) showed that ET was involved in maize plants' susceptibility to infection by A. flavus. Interestingly, the same authors observed that both colonization of maize kernels by A. flavus and conidia production exposed to an ET biosynthesis inhibitor were reduced.

Photosynthesis is the main physiological process affected in plants infected by pathogens of different lifestyles and has been investigated for the maize-S. macrospora and -E. turcicum (Bermúdez-Cardona et al. 2015; Silveira et al. 2019) and soybean-Corynespora cassiicola, -Colletotrichum truncatum, -Cercospora sojina, and -P. pachyrhizi (Dias et al. 2018; Fortunato et al. 2018; Nascimento et al. 2018; Rios et al. 2018) interactions. In the present study, the photosynthesis in maize leaves was impaired upon E. turcicum infection, as noticed by the lower A, g_s, and E values linked to high C_i values. The decrease in A in infected leaves was associated with reduced CO_2 influx due to stomatal closure and limitations for its fixation at the biochemical level. Lower E values were linked to a reduction in g_s in the leaves of soybean plants infected by P. pachyrhizi and, therefore, associated with stomatal closure (Rios et al. 2018).

Despite the increase in NLB symptoms on ET or AOA-sprayed plants, photosynthesis was not impaired as noticed by no quantitative changes in the values of Chl a fluorescence parameters. Differences were only noticed for non-inoculated plants and those inoculated with E. turcicum. There were no changes in the F_v/F_m, Y(NPQ), and Y(NO) values as well as on the concentrations of total chlorophylls and carotenoids during the biotrophic phase of E. turcicum, indicating, therefore, its incapacity to perturb the photosynthetic apparatus in maize leaves. Leaf tissues necrosis is only noticeable during the necrotrophic phase of E. turcicum (Kotze et al. 2019). However, as the lesions of NLB were noticed in the leaves, decreases in F_v/F_m (values lower than 0.8) occurred, indicating that the photosynthetic apparatus was damaged. Lower Y(NPQ) and Y(NO) values occurred at advanced stages of E. turcicum infection. Baghbani et al. (2019) demonstrated the PSII was damaged, and the photosynthetic process was

compromised as the infection process of F. verticillioides took place on maize plants (Baghbani et al. 2019).

As the NLB symptoms developed, the concentration of photosynthetic pigments decreased due to the appearance of necrotic lesions surrounded by intense chlorosis that irreversibly impacted the photosynthetic tissue and reduced the amount of green tissue for light capture for the photosynthetic processes. According to Fortunato et al. (2018), the coalescence of target spot lesions in soybean leaves and a progressive yellowing of the leaf tissues due to the action of non-host selective toxins released by C. cassiicola were associated with the lower concentration of Chl a+b and, to a lesser extent, to the Chl a+b/carotenoids ratio. Cuq et al. (1993) reported that E. turcicum produces the lipophilic toxin monocerin that causes brown necrotic lesions in maize leaves. Considering that the aggressiveness of E. turcicum is directly proportional to the release of hydrolytic enzymes and non-host selective toxins, it is plausible to hypothesize that reduction in the concentration of photosynthetic pigments was linked to lipid peroxidation in the plasmatic membrane. The MDA concentration, a biochemical indicator of lipid peroxidation, was high at advanced stages of E. turcicum infection, especially in ET-sprayed plants, which exhibited the greatest disease symptoms.

The oxidative burst as a response of the plant against pathogen infection gives rise to a localized accumulation of reactive oxygen species (ROS) that can indicate defense response. The production and release of ROS (e.g., hydrogen peroxide (H_2O_2), singlet oxygen ($^1O_2$), superoxide anion (O_2^-), and hydroxyl radical (OH)) in the cells may damage them or serve as signaling molecules (Camejo et al. 2016). In the present study, the highest accumulation of O_2^- occurred from 12 to 16 dai and was accompanied by the appearance of lesions and their expansion even though there was no difference among the control, AOA, and ET treatments. The highest accumulation of H_2O_2 also occurred at 12 and 16 dai and was more expressive for ET-sprayed plants. The H_2O_2 interplays with the diverse phytohormones to regulate the

developmental processes of plants and their stress response. Cui et al. (2019) observed that H_2O_2 production stimulated the ET biosynthesis. Moreover, Wi et al. (2012) reported that ET and ROS levels correlated with the infection process of Phytophthora parasitica in tobacco plants. Therefore, ET production reflected pathogen penetration into the plant tissues, and later ET and ROS production were of detrimental importance for disease development (Wi et al. 2012).

Plants have developed an efficient antioxidant system to lower the damage caused by the ROS to the cells, which involves the enzymes SOD (catalyzes the removal of O_2^- by dismutating it into O_2 and H_2O_2), CAT (responsible for catalyzing the dismutation of H_2O_2 into H_2O and O_2), and APX (reduces the H_2O_2 to H_2O) (Das and Roychoudhury 2014). The POX, CAT, and SOD genes are involved in the antioxidative system and are expressed in the first hours (12 and 60 hai) in maize leaves in response to S. turcica infection (Shi et al. 2018). In the present study, inoculated plants displayed a significant increase in the activities of CAT, GR, and APX from 4 to 16 dai. Moreover, ET-sprayed plants showed lower activities of SOD (4 and 12 dai), GR (12 dai), and APX (4, 12, and 16 dai), indicating that ET was able to manipulate the antioxidant system of maize plants in favor of E. turcicum infection.

The interaction between host and pathogen is complex and involves the pathogen's strategies to efficiently infect its host, responding through the activation of defense responses (Carere et al. 2016). In the present study, the concentration of phenolics was high for inoculated plants regardless if they were sprayed with water, ET, or AOA. The CHI is an important lytic enzyme that degrades chitin in the fungal cell wall (Malik 2019). The GLU can act directly against fungal pathogens by degrading β-1,3/1,6-glucans in their cell wall rendering the fungal cell lysis (Zhang et al. 2019). In addition to these enzymes, others are important for plant defense, such as POX, LOX, and PAL (Debona et al. 2018; Fagundes-Nacarath et al. 2018; Silva et al. 2019). In the present study, CHI, GLU, POX, PPO, LOX, and PAL activities

increased for inoculated plants and reduced NLB symptoms. The GLU activity increased in maize leaves infected by E. turcicum (Jondle et al. 1989). Maize plants infected by U. maydis displayed induction of genes of the shikimate pathway beside a 20-fold increase in PAL activity and an accumulation of phenolics (Doehlemann et al. 2008). In the present study, CHI, GLU, LOX, and PAL activities were lower for ET-sprayed plants. Reductions in lignin concentration may be associated with lower PAL activity and may lower the resistance of maize plants against E. turcicum infection. The PAL comprises the first enzyme involved in the phenylpropanoid pathway, which is involved in the synthesis of phenolics, lignin, and salicylic acid (Yadav et al. 2020). A recent study with Arabidopsis-P. syringae interaction indicated that ET likely exerted effective repression on the SA pathway by repressing multiple genes involved in the biosynthesis, transport, and signaling of this hormone, making the plants more susceptible to bacterial infection (Li et al. 2020).

Based on the experiments carried out by Tanaka et al. (2014), it was demonstrated that modifying lignin composition in maize plants increased the chance of them to become susceptible to U. maydis infection because of the reduced strength of cell walls that will increase the access of fungal hyphae to nutrients. According to Chen et al. (2009b), mutant plants of Arabidopsis with reduced ET signaling or perception were more resistant against F. graminearum infection than wild-type plants while mutants plants with enhanced ET production were susceptible.

In summary, we have shown that an exogenous ET supply to the leaves of maize plants played a negative role in the infection process of E. turcicum besides modulating fungal-induced ROS formation. The ET biosynthesis was noticed in the leaves infected by E. turcicum and was closely associated with NLB development. The increase in NLB symptoms can probably be attributed to the lower activities of enzymes related to the antioxidative (SOD, GR, and APX) and defense (CHI, GLU, LOX, and PAL) metabolisms.

References

Abdelsamad NA, MacIntosh GC, Leandro LFS (2019) Induction of ethylene inhibits development of soybean sudden death syndrome by inducing defense-related genes and reducing Fusarium virguliforme growth. PLoS ONE 14:e0215653

Baghbani F, Lotfi R, Moharramnejad S, Bandehagh A, Roostaei M, Rastogi, A, Kalaji H. M (2019) Impact of Fusarium verticillioides on chlorophyll fluorescence parameters of two maize lines. European Journal of Plant Pathology 154:337–346

Berens ML, Berry HM, Mine A, Argueso CT, Tsuda K (2017) Evolution of hormone signaling networks in plant defense. Annual Review of Phytopathology 55:401–425

Berger S, Sinha AK, Roitsch T (2007) Plant physiology meets phytopathology: plant primary metabolism and plant–pathogen interactions. Journal of Experimental Botany 58: 4019-4026

Bermúdez-Cardona MB, Bispo WMS, Rodrigues FA (2015a) Physiological and biochemical alterations on maize leaves infected by Stenocarpella macrospora. Acta Physiologiae Plantarum 37:158

Bermúdez-Cardona MB, Wordell Filho JA, Rodrigues FA (2015b) Leaf gas exchange and chlorophyll a fluorescence in maize leaves infected with Stenocarpella macrospora. Phytopathology 105:26–34

Bradford MM (1976) A rapid and sensitive method for the quantitation of microgram quantities of protein utilizing the principle of protein-dye binding. Analytical Biochemistry 72:248–254

Camejo D, Guzmán-Cedeño A, Moreno A (2016) Reactive oxygen species, essential molecules, during plant-pathogen interactions. Plant Physiology and Biochemistry 103: 10–23

Carere J, Colgrave ML, Stiller J, Liu C, Manners JM, Kazan K, Gardiner DM (2016) Enzyme-driven metabolomic screening: a proof-of-principle method for discovery of plant defence compounds targeted by pathogens. New Phytologist 212:770–779

Chaitanya KSK, Naithani SC (1994) Role of superoxide, lipid peroxidation and superoxide

dismutase in membrane perturbation during loss of viability in seeds of Shorea robusta Gaertn.f. New Phytologist 126:623–627

Chen H, Xue L, Chintamanani S, Germain H, Lin H, Cui H, Cai R, Zuo J, Tang X, Li X, Guo H, Zhou JM (2009a) ETHYLENE INSENSITIVE3 and ETHYLENE INSENSITIVE3-LIKE1 repress SALICYLIC ACID INDUCTION DEFICIENT2 expression to negatively regulate plant innate immunity in Arabidopsis. Plant Cell 21:2527–2540

Chen X, Steed A, Travella S, Keller B, Nicholson, P. (2009b). Fusarium graminearum exploits ethylene signalling to colonize dicotyledonous and monocotyledonous plants. New Phytologist 182:975–983

Cristescu SM, De Martinis D, Hekkert STL, Parker DH, Harren FJM (2002) Ethylene production by Botrytis cinerea in vitro and in tomatoes. Applied and Environmental Microbiology 68:5342–5350

Cui Z, Yang Z, Xu D (2019) Synergistic roles of biphasic ethylene and hydrogen peroxide in wound-induced vessel occlusions and essential oil accumulation in Dalbergia odorifera. Frontiers in Plant Science 10:250

Cuq F, Petitprez M, Herrmann-Gorline S, Klaebe A, Rossignol M (1993) Monocerin in Exserohilum turcicum isolates from maize and a study of its phytotoxicity. Phytochemistry 34:1265–1270

Das K, Roychoudhury A (2014) Reactive oxygen species (ROS) and response of antioxidants as ROS-scavengers during environmental stress in plants. Frontiers in Environmental Science 2:53

De Vleesschauwer D, Yang Y, Cruz CV, Hofte M (2010) Abscisic acid-induced resistance against the brown spot pathogen Cochliobolus miyabeanus in rice involves MAP kinase-mediated repression of ethylene signaling. Plant Physiology 152:2036–2052

Debona D, Fortunato AA, Araújo L, Rodrigues AL, Rodrigues FA (2018) Rice defense responses to Bipolaris oryzae mediated by a strobilurin fungicide. Tropical Plant Pathology 43:389–401

Di X, Gomila J, Takken FLW (2017) Involvement of salicylic acid, ethylene and jasmonic acid signalling pathways in the susceptibility of tomato to Fusarium oxysporum. Molecular Plant Pathology 18:1024–1035

Dias CS, Araujo L, Chaves JAA, DaMatta FM, Rodrigues FA (2018) Water relation, leaf gas exchange and chlorophyll a fluorescence imaging of soybean leaves infected with Colletotrichum truncatum. Plant Physiology and Biochemistry 127:119–128

Doehlemann G, Wahl R, Horst RJ, Voll LM, Usadel B, Poree F, Stitt M, Pons-Kühnemann J, Sonnewald U, Kahmann R, Kämper J (2008) Reprogramming a maize plant: transcriptional and metabolic changes induced by the fungal biotroph Ustilago maydis. The Plant Journal 56:181–195

Fagundes-Nacarath IRF, Debona D, Oliveira ATH, Hawerroth C, Rodrigues FA (2018) Biochemical responses of common bean to white mold potentiated by phosphites. Plant Physiology and Biochemistry 132:308–319

Fortunato AA, Debona D, Bernardeli AMA, Rodrigues FA (2015) Defence-related enzymes in soybean resistance to target spot. Journal of Phytopathology 163:731–742

Fortunato AA, Debona D, Aucique-Pérez CE, Fialho Corrêa E, Rodrigues FA (2018) Chlorophyll a fluorescence imaging of soybean leaflets infected by Corynespora cassiicola. Journal of Phytopathology 166:782–789

Gaige AR, Ayella A, Shuai B (2010) Methyl jasmonate and ethylene induce partial resistance in Medicago truncatula against the charcoal rot pathogen Macrophomina phaseolina. Physiological and Molecular Plant Pathology 74:412–418

Guan R, Su J, Meng X, Li S, Liu Y, Xu J, Zhang S (2015) Multilayered regulation of ethylene induction plays a positive role in Arabidopsis resistance against Pseudomonas syringae. Plant Physiology 169:299–312

Hao D, Sun X, Ma B, Zhang J, Guo H (2017) Ethylene. In: Li J, Li C, Smith SM (eds). Hormone Metabolism and Signaling in Plants. ELSEVIER Academic Press, London (United Kingdom). pp. 203-241

Helliwell EE, Wang Q, Yang Y (2013) Transgenic rice with inducible ethylene production exhibits broad-spectrum disease resistance to the fungal pathogens Magnaporthe oryzae and Rhizoctonia solani. Plant Biotechnology Journal 11:33–42

Helliwell EE, Wang Q, Yang Y (2016) Ethylene biosynthesis and signaling is required for rice immune response and basal resistance against Magnaporthe oryzae infection. Molecular Plant-Microbe Interactions 29:831–843

Hennessy GG, Demilliano WAJ, Mclaren CG (1990) Influence of primary weather variables on sorghum leaf-blight severity in Southern Africa. Phytopathology 80:943–945

Hodges DM, Delong JM, Forney CF, Prange RK (1999) Improving the thiobarbituric acid-reactive-substances assay for estimating lipid peroxidation in plant tissues containing anthocyanin and other interfering compounds. Planta 207:604–611

Hooda KS, Khokhar MK, Shekhar M, Karjagi CG, Kumar B, Mallikarjuna N, Devlash RK, Chandrashekara C, Yadav OP (2017) Turcicum leaf blight-sustainable management of a re-emerging maize disease. Journal of Plant Diseases and Protection 124:101–113

Horst RJ, Engelsdorf T, Sonnewald U, Voll LM (2008) Infection of maize leaves with Ustilago maydis prevents establishment of C4 photosynthesis. Journal of Plant Physiology 165:19–28

Hurni S, Scheuermann D, Krattinger SG, Kessel B, Wicker T, Herren G, Fitze MN, Breen J, Presterl T, Ouzunova M, Keller B (2015) The maize disease resistance gene Htn1 against

northern corn leaf blight encodes a wall-associated receptor-like kinase. Proceedings of the National Academy of Sciences 112:8780–8785

Jondle DJ, Coors JG, Duke SH (1989) Maize leaf β-1,3-glucanase activity in relation to resistance to Exserohilum turcicum. Canadian Journal of Botany 67:263–266

Kramer DM, Johnson G, Kiirats O, Edwards GE (2004) New fluorescence parameters for the determination of QA redox state and excitation energy fluxes. Photosynthesis Research 79:209–218

Kotze RG, Van der Merwe CF, Crampton BG, Kritzinger Q (2019) A histological assessment of the infection strategy of Exserohilum turcicum in maize. Plant Pathology 68:504–512

Leonard KJ, Suggs EG (1974) Setosphaeria prolata, the Ascigerous State of Exserohilum prolatum. Mycologia 66:281

Li Z, Liu H, Ding Z, Yan J, Yu H, Pan R, Hu J, Guan Y, Hua J (2020) Low temperature enhances plant immunity via salicylic acid pathway genes that are repressed by ethylene. Plant Physiology 182:626–639

Lund ST, Stall RE, Klee HJ (1998) Ethylene regulates the susceptible response to pathogen infection in tomato. Plant Cell 10:371–382

Luttrell ES, Bacon CW (1977) Classification of Myriogenospora in the Clavicipitaceae. Canadian Journal of Botany 55:2090–2097

Malca I, Ullstrup AJ (1962) Effects of carbon and nitrogen nutrition on growth and sporulation of two species of Helminthosporium. Bulletin of the Torrey Botanical Club 89:240–249

Malik A (2019) Purification and properties of plant chitinases: A review. Journal of Food Biochemistry 43:e12762

Meyer J, Berger DK, Christensen SA, Murray SL (2017) RNA-Seq analysis of resistant and susceptible sub-tropical maize lines reveals a role for kauralexins in resistance to grey leaf spot disease, caused by Cercospora zeina. BMC Plant Biology 17:1–20

Munkvold GP, White DG (2016) Compendium of Corn Diseases. 4th Ed. St. Paul, The American Phytopathological Society, Minnesota

Nascimento KJT, Debona D, Rezende D, DaMatta FM, Rodrigues FA (2018) Changes in leaf gas exchange and chlorophyll a fluorescence on soybean plants supplied with silicon and infected by Cercospora sojina. Journal of Phytopathology 166:747–760

Pantelides IS, Tjamos SE, Pappa S, Kargakis M, Paplomatas EJ (2013) The ethylene receptor ETR1 is required for Fusarium oxysporum pathogenicity. Plant Pathology 62:1302–1309

Polanco LR, Rodrigues FA, Nascimento KJT, Shulman P, Silva LC, Neves FW, Vale FXR (2012) Biochemical aspects of bean resistance to anthracnose mediated by silicon. Annals of Applied Biology 161:140–150

Rios JA, Rodrigues FA, Debona D, Resende RS, Moreira WR, Andrade CCL (2014) Induction of resistance to Pyricularia oryzae in wheat by acibenzolar-S-methyl, ethylene and jasmonic acid. Tropical Plant Pathology 39:224–233

Rios JA, Aucique-Pérez CE, Debona D, Cruz Neto LBM, Rios VS, Rodrigues FA (2017) Changes in leaf gas exchange, chlorophyll a fluorescence and antioxidant metabolism within wheat leaves infected by Bipolaris sorokiniana. Annals of Applied Biology 170:189–203

Rios VS, Rios JA, Aucique-Pérez CE, Silveira PR, Barros AV, Rodrigues FA (2018) Leaf gas exchange and chlorophyll a fluorescence in soybean leaves infected by Phakopsora pachyrhizi. Journal of Phytopathology 166:75–85

Rodriguez-Moreno L, Ebert MK, Bolton MD, Thomma BPHJ (2018) Tools of the crook-infection strategies of fungal plant pathogens. The Plant Journal 93: 664–674

Shaner G, Finney RE (1977) The effect of nitrogen fertilization on the expression of slow-mildewing resistance in knox wheat. Phytopathology 67:1051–1056

Santos RP, Cruz ACF, Iarema L, Kuki KN, Otoni WC (2008) Protocolo para extração de pigmentos foliares em porta-enxertos de videira micropropagados. Ceres 55:356–364

Shi F, Zhang Y, Wang K, Meng Q, Liu X, Ma L, Li Y, Liu J, Ma L (2018) Expression profile analysis of maize in response to Setosphaeria turcica. Gene 659:100–108

Sergiev I, Alexieva V, Karanov E (1997) Effect of spermine, atrazine and combination between them on some endogenous protective systems and stress markers in plants. Comptes Rendus de l'Academie Bulgare des Sciences 51:121–124

Shigenaga AM, Argueso CT (2016) No hormone to rule them all: interactions of plant hormones during the responses of plants to pathogens. Seminars in Cell & Developmental Biology 56:174–189

Sibiya J, Tongoona P, Derera J (2013) Combining ability and GGE biplot analyses for resistance to northern leaf blight in tropical and subtropical elite maize inbred lines. Euphytica 191:245–257

Silva PO, Medina EF, Barros RS, Ribeiro DM (2014) Germination of salt-stressed seeds as related to the ethylene biosynthesis ability in three Stylosanthes species. Journal of Plant Physiology 171:14–22

Silva ET, Rios JA, Araujo MUP, Silveira PR, Rodrigues FA (2019) Defence responses in flag leaves and spikes of common wheat Triticum aestivum cultivars with contrasting levels of basal resistance to blast caused by Pyricularia oryzae. Plant Pathology 68:645–658

Silveira PR, Milagres PO, Corrêa EF, Aucique-Pérez CE, Wordell Filho JA, Rodrigues FA (2019) Changes in leaf gas exchange, chlorophyll a fluorescence, and antioxidant metabolism within maize leaves infected by Exserohilum turcicum. Biologia Plantarum 63:643–653

Sivanesan A (1984) The bitunicate ascomycetes and their anamorphs. Canadian Journal of Botany 67:1500–1599

Sugano S, Sugimoto T, Takatsuji H, Jiang C-J (2013) Induction of resistance to Phytophthora sojae in soybean (Glycine max) by salicylic acid and ethylene. Plant Pathology 62:1048–1056

Tanaka S, Brefort T, Neidig N, Djamei A, Kahnt J, Vermerris W, Koenig S, Feussner K, Feussner I, Kahmann R (2014) A secreted Ustilago maydis effector promotes virulence by targeting anthocyanin biosynthesis in maize. Elife 3:e01355

Tatagiba SD, DaMatta FM, Rodrigues FA (2015) Leaf gas exchange and chlorophyll a fluorescence imaging of rice leaves infected with Monographella albescens. Phytopathology 105:180–188

Vale FXR, Fernandes Filho EI, Liberato JR (2003) QUANT. A software plant disease severity assessment. In: 8th International Congress of Plant Pathology. Christchurch, New Zeland, p. 105

Van Bockhaven J, Spíchal L, Novák O, Strnad M, Asano T, Kikuchi S, Höfte M, De Vleesschauwer D (2015) Silicon induces resistance to the brown spot fungus Cochliobolus miyabeanus by preventing the pathogen from hijacking the rice ethylene pathway. New Phytologist 206:761–773

Völz R, Park JY, Kim S, Park SY, Harris W, Chung H, Lee YH (2020) The rice/maize-pathogen Cochliobolus spp. infect and reproduce on Arabidopsis revealing differences in defensive phytohormone function between monocots and dicots. The Plant Journal 103:412–429

Wang S, Park YS, Yang Y, Borrego EJ, Isakeit T, Gao X, Kolomiets MV (2017) Seed-derived ethylene facilitates colonization but not aflatoxin production by Aspergillus flavus in maize. Frontiers in Plant Science 8:1–12

Wellburn AR (1994) The spectral determination of chlorophylls a and b, as well as total carotenoids, using various solvents with spectrophotometers of different resolution. Journal of Plant Physiology 144:307–313

Wi SJ, Ji NR, Park KY (2012) Synergistic biosynthesis of biphasic ethylene and reactive oxygen species in response to hemibiotrophic Phytophthora parasitica in tobacco plants. Plant Physiology 159:251–265

Yadav V, Wang Z, Wei C, Amo A, Ahmed B, Yang X, Zhang X (2020) Phenylpropanoid pathway engineering: an emerging approach towards plant defense. Pathogens 9:312

Yang C, Li W, Cao J, Meng F, Yu Y, Huang J, Jiang L, Liu M, Zhang Z, Chen X, Miyamoto K, Yamane H, Zhang J, Chen S, Liu J (2017) Activation of ethylene signaling pathways enhances disease resistance by regulating ROS and phytoalexin production in rice. The Plant Journal 89:338–353

Ye JR, Guo YL, Zhang DF, Zhang N, Wang C, Xu ML (2013) Cytological and molecular characterization of quantitative trait locus qrfg1, which confers resistance to gibberella stalk rot in maize. Molecular Plant-Microbe Interactions 26:1417–1428

Zhang SB, Zhang WJ, Zhai HC, Lv YY, Cai JP, Jia F, Wang JS, Hu YS (2019) Expression of a wheat β-1, 3-glucanase in Pichia pastoris and its inhibitory effect on fungi commonly associated with wheat kernel. Protein Expression and Purification 154:134–139

Zhang X, Fernandes SB, Kaiser C, Adhikari P, Brown PJ, Mideros SX, Jamann TM (2020) Conserved defense responses between maize and sorghum to Exserohilum turcicum. BMC Plant Biology 20:67

Zhou S, Zhang YK, Kremling KA, Ding Y, Bennett JS, Bae JS, Kim DK, Ackerman HH, Kolomiets MV, Schmelz EA, Schroeder, FC, Buckler ES, Jander G (2018) Ethylene signaling regulates natural variation in the abundance of antifungal acetylated diferuloylsucroses and Fusarium graminearum resistance in maize seedling roots. New Phytologist 221:2096–2111

Zhu P, Xu Z, Cui Z, Zhang Z, Xu L (2017) Ethylene production by Alternaria alternata and its association with virulence on inoculated grape berries. Phytoparasitica 45:273–279

Table and Figures

Table 1. Analysis of variance for the effects of foliar treatments (T), plant inoculation (PI), and the T × PI interaction for severity, area under disease progress curve (AUDPC), ethylene production, leaf gas exchange parameters (net CO_2 assimilation rate (A), stomatal conductance to water vapor (g_s), internal CO_2 concentration (C_i), and transpiration rate (E)), chlorophyll (Chl) a fluorescence parameters (maximal photosystem II quantum efficiency (F_v/F_m), effective PSII quantum yield (Y(II)), quantum yield of regulated energy dissipation (Y(NPQ)), and quantum yield of non-regulated energy dissipation (Y(NO))), concentrations of carotenoids (CAR), Chl a+b, superoxide anion radical (O_2^-), hydrogen peroxide (H_2O_2), malondialdehyde (MDA), total soluble phenolics (TSP), and lignin-thioglycolic acid (LTGA) derivatives, antioxidant enzymes activities (superoxide dismutase (SOD), catalase (CAT), glutathione reductase (GR), and ascorbate peroxidase (APX)), defence-related enzymes (chitinase (CHI), β-1,3-glucanase (GLU), peroxidase (POX), polyphenoloxidase (PPO), lipoxygenase (LOX), and phenylalanine ammonia-lyase (PAL)).

Variables/Parameters	T	PI	T × PI
Severity	< 0.001	-	-
AUDPC	0.001	-	-
Ethylene production	< 0.001	< 0.001	0.777
A	0.431	< 0.001	0.305
g_s	0.08	< 0.001	0.294
C_i	0.361	< 0.001	0.563
E	0.993	< 0.001	0.520
F_v/F_m	0.455	< 0.001	0.744
Y(II)	0.477	0.002	0.601
Y(NPQ)	0.937	< 0.001	0.668
Y(NO)	0.581	< 0.001	0.555
CAR	0.024	< 0.001	0.658
Chl a+b	0.063	< 0.001	0.314
O_2^-	0.382	< 0.001	0.491
H_2O_2	0.003	< 0.001	< 0.001
MDA	< 0.001	< 0.001	< 0.001
TSP	0.019	< 0.001	0.052
LTGA derivatives	< 0.001	0.003	0.010
SOD	0.087	< 0.001	0.181
CAT	< 0.001	< 0.001	0.011
GR	< 0.001	< 0.001	0.003
APX	< 0.001	< 0.001	< 0.001
CHI	< 0.001	< 0.001	< 0.001
GLU	0.659	< 0.001	0.725
POX	0.055	< 0.001	0.017
PPO	0.076	< 0.001	0.725
LOX	< 0.001	< 0.001	< 0.001
PAL	0.026	< 0.001	< 0.001

- = not determined.

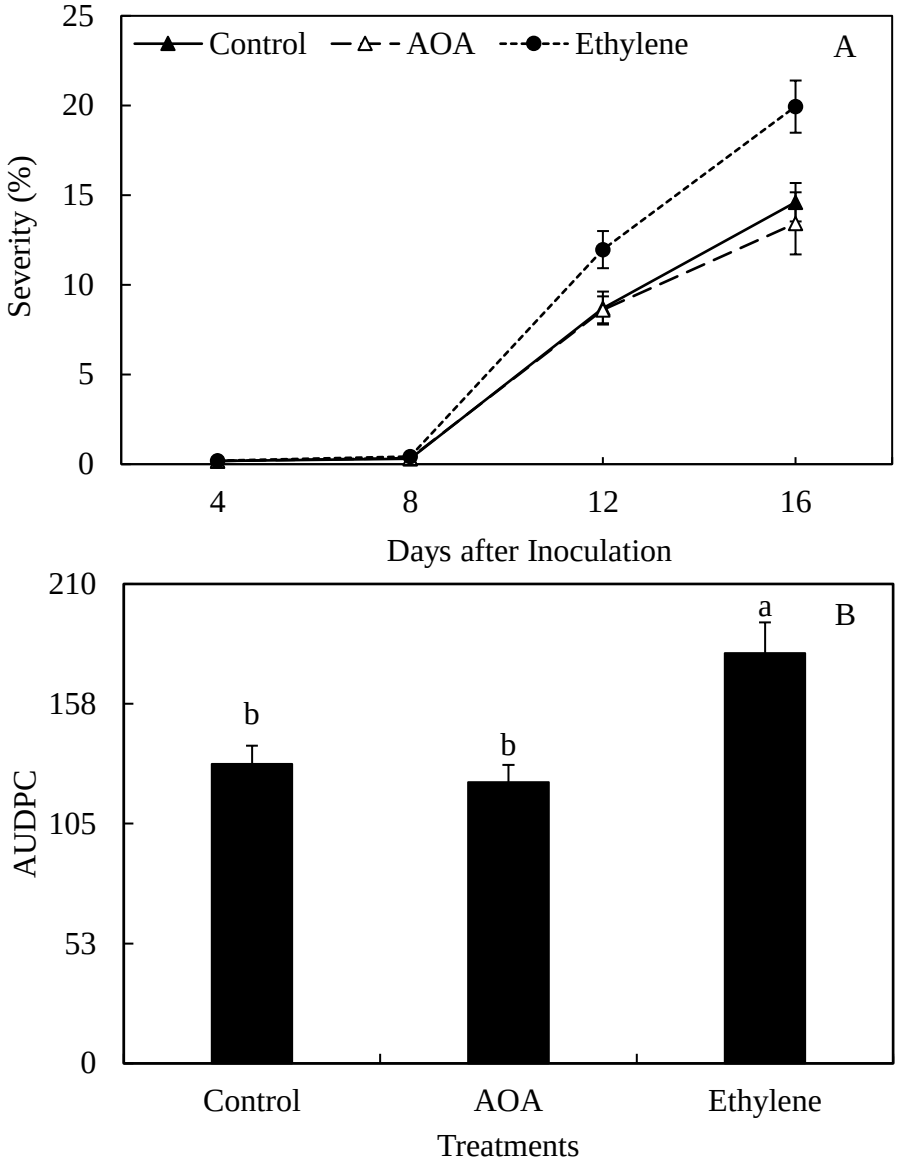

Figure 1. Severity of northern leaf blight (A) and area under disease progress curve (AUDPC) (B) for maize plants sprayed with distilled water (control), aminooxyacetic acid (AOA), and ethylene. For AUDPC, treatments means followed by different letters are significantly different ($P \leq 0.05$) according to Tukey's test. Bars represent the standard error of the means. n = 4.

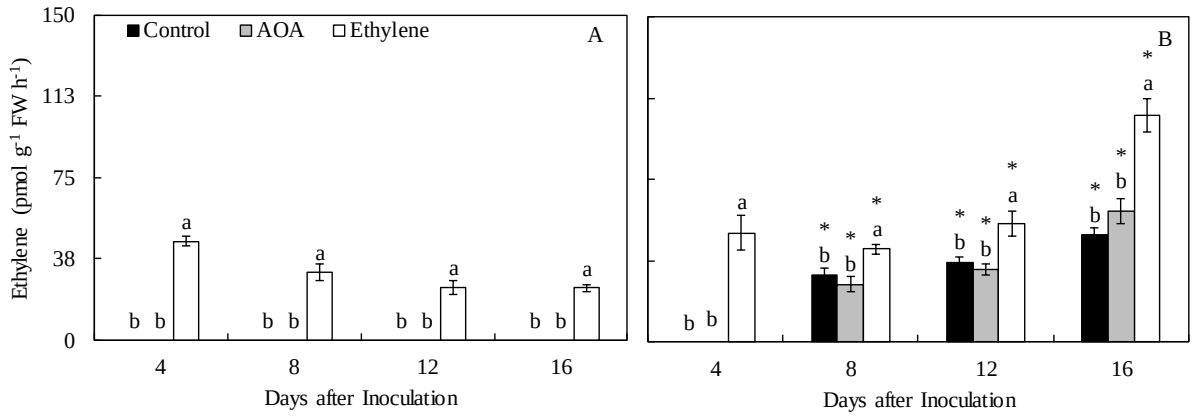

Figure 2. Ethylene production for maize plants non-inoculated (A) and inoculated with Exserohilum turcicum (B) sprayed with distilled water (control), aminooxyacetic acid (AOA), and ethylene. For each evaluation time, treatments means followed by different letters and non-inoculated and inoculated plants, for each treatment, followed by an asterisk (*) are significantly different ($P \leq 0.05$) according to Tukey's test. Bars represent the standard error of the means. FW = fresh weight. n = 4.

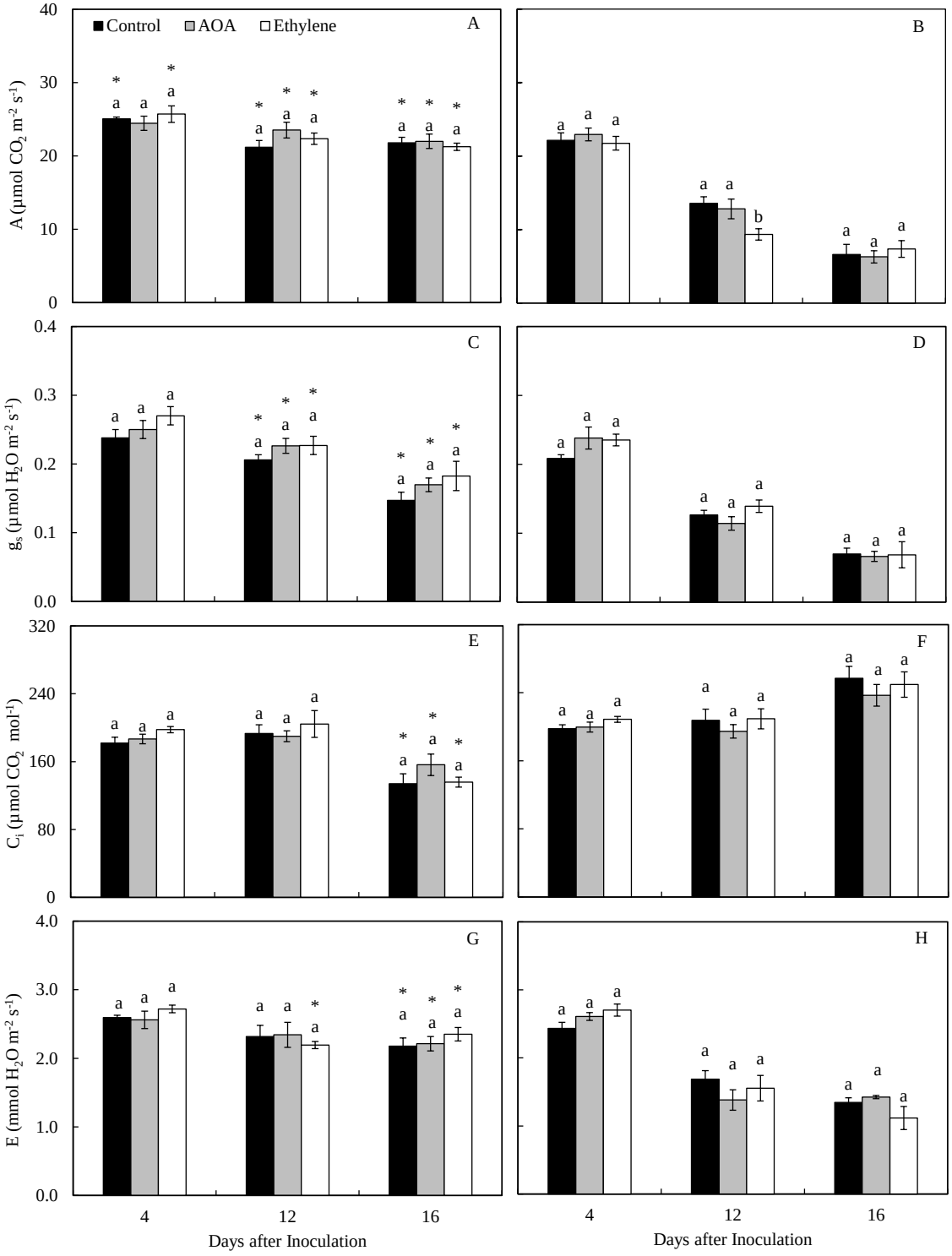

Figure 3. Leaf gas exchange parameters: net carbon assimilation rate (A) (A and B), stomatal conductance to water vapor (g_s) (C and D), internal CO_2 concentration (C_i) (E and F), and transpiration rate (E) (G and H) determined in the fifth leaf of maize plants sprayed with distilled water (control), aminooxyacetic acid (AOA), and ethylene and non-inoculated (A, C,

E, and G) or inoculated with Exserohilum turcicum (B, D, F, and H). For each evaluation time, treatments means followed by different letters and non-inoculated and inoculated plants, for each treatment, followed by an asterisk (*) are significantly different ($P \leq 0.05$) according to Tukey's test. Bars represent the standard error of the means. n = 4.

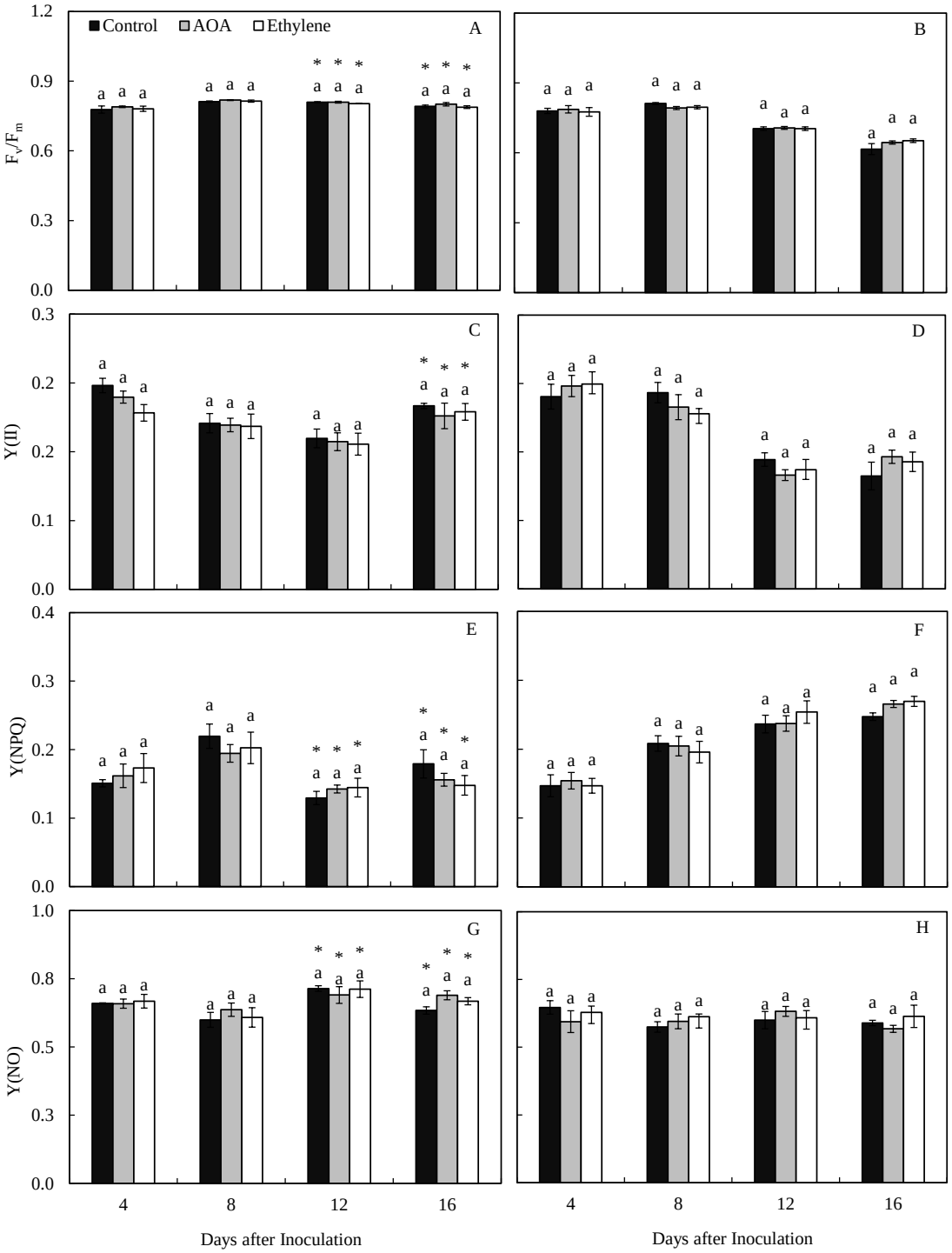

Figure 4. Chlorophyll a parameters: variable-to-maximum chlorophyll a fluorescence ratio (F_v/F_m) (A and B), effective PSII quantum yield (Y(II)) (C and D), quantum yield of regulated energy dissipation (Y(NPQ)) (E and F), and quantum yield of non-regulated energy dissipation (Y(NO)) (G and H) determined in the fifth leaf of maize plants sprayed with distilled water

(control), aminooxyacetic acid (AOA), and ethylene and non-inoculated (A, C, E, and G) or inoculated with Exserohilum turcicum (B, D, F, and H). For each evaluation time, treatments means followed by different letters and non-inoculated and inoculated plants, for each treatment, followed by an asterisk (*) are significantly different ($P \leq 0.05$) according to Tukey's test. Bars represent the standard error of the means. n = 4.

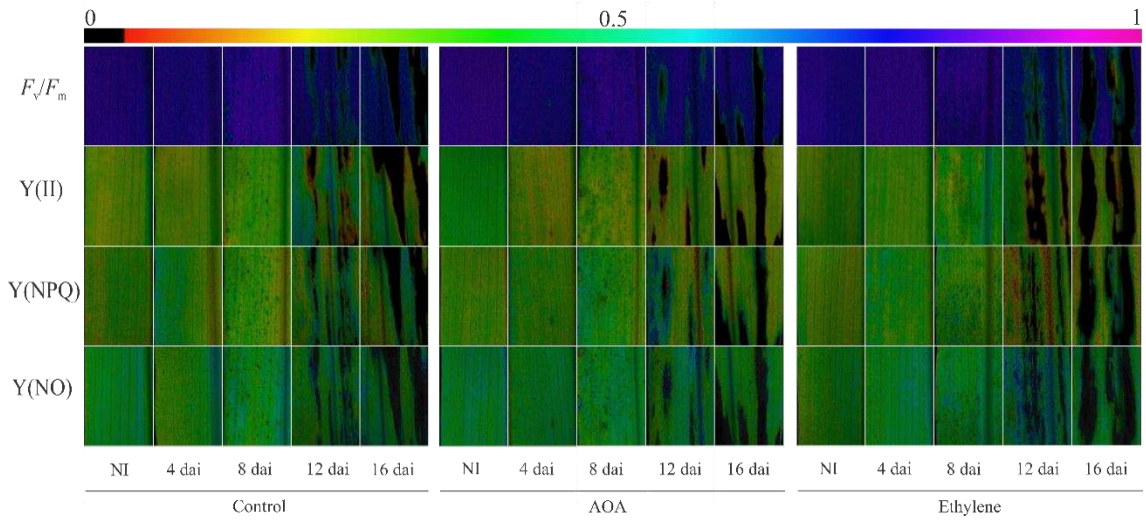

Figure 5. Images of chlorophyll a fluorescence parameters: maximum PSII quantum efficiency (F_v/F_m), photochemical yield (Y(II)), yield for dissipation by down-regulation (Y(NPQ)), and yield for non-regulated dissipation (Y(NO)) determined in the fifth leaf of maize plants sprayed with distilled water (control), aminooxyacetic acid (AOA), and ethylene and inoculated with Exserohilum turcicum. Non-inoculated (NI) plants were considered as the control treatment.

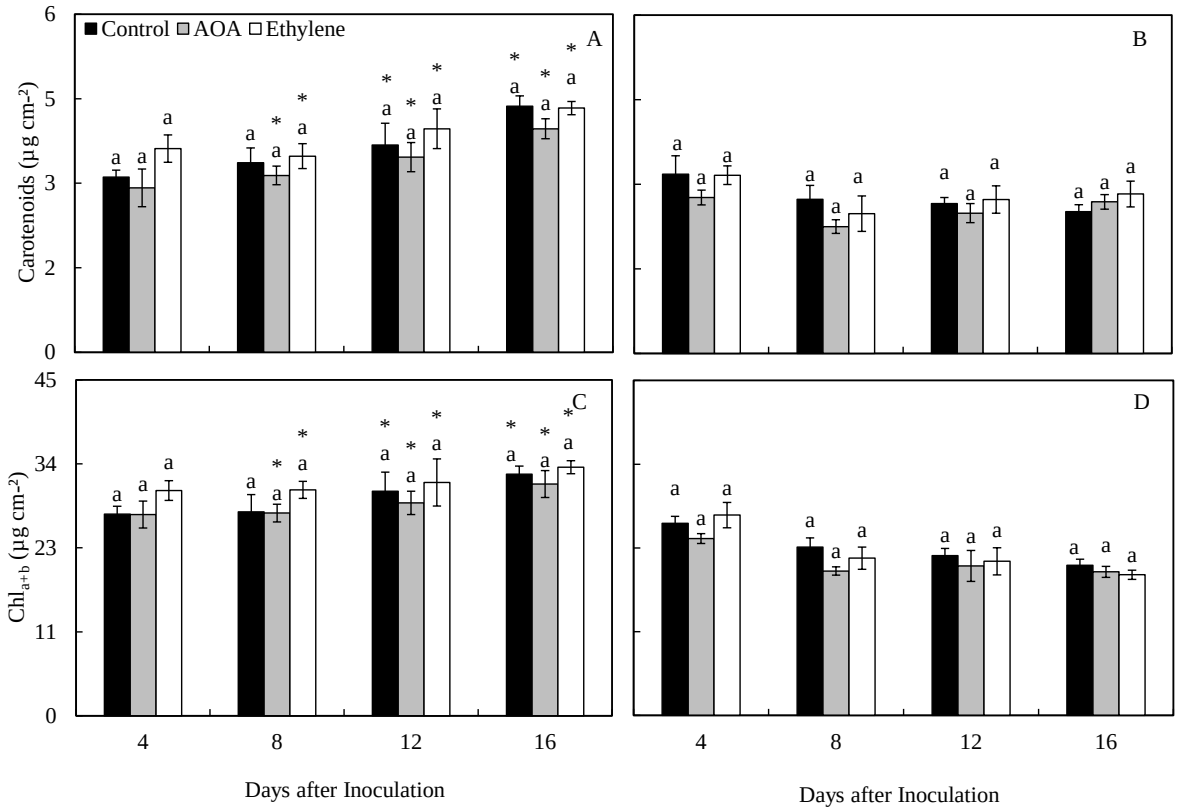

Figure 6. Concentrations of carotenoids (A and B) and total chlorophyll (Chl a+b) (C and D) determined in the fifth leaf of maize plants sprayed with water (control), aminooxyacetic acid (AOA), and ethylene and non-inoculated (A and C) or inoculated with Exserohilum turcicum (B and D). For each evaluation time, treatments means followed by different letters and non-inoculated and inoculated plants, for each treatment, followed by an asterisk (*) are significantly different ($P \leq 0.05$) according to Tukey's test. Bars represent the standard error of the means. FW = fresh weight. n = 4.

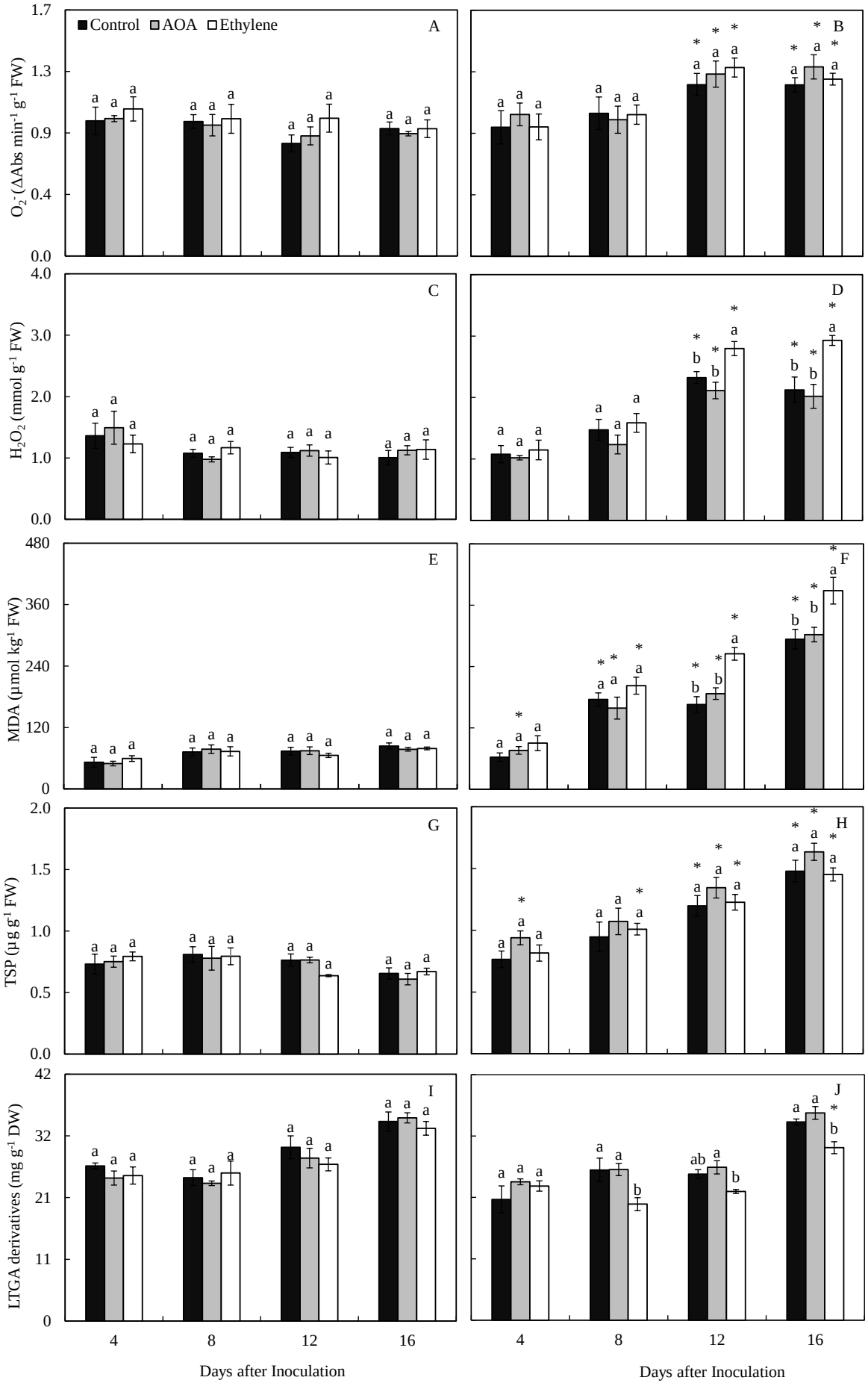
Control
AOA
Ethylene
A
B
C
D
E
F
G
H
I
J
O_2^- (ΔAbs min^{-1} g^{-1} FW)
H_2O_2 (mmol g^{-1} FW)
MDA (μmol kg^{-1} FW)
TSP (μg g^{-1} FW)
LTGA derivatives (mg g^{-1} DW)
Days after Inoculation
Days after Inoculation

Figure 7. Concentrations of superoxide anion radical (O_2^-) (A and B), hydrogen peroxide (H_2O_2) (C and D), malondialdehyde (MDA) (E and F), total soluble phenolics (TSP) (G and H), and lignin-thioglycolic acid (LTGA) derivatives (I and J) determined in the leaves of maize plants sprayed with distilled water (control), aminooxyacetic acid (AOA), and ethylene and non-inoculated (A, C, E, and G) or inoculated with Exserohilum turcicum (B, D, F, and H). For each evaluation time, treatments means followed by different letters and non-inoculated and inoculated plants, for each treatment, followed by an asterisk (*) are significantly different ($P \leq 0.05$) according to Tukey's test. Bars represent the standard error of the means. FW = fresh weight. DW=dry weight. n = 4.

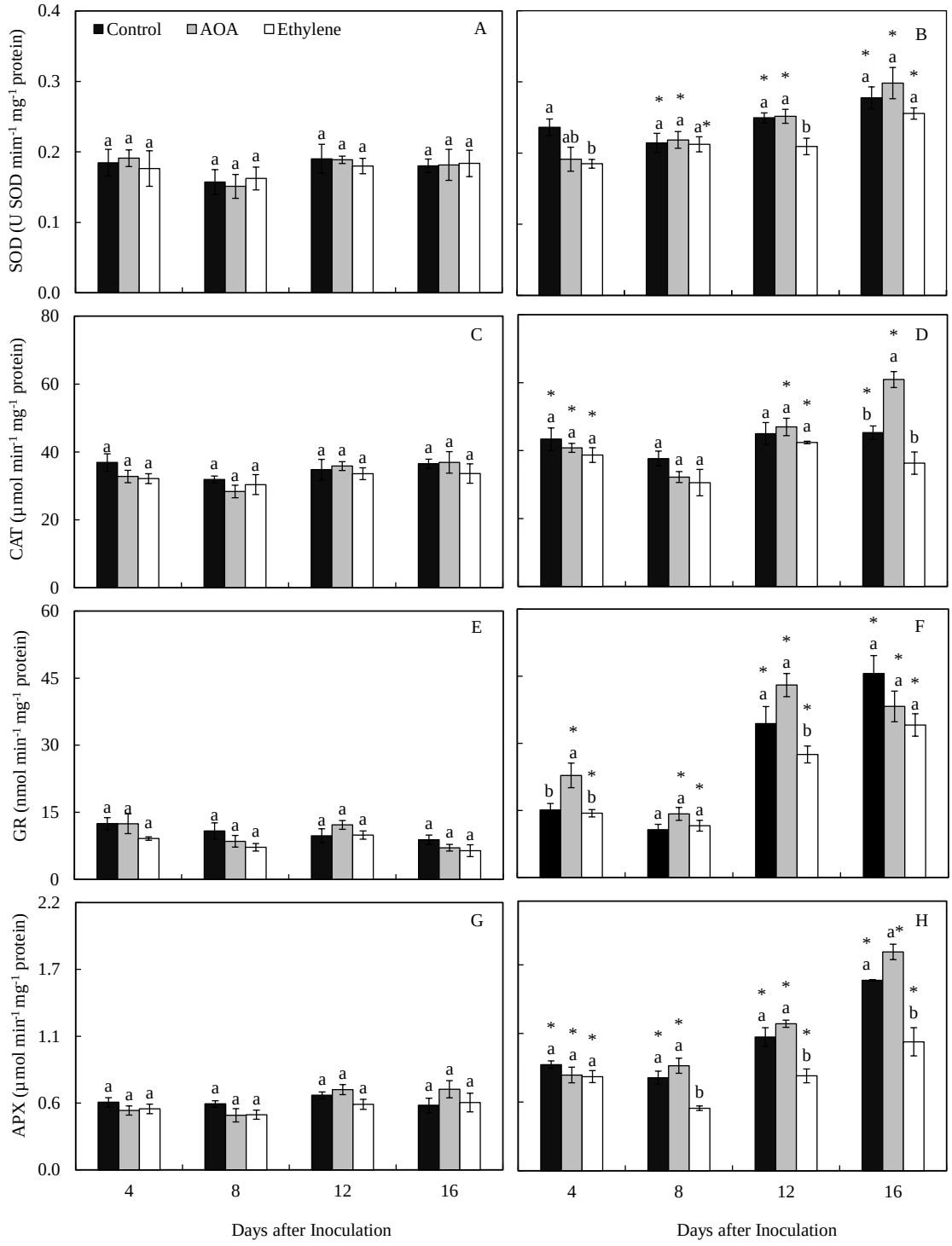

Figure 8. Activities of superoxide dismutase (SOD) (A and B), catalase (CAT) (C and D), glutathione reductase (GR) (E and F), and ascorbate peroxidase (APX) (G and H) determined in the leaves of maize plants sprayed with distilled water (control), aminooxyacetic acid (AOA), and ethylene and non-inoculated (A, C, E, and G) or inoculated with Exserohilum turcicum (B,

D, F, and H). For each evaluation time, treatments means followed by different letters and non-inoculated and inoculated plants, for each treatment, followed by an asterisk (*) are significantly different ($P \leq 0.05$) according to Tukey's test. Bars represent the standard error of the means. n = 4.

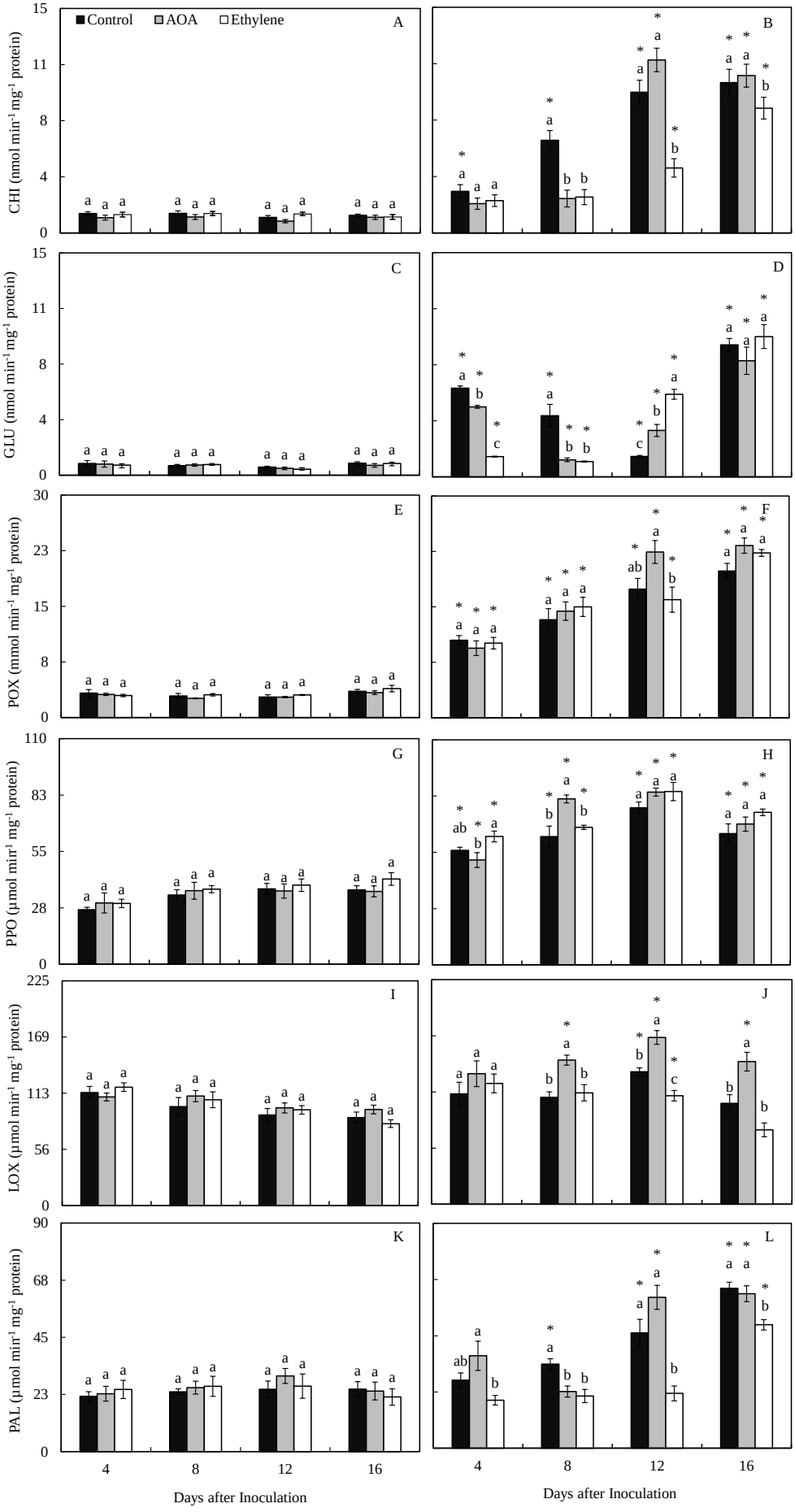
Control
AOA
Ethylene
A
B
C
D
E
F
G
H
I
J
K
L
CHI (nmol min-1 mg-1 protein)
GLU (nmol min-1 mg-1 protein)
POX (mmol min-1 mg-1 protein)
PPO (μmol min-1 mg-1 protein)
LOX (μmol min-1 mg-1 protein)
PAL (μmol min-1 mg-1 protein)
Days after Inoculation
Days after Inoculation

Figure 9. Activities of chitinase (CHI) (A and B), β-1,3-glucanase (GLU) (C and D), peroxidase (POX) (E and F), polyphenoloxidase (PPO) (G and H), lipoxygenase (LOX) (I and J), and phenylalanine ammonia-lyase (PAL) (K and L) determined in the leaves of maize plants sprayed with distilled water (control), aminooxyacetic acid (AOA), and ethylene and non-inoculated (A, C, E, G, I, and K) or inoculated (B, D, F, H, J, and L) with Exserohilum turcicum. For each evaluation time, treatments means followed by different letters and non-inoculated and inoculated plants, for each treatment, followed by an asterisk (*) are significantly different ($P \leq 0.05$) according to Tukey's test. Bars represent the standard error of the means. n = 4.

Chapter II

Physiological and Biochemical Aspects of Maize Resistance to Northern Leaf Blight Potentiated by Nickel

Abstract

The northern leaf blight (NLB), caused by Exserohilum turcicum, is one of the most devastating diseases in maize production worldwide. The nickel (Ni) supply to maize plants may be an interesting strategy for NLB management. This study investigated the effect of foliar Ni spray on the potentiation of maize resistance against E. turcicum infection by examining alterations in the photosynthesis (leaf gas exchange and chlorophyll a fluorescence parameters), foliar concentrations of micronutrients, production of ethylene and reactive oxygen species (ROS) as well as activities of both defense and antioxidant enzymes. Ni inhibited the mycelial growth of E. turcicum. High foliar concentrations of manganese and Ni were noticed for inoculated and +Ni plants, which exhibited decreases of 33 and 24%, respectively, for NLB severity at 12 and 16 days after inoculation. Photosynthesis was impaired as the NLB lesions expanded in the leaves of inoculated -Ni plants mainly due to biochemical limitations and destruction of pigments. Lower malondialdehyde and hydrogen peroxide concentrations were noticed for the leaves of inoculated +Ni plants. The activities of antioxidant enzymes were not affected by Ni, except for an increase in glutathione reductase activity for non-inoculated +Ni plants. The decrease in NLB severity gained by Ni supply was related to a direct effect of this micronutrient against E. turcicum infection associated with the potentiation of host defense responses mainly through great lipoxygenase and polyphenoloxidase activities as well as more production of phenolics and lignin.

Keywords: Exserohilum turcicum. Zea mays. Host defense enzymes. Leaf gas exchange. Mineral nutrition. Photosynthesis. Plant nutrition.

Resumo

A queima foliar, causada por Exserohilum turcicum, é uma das doenças mais devastadoras na produção de milho em todo o mundo. O fornecimento de níquel (Ni) para plantas de milho pode ser uma estratégia interessante para o manejo da queima foliar. Este estudo investigou o efeito da pulverização foliar de Ni na potenciação da resistência do milho contra a infecção por E. turcicum, examinando alterações na fotossíntese (trocas gasosas e parâmetros de fluorescência da clorofila a), concentrações foliares de micronutrientes, produção de etileno e espécies reativas de oxigênio (EROS), bem como atividades de enzimas de defesa e antioxidantes. O Ni inibiu o crescimento micelial de E. turcicum. Altas concentrações foliares de manganês e Ni foram observadas nas plantas inoculadas e +Ni, que exibiram reduções de 33 e 24%, respectivamente, para a severidade da queima foliar aos 12 e 16 dias após a inoculação. A fotossíntese foi prejudicada à medida que as lesões da queima foliar se expandiram nas folhas das plantas -Ni inoculadas, principalmente, devido a limitações bioquímicas e destruição de pigmentos. Baixas concentrações de malonaldeído e peróxido de hidrogênio foram observadas nas folhas das plantas inoculadas +Ni. As atividades das enzimas antioxidantes não foram afetadas pelo Ni, exceto por um aumento na atividade da glutationa redutase para plantas não inoculadas +Ni. A diminuição da severidade da queima foliar obtida pelo suprimento de Ni foi relacionada a um efeito direto deste micronutriente contra a infecção por E. turcicum associada à potencialização das respostas de defesa do hospedeiro principalmente através de grandes atividades da lipoxigenase e polifenoloxidase, bem como maior produção de fenólicos e lignina.

Palavras-chave: Exserohilum turcicum. Zea mays. Enzimas de defesa da planta. Fotossíntese. Nutrição de plantas. Trocas gasosas.

Introduction

Many diseases greatly impact maize production worldwide, and northern leaf blight (NLB), caused by the fungus Exserohilum turcicum (Passerini) Leonard and Suggs (syn. Setosphaeria turcica [Luttrell] Leonard and Suggs) (Leonard and Suggs 1974; Luttrell and Bacon 1977; Sivanesan 1984) stands out as one of the most important. The NLB is more devastating in maize growing regions with high humidity levels and moderate temperatures resulting in yield losses greater than 50% (Hennessy et al. 1990; Hooda et al. 2017; Zhang et al. 2020). Long elliptical, greyish-green, or tan lesions are noticed mainly in the older leaves of maize plants, and as they expand, the photosynthesis becomes seriously compromised (Kotze et al. 2019; Silveira et al. 2019). Also, monocerine, a non-host selective toxin released by E. turcicum at the infection sites, maximizes leaf tissues necrosis (Cuq et al. 1993).

The infection process of E. turcicum on maize leaves results in lower values of net assimilation rate, stomatal conductance to water vapor, transpiration rate, internal CO_2 concentration, maximum quantum yield of photosystem (PS) II, and effective quantum yield of PS II (Pant et al. 2001; Silveira et al. 2019). Silveira et al. (2019) reported that on maize leaves infected by E. turcicum, the quantum yield of regulated energy dissipation increased, the concentrations of hydrogen peroxide, malondialdehyde, and electrolyte leakage were higher, and the antioxidative system (great activities of ascorbate peroxidase, catalase, glutathione peroxidase, glutathione-S-transferase, glutathione reductase, peroxidase, and superoxide dismutase) was more robust. The β-1,3-glucanase activity also increased on maize leaves with NLB symptoms (Jondle et al. 1989).

Cultural practices such as crop rotation, use of resistant hybrids, and foliar spray of fungicides have been used by the growers to reduce the impact of NLB on yield (Nelson et al. 2018). Thus, more sustainable methods for NLB control need to be investigated to be integrated with the cultural strategies available, aiming to reduce the production costs. Mineral nutrition

stands out as an effective strategy to increase commercial crops' resistance against their most important diseases (Datnoff et al. 2007). Included in the list of essential nutrients to plants, nickel (Ni), applied to both soil and foliarly, increases plant growth, decreases urea concentration on plant tissues, and maximizes urease activity (Brown et al. 1987; Broadley et al. 2012). The importance of Ni to improve maize growth has been highlighted (Sabir et al. 2011). The involvement of Ni for optimum functioning of some enzymes (e.g., acetyl-CoA decarbonylase synthase, aci-reductone dioxygenase, carbon monoxide dehydrogenase, hydrogenase, methyl-coenzyme M reductase, Ni-dependent glyoxalase, NiFe-hydrogenase, methyleneurease, superoxide dismutase, and urease) explain its role in improving plant growth and development (Broadley et al. 2012).

Some crops supplied with Ni are less prone to be affected by some foliar diseases due to a direct effect of Ni against the pathogens or due to the antifungal property of ureases at the infection sites (Becker-Ritt et al. 2007; Wiebke-Strohm et al. 2012; Wood et al. 2012; Carlini and Ligabue-Braun 2016). The Ni has been reported to reduce the severities of diseases in the following host-pathogen interactions: milkwort jewel flower-Erysiphe polygoni, -Xanthomonas campestris pv. campestris and -Alternaria brassicicola (Boyd et al. 1994), pecan-Fusicladium effusum (Wood et al. 2004, 2012), soybean-Microsphaera diffusa (Barcelos et al. 2018), cucumber-cucumber mosaic virus (Derbalah and Elsharkawy 2019), and soybean-Phakopsora pachyrhizi (Einhardt et al. 2020a,b). According to Barcelos et al. (2018), high activities of enzymes of the antioxidative system (e.g., catalase, peroxidase, and superoxide dismutase) were associated with a reduction in powdery mildew severity on the leaves of soybean plants supplied with Ni due to damage to conidia and fungal mycelia on the leaf surface. Soybean plants supplied with Ni showed less Asian soybean rust severity, and consequently, the concentrations of malondialdehyde, anion superoxide, and hydrogen peroxide were lower while β-1,3-glucanase activity was high (Einhardt et al. 2020a,b). Moreover, the URE gene expression and

the defense-related genes PAL1.1, PAL2.1, CHI1B1, and *PR-1A* were up-regulated in the leaves of Ni-treated plants infected by P. pachyrhizi (Einhardt et al. 2020a,b). Moreover, the values of the parameters related to leaf gas exchange (net carbon assimilation, stomatal conductance to water vapor, and transpiration rate) and chlorophyll a fluorescence (maximum photochemical efficiency of photosystem II (PSII), effective yield of PSII, and electron transport rate) were higher, and the yield for other non-regulated losses and internal CO_2 concentration values were lower for soybean plants sprayed with Ni and infected by P. pachyrhizi (Einhardt et al. 2020b).

Ethylene negatively affects plants' resistance to pathogens due to its interaction with other plant hormones (Chen et al. 2009; De Vleesschauwer et al. 2010; Pantelides et al. 2013). It is plausible that a reduction in the levels of ethylene in plant tissues may be linked to the beneficial effect gained by Ni supply. The Ni had the potential to inhibit ethylene biosynthesis (Pennazio and Roggero 1992) and increase the post-harvest longevity of fruits and flowers (Smith and Woodburn 1983; Zheng et al. 2006; Kazemi et al. 2012).

Taking into consideration the role played by Ni on host defense responses against the infection by pathogens, the present study aimed to investigate its effect in the potentiation of maize resistance against infection by E. turcicum at both biochemical and physiological levels considering the scarcity of studies in the literature regarding this subject.

Material and Methods

Plant growth

Seeds of the maize cultivar P-1630 Hx (susceptible to E. turcicum) (Silveira et al. 2019) were sown in plastic pots containing 2 kg of a substrate (1:1:1 mixture of pine bark, peat, and expanded vermiculite) amended with 1.63 g of calcium phosphate monobasic. Plants were kept in a greenhouse (temperature of 25 ± 3°C (day) and 21 ± 2°C (night) and relative humidity of 75 ± 5%). Plants in each pot were fertilized, weekly, with 50 mL of a nutrient solution

composed, in mg/L, of 192 KCl, 104.52 K_2SO_4, 150.37 $MgSO_4$, 61 CH_4N_2O, 100 NH_4NO_3, 0.27 $(NH_4)_6MO_7O_{24}$, 1.61 H_3BO_3, 6.67 $ZnSO_4$, 1.74 $CuSO_4$, 4.10 $MnCl_2$, 4.08 $FeSO_4$, and 5.58 ethylenediaminetetraacetic acid (EDTA).

Inoculum production, plant inoculation, and treatments

Plants were inoculated with the monosporic UFV-DFP Et22 isolate of E. turcicum. The fungus was grown in Petri dishes containing lactose casein hydrolysate (LCH) medium (Malca and Ullstrup 1962) kept in an incubator (25°C and photoperiod of 16 hours light and 8 hours dark) for ten days. Plants were inoculated with a conidial suspension (1×10^4 conidia/ml) of E. turcicum at 20 days after emergence (plants with five fully expanded leaves) using a VL Airbrush atomizer (Paasche Airbrush Co., Chicago, IL). Gelatin (0.5% w/v) was added to the conidial suspension to aid conidia adhesion to the leaves. At eight days after inoculation, leaf fragments containing necrotic lesions were collected, disinfected in solutions of 70% (v/v) aqueous alcohol and 2% sodium hypochlorite (v/v), and transferred to Petri dishes (three-leaf fragments per dish) containing LCH medium. Petri dishes were transferred to an incubator (25°C and photoperiod of 16 hours of light and 8 hours of dark) for ten days. After this period, a total of 1 ml of sterile distilled water was added to each Petri dish, and fungal mycelia were carefully disrupted using a camel hair brush within a laminar flow chamber to induce fungal sporulation. After this procedure, Petri dishes were transferred to an incubator (25°C and photoperiod of 12 h with blacklight lamps emitting light near-ultraviolet (320-400 nm) and 12 h dark) for five days.

Plants with five fully expanded leaves were inoculated with a conidial suspension of E. turcicum as described above and kept in a growth chamber (temperature of 25 ± 2°C and relative humidity of 90 ± 5%) under dark for the first 12 h to allow conidia germination and fungal penetration. Thereafter, plants were transferred to a greenhouse (25 ± 2°C, the relative humidity

of 75 ± 5%, and natural photon flux density) for the experiments' duration. Plants were sprayed with a solution (7.5 mL per plant) of 0.41 g $NiSO_4.6H_2O$ L^{-1} (50 g Ni ha^{-1}) and 0.01% (v/v) Tween-20 at 72 h before inoculation with E. turcicum by using a VL Airbrush atomizer (Paasche Airbrush Co., Chicago, IL). Plants sprayed with water served as the control treatment.

Determination of Ni concentration in the substrate and foliar concentration of nutrients

Samples of the substrate used to grow the maize plants were collected before sowing, and Ni concentration was determined by flame atomic absorption spectrophotometry following the method 7000B (US EPA 2007). This Ni concentration in the substrate was 41.51 mg kg^{-1}. For determination of foliar nutrients concentration, leaves from plants used to evaluated NLB severity (16 dai) and also from non-inoculated plants were collected, washed in deionized water, and dried in a drying oven with forced ventilation. The leaf tissue was digested with a nitric-perchloric acid solution (Sarruge and Haag 1974). Foliar concentrations of copper (Cu), iron (Fe), manganese (Mn), nickel (Ni), and zinc (Zn) were determined by optical emission spectrometry with inductively coupled plasma (ICP-OES) (DV8300, PerkinElmer).

In vitro assays

The sensitivity of E. turcicum to Ni was evaluated in vitro using the concentrations of 0, 0.125, 0.25, 0.375, 0.5, and 1 g Ni L^{-1}. The nickel sulfate ($NiSO_4.6H_2O$ L^{-1}) was the Ni source. Melted lactose casein hydrolysate (MLCH) medium was amended with each Ni rate and then poured into Petri plates (20 mL per plate). Then, one plug of MLCH medium (10 mm in diameter) containing fungal mycelia obtained from the edge of a ten-day-old colony of E. turcicum was placed in the center of each Petri dish. The dishes were kept in a growth chamber (25°C and photoperiod of 16 hours of light and 8 hours of dark). The fungal colony in each Petri dish was measured to obtain its diameter in two orthogonal directions at 10 days using a digital caliper.

The surface area of the plug was subtracted from the total surface area measured on each Petri dish. The percent of mycelial growth inhibition was calculated as follows: 100 - [(mycelia surface area of each replication per treatment from the Ni rates/mycelia surface area of the medium non-amended with Ni) × 100] (Weems and Bradley 2017). A linear interpolation method was used to calculate the effective concentration (EC) to reduce fungal mycelia growth by 50% (EC_{50}) (Weems and Bradley 2017).

Assessment of NLB severity

The NLB severity was evaluated on the fifth fully expanded leaf, from basis to top, of each plant per replication of each treatment at 4, 8, 12, and 16 days after inoculation (dai). The leaves were scanned at 600 dpi resolution, and the images were processed using the QUANT software (Vale et al. 2003) to obtain the severity values. The area under the disease progress curve (AUDPC) was calculated using the trapezoidal integration of NLB progress curves over time, according to Shaner and Finney (1977).

Determination of ethylene (ET) concentration

The ET was measured on the fourth fully expanded leaf, from basis to top, of each plant per replication of each treatment at 4, 8, 12, and 16 dai. The leaves were weighed to obtain their fresh weight and placed in Erlenmeyer flasks hermetically sealed. After an incubation of 12 h, an air sample of 1 mL was taken from the flask headspace and injected into a gas chromatograph (Hewlett-Packard 5890, series II) following the procedures described by Silva et al. (2014).

Determination of the leaf gas exchange parameters

A portable open-system infrared gas analyzer (LI-6400XT, LI-COR, Lincoln, NE, USA) was used to obtain the values of net carbon assimilation rate (A), stomatal conductance to water

vapor (g_s), internal CO_2 concentration (C_i), and transpiration rate (E) on the fifth fully expanded leaf, from basis to top, of each plant per replication of each treatment at 4, 12, and 16 dai. Evaluations were performed from 10:00 to 12:00 a.m. under artificial and saturating photon irradiance (1200 µmol m^{-2} s^{-1}) and CO_2 concentration of ± 400 ppm.

Imaging of the Chlorophyll (Chl) a fluorescence

The images and fluorescence parameters of Chl a were obtained at 4, 8, 12, and 16 dai using an IMAGING-PAM fluorometer (Maxi version) and the Imaging Win software (Heinz Walz GmbH, Effeltrich, Germany). The images were obtained with a resolution of 640 × 480 pixels in the fifth fully expanded leaf, from basis to top, of each replication per treatment. The Chl a fluorescence emission transients were captured by a CCD (charge-coupled device) camera with a resolution of 640 × 480 pixels in a visible sample area of 24 × 32 mm on each leaf. The leaves were then exposed to a weak and modulated measuring beam (0.5 µmol m^{-2} s^{-1}, 100 µs, 1 Hz) to determine the initial fluorescence (F_0) when all the PSII reaction centers were open. Next, a saturating white light pulse of 2.400 µmol m^{-2} s^{-1} (10 Hz) was applied for 0.8 s to ensure maximum fluorescence emission (F_m) when all the PSII reaction centers are expected to be closed. The leaves were initially adapted to darkness for 30 min, after which they were carefully and individually fixed in support at a distance of 18.5 cm from the CCD camera. From these initial measurements, the maximum PSII photochemical efficiency of the dark-adapted leaves was estimated through the variable-to-maximum Chl fluorescence ratio as follows: $F_v/F_m = [(F_m - F_0)/F_m)]$. Following the calculations proposed by Kramer et al. (2004), the energy absorbed by the PSII for the following two yield components for dissipative processes was determined: the yield of photochemistry [(YII = F'_m - F/F'_m], the yield for dissipation by downregulation [$Y(NPQ) = (F_s/F'_m) - (F_s/F_m)$], and the yield for other non-photochemical (non-

regulated) losses [Y(NO) = F_s/F_m]. These parameters were calculated using the Imaging Win software (Kramer et al. 2004).

Determination of the concentration of photosynthetic pigments

Five leaf discs (8 mm in diameter) obtained from the fifth fully expanded leaf, from basis to top, of each plant per replication, were placed in glass vials with 5 ml of dimethylsulfoxide (DMSO), and the absorbances of the extracts were read at 480, 649, and 665 nm using DMSO as a blank after 24 h at 25°C (Wellburn 1994, Santos et al. 2008).

Biochemical assays

The fourth and fifth fully expanded leaves, from basis to top, of each plant per replication of each treatment were collected at 4, 8, 12, and 16 dai. Leaves were kept in liquid nitrogen during sampling and stored at -80°C thereafter.

Determination of superoxide anion radical (O_2^-) concentration

A total of 0.2 g of leaf tissue was ground into a fine powder with liquid nitrogen using a vibration ball mill and homogenized in 2 ml of a solution containing 100 mM sodium phosphate buffer (pH 7.2) and 1 mM sodium diethyldithiocarbamate (SDD). The homogenate was centrifuged at 22.000 g for 20 min at 4°C. After centrifugation, an aliquot of the supernatant was placed to react with a solution containing 100 mM sodium phosphate buffer (pH 7.2), 1 mM SDD, and 0.25 mM nitroblue tetrazolium (NBT). The O_2^- concentration was determined by subtracting the absorbance of the final product from the initial absorbance at 540 nm (Chaitanya and Naithani 1994).

Determination of hydrogen peroxide (H_2O_2) concentration

A total of 0.1 g of leaf tissue was ground into a fine powder with liquid nitrogen using a vibration ball mill and homogenized in 2 ml of 0.1% (w/v) of trichloroacetic acid (TCA). The homogenate was centrifuged at 12.000 g for 15 min at 4°C, and an aliquot of the supernatant reacted with a mixture containing 10 mM potassium phosphate buffer (pH 7.0) and potassium iodide solution and incubated for 5 min. Absorbance was determined at 390 nm. The H_2O_2 concentration was determined based on a standard curve made with known concentrations of H_2O_2 (Sergiev et al. 1997).

Determination of malondialdehyde (MDA) concentration

A total of 0.1 g of leaf tissue was ground into a fine powder with liquid nitrogen using a vibration ball mill and homogenized and homogenized in 2 ml of a solution of TCA 0.1% (w/v). The homogenate was centrifuged at 12.000 g for 15 min at 4°C. An aliquot of the supernatant was mixed with 0.75 ml of 0.5% thiobarbituric acid (TBA) solution (w/v) (prepared in 20% (w/v) TCA) and incubated in a water bath at 95°C for 60 min. Thereafter, the reaction was quenched in an ice bath following centrifugation at 10.000 g for 10 min. The specific absorbance of the supernatant was determined at 532 nm. Non-specific absorbance was measured at 600 nm and subtracted from the value of the specific absorbance. The extinction coefficient of 155 mM^{-1} cm^{-1} was used to calculate the MDA concentration (Hodges et al. 1999).

Determination of total soluble phenolics (TSP) and lignin-thioglycolic acid (LTGA) derivatives concentrations

A total of 0.1 g of leaf tissue was ground into a fine powder with liquid nitrogen using a vibration ball mill and homogenized in 1.5 ml of 80% (v/v) methanol solution. The crude extract

was shaken at 300 rpm at 25°C for 12 h, and the mixture was centrifuged at 13.000 g for 30 min. The TSP concentration was determined in the methanolic extract, and the pellet was kept at 20°C to determine the LTGA derivatives concentration, according to Fortunato et al. (2015).

Determination of antioxidant enzymes activities

A total of 0.2 g of leaf tissue was macerated in a vibration ball mill with liquid nitrogen to obtain a fine powder, which was homogenized in 2 ml of potassium phosphate buffer 100 mM (pH 6.8) containing 0.1 mM EDTA, 1 mM phenylmethyl-sulphonyl fluoride (PMSF), and 0.5% (w/v) polyvinylpolypyrrolidone (PVPP). The homogenate was centrifuged at 13.000 g for 15 min at 4°C, and the supernatant was divided into aliquots which were used as extracts for the determinations of superoxide dismutase (SOD, EC 1.15.1.1), catalase (CAT, EC 1.11.1.6), glutathione reductase (GR, EC 1.8.1.7), and ascorbate peroxidase (APX, EC 1.11.1.11) activities as previously described (Bermúdez-Cardona et al. 2015a, Tatagiba et al. 2015, Rios et al. 2017). Proteins concentration was measured using the Bradford assay with bovine serum albumin as a standard (Bradford 1976).

Determination of defense enzymes activities

A total of 0.2 g of leaf tissue was macerated in a vibration ball mill with liquid nitrogen to obtain a fine powder to determine the activities of chitinase (CHI) (EC 3.2.1.14), β-1,3-glucanase (GLU) (EC 3.2.1.39), peroxidase (POX) (EC 1.11.1.7), polyphenoloxidase (PPO), lipoxygenase (LOX) (EC 1.13.11.12), and phenylalanine ammonia-lyase (PAL) (EC 4.3.1.5). The fine powder was homogenized in 2 ml of a solution containing 50 mM potassium phosphate buffer (pH 6.8), 1 mM EDTA, 1 mM PMSF, and 0.5% (w/v) PVPP. The homogenate was centrifuged at 12.000 g for 15 min at 4 °C, and the supernatant was used to determine CHI, GLU, PAL, PPO, and LOX activities as previously described (Polanco et al. 2012; Fortunato

et al. 2015; Fagundes-Nacarath et al. 2018). Proteins concentration was measured as described above.

Experimental design and statistical analysis

A 2 × 2 factorial experiment, consisting of plants non-supplied or supplied with Ni (referred to as treatments (T) thereafter) and plant inoculation (PI) (non-inoculated and inoculated plants), was arranged in a completely randomized design with eight replications. Each replication corresponded to a plastic pot containing two plants. The experiment was repeated once. All parameters and variables evaluated were subjected to analysis of variance, and treatments means were compared by F test ($P \leq 0.05$). Data were analyzed using the Minitab software (version 18; Minitab Corporation).

Results

Analysis of variance

The factors foliar treatments (T) and plant inoculation (PI), as well as the T × PI interaction, were significant for most of the variables and parameters evaluated. The T × PI interaction was significant for Mn, Ni, and H_2O_2 concentrations as well as for SOD and GR activities (Table 1).

In vitro assay

Fungal mycelial growth was affected from the dose of 0.125 g Ni L^{-1} (Fig. 1). Fungal mycelial growth was significantly inhibited by 19, 36, 53, 63, and 90% for the Ni concentrations of 0.125, 0.25, 0.375, 0.5, and 1 g L^{-1}, respectively (Fig. 2A). The EC_{50} value was of 0.45 g Ni L^{-1} (Fig. 2B).

Foliar nutrients concentrations

The foliar spray of Ni to non-inoculated plants significantly increased the foliar Mn and Ni concentrations (Fig. 3A). The foliar Mn and Ni concentrations were of 16 and 533% higher, respectively, for +Ni plants compared to -Ni plants (Fig. 3A). For inoculated plants, foliar Ni concentration was 375% higher for +Ni plants compared to -Ni plants (Fig. 3B). There were significant increases for foliar concentrations of Cu (24%), Fe (23%), Mn (18%), and Zn (31%) for non-inoculated -Ni plants in comparison to their inoculated counterparts (Fig. 3A and B). For non-inoculated +Ni plants in comparison to their inoculated counterparts, there were significant increases only for foliar concentrations of Mn (41%) and Ni (81%) (Fig. 3A and B).

Disease severity

On the leaves of -Ni plants, the NLB progressed much faster in comparison to the leave of +Ni plants (Fig. 4A). The NLB severity for +Ni plants was significantly reduced by 33 and 24% at 12 and 16 dai, respectively, in comparison to -Ni plants (Fig. 4A). The AUDPC for +Ni plants was significantly reduced by 27% in comparison to -Ni plants (Fig. 4B).

ET production

In the leaves of non-inoculated plants, ET was not detected regardless of Ni treatments, while its production occurred from 8 dai in the leaves of inoculated plants (Fig. 5A and B). The ET production was significantly reduced by 47% for +Ni plants in comparison to -Ni plants at 16 dai (Fig. 5B). The ET production was significantly higher for inoculated plants in comparison to non-inoculated plants regardless of Ni treatments from 8 to 16 dai (Fig. 5A and B).

Leaf gas exchange parameters

For non-inoculated plants, there was no significant difference for A, g_s, C_i, and E regardless of Ni treatments and evaluation time (Fig. 6A, C, E, and G), except for C_i at 16 dai in which +Ni plants showed a reduction of 11% in comparison to -Ni plants (Fig. 6E). For inoculated plants, there was no significant difference between -Ni and +Ni plants for none of the leaf gas exchange parameters evaluated (Fig. 6B, D, F, and H), except for E at 12 dai in which there was a significant decrease of 23% for +Ni plants in comparison to -Ni plants (Fig. 6H). As the NLB developed during the evaluation time, the values of A, g_s, and E decreased. The A values were significantly lower by 22 and 21% at 4 dai, by 18 and 11% at 8 dai, by 14 and 24% at 12 dai, and by 58 and 44% at 16 dai, respectively, for -Ni and +Ni inoculated plants in comparison to their non-inoculated counterparts (Fig. 6A and B). For inoculated -Ni plants, there were significant decreases for g_s of 16% at 8 dai, of 43% at 12 dai, and of 56% at 16 dai in comparison to their non-inoculated counterparts (Fig. 6C and D). For inoculated +Ni plants, there were significant decreases for g_s of 42% at 12 dai, and of 56% at 16 dai in comparison to their non-inoculated counterparts (Fig. 6C and D). The C_i significantly increased by 18 and 26% at 8 dai, by 47 and 47% at 12 dai, and by 21 and 22% at 16 dai, respectively, for -Ni and +Ni inoculated plants in comparison to their non-inoculated counterparts (Fig. 6E and F). For inoculated -Ni plants, E values were significantly lower by 3% at 8 dai and by 55 at 16 dai in comparison to their non-inoculated counterparts (Fig. 6G and H). However, for inoculated +Ni plants, E values were significantly lower by 33 and 50%, respectively, at 12 and 16 dai in comparison to their non-inoculated counterparts (Fig. 6G and H).

Chl a fluorescence parameters

Based on the images of Chl a fluorescence parameters Y(II), Y(NPQ), Y(NO), and F_v/F_m from the leaves of non-inoculated plants, there was no visible difference among the treatments (Fig.

7). The leaves of inoculated plants showed alterations in the Chl a fluorescence parameters with progressive loss of their photosynthetic capacity as indicated by the dark areas in the images (Fig. 7). The Y(II), Y(NPQ), Y(NO), and F_v/F_m were not affected by Ni treatments regardless of plant inoculation during the time-course evaluated (Fig. 8A-H), except for Y(NO) at 12 dai in which there was a significant decrease of 12% for +Ni plants in comparison to -Ni plants (Fig. 8F). For inoculated -Ni plants, the values were significantly lower for Y(II) by 5, 15, and 33% and for F_v/F_m by 3, 11, and 11% at 8, 12, and 16 dai, respectively, in comparison to non-inoculated -Ni plants (Fig. 8A-B and G-H). For inoculated +Ni plants, the values for Y(II) (18, and 30% at 12, and 16 dai) and F_v/F_m (2, 12, and 10% at 8, 12, and 16 dai) were significantly lower in comparison to non-inoculated ones (Fig. 8A-B and G-H). On the other hand, for inoculated +Ni plants, there was a significant increase for Y(NPQ) by 22% at 12 dai in comparison to non-inoculated ones (Fig. 8C and D). For Y(NO) of inoculated -Ni plants, there were significant increases of 16 and 27% at 8 and 16 dai in comparison to non-inoculated -Ni plants (Fig. 8E). The inoculated +Ni plants showed a significant increase of 18% for Y(NO) only at 16 dai compared to non-inoculated +Ni plants (Fig. 8F).

Photosynthetic pigments

The concentrations of Chl a, Chl b, and Chl a+b followed the same trend among the treatments. In comparison to inoculated plants, the concentrations of Chl a (49-71% and 39-54%, respectively, for -Ni and +Ni plants), Chl b (61-77% and 66-63%, respectively, for -Ni and +Ni plants), and Chl a+b (53-72% and 45-55%, respectively, for -Ni and +Ni plants) significantly decreased in comparison to their non-inoculated counterparts at 12 and 16 dai (Fig. 9A-D and G-H). For non-inoculated -Ni plants, the concentration of carotenoids significantly increased by 16, 21, and 48%, respectively, at 8, 12, and 16 dai compared to inoculated -Ni plants (Fig. 9E and F). For non-inoculated +Ni plants, the concentration of carotenoids significantly

increased by 13, 16, and 28%, respectively, at 8, 12, and 16 dai compared to inoculated +Ni plants (Fig. 9E and F). For inoculated plants, the concentrations of Chl a, Chl b, and Chl a+b were influenced by the Ni treatments (Fig. 9B, D, F, and H). There were significant increases for the concentrations of Chl a (9, 15, and 63% at 4, 12, and 16 dai, respectively), Chl b (53% at 16 dai), and Chl a+b (14, 15, and 61% at 4, 12, and 16 dai, respectively) for +Ni plants in comparison to -Ni plants (Fig. 9B, D, and H).

Concentrations of O_2^-, H_2O_2, MDA, TSP, and LTGA derivatives

For non-inoculated plants, there was no significant difference for the O_2^-, H_2O_2, MDA, and LTGA concentrations between -Ni and +Ni treatments regardless of the evaluation time (Fig. 10A, C, E, and I), except for TSP at 8 dai in which +Ni plants showed an increase of 39% in comparison to -Ni plants (Fig. 10G). The deleterious effect of E. turcicum infection was confirmed by significant increases in the concentrations of O_2^-, H_2O_2, and MDA (Fig. 10B, D, and F). For inoculated +Ni plants, there were significant increases in the concentrations of O_2^- (12% at 8dai), TSP (36% at 8 dai), and LTGA derivatives (23% at 8 dai) and significant decreases in the concentrations of H_2O_2 (36 and 11% at 8 and 16 dai, respectively), MDA (30 and 18% at 8 and 16 dai, respectively), and TSP (13% at 12 dai) in comparison to inoculated -Ni plants (Fig. 8D, F, and J). The concentration of O_2^- significantly increased by 48, 52, and 39%, respectively, at 8, 12, and 16 dai for inoculated -Ni plants in comparison to non-inoculated -Ni plants (Fig. 10A and B). For inoculated +Ni plants, the concentration of O_2^- significantly increased by 46, 52, and 35%, respectively, at 8, 12, and 16 dai in comparison to non-inoculated +Ni plants (Fig. 10A and B). The H_2O_2 concentration significantly increased by 71, 172, 86, and 209%, respectively, at 4, 8, 12, and 16 dai for inoculated -Ni plants in comparison to non-inoculated -Ni plants (Fig. 10C and D). For inoculated +Ni plants, the H_2O_2 concentration significantly increased by 56, 74, 54, and 142%, respectively, 4, 8, 12, and 16 dai in comparison

to inoculated +Ni plants (Fig. 10C and D). For MDA concentration, there were significant increases for inoculated -Ni plants at 8 (34%), 12 (69%), and 16 dai (97%) in comparison to non-inoculated -Ni plants (Fig. 10E and F). The MDA concentration significantly increased by 65 and 48%, respectively, at 12 and 16 dai for inoculated +Ni plants in comparison to inoculated +Ni plants (Fig. 10E and F). The TSP concentration significantly increased by 87, 108, 154%, respectively, at 8, 12, and 16 dai for inoculated -Ni plants compared to non-inoculated -Ni plants (Fig. 10G and H). For inoculated +Ni plants, the TSP concentration significantly increased by 83, 98, and 124%, respectively, at 8, 12, 16 dai when compared to non-inoculated +Ni plants (Fig. 10G and H). The LTGA derivatives concentration significantly increased by 44 and 46%, respectively, at 12 and 16 dai for inoculated -Ni plants in comparison to non-inoculated -Ni plants (Fig. 10I and J). Significant increases of 51, 47, and 70%, respectively, at 8, 12, 16 dai for the LTGA derivatives concentration occurred for inoculated +Ni plants in comparison to non-inoculated +Ni plants (Fig. 10I and J).

Activities of antioxidant enzymes

Activities of SOD, CAT, GR, and APX for non-inoculated plants were not influenced by Ni treatments regardless of the sampling time, except for GR. At 8 and 16 dai for non-inoculated -Ni plants, GR activity significantly increased by 60 and 70% in comparison to inoculated -Ni plants (Fig. 11E). The activities of antioxidant enzymes significantly increased in response to E. turcicum infection regardless of Ni treatments and evaluation time (Fig. 11B, D, F, and H). Inoculated +Ni plants displayed significant decreases for GR activity by 37 and 40% at 4 and 12 dai, respectively, in comparison to inoculated -Ni plants (Fig. 11F). For SOD activity, there were significant increases for inoculated -Ni plants at 4 (28%), 8 (28%), 12 (50%), and 16 dai (40%) when compared to non-inoculated -Ni plants (Fig. 11A and B). For inoculated +Ni plants, the SOD activity significantly increased by 19 and 29%, respectively, at 12 and 16 dai

in comparison to non-inoculated +Ni plants (Fig. 11A and B). The CAT activity significantly increased by 48, 21, 60, and 35%, respectively, at 4, 8, 12, and 16 dai for inoculated -Ni plants in comparison to non-inoculated -Ni plants (Fig. 11C and D). For inoculated +Ni plants, CAT activity significantly increased by 21, 47, 82, and 67%, respectively, at 4, 8, 12, and 16 dai in comparison to non-inoculated +Ni plants (Fig. 11C and D). The GR activity was significantly higher by 111, 355, 556, 428%, respectively, at 4, 8, 12, and 16 dai for inoculated -Ni plants in comparison to non-inoculated -Ni plants (Fig. 11E and F). For inoculated +Ni plants, GR activity significantly increased by 46, 138, 216, and 215%, respectively, at 4, 8, 12, and 16 in comparison to non-inoculated +Ni plants (Fig. 11E and F). The APX activity significantly increased by 55, 83, and 68%, respectively, at 4, 12, and 16 dai for inoculated -Ni plants compared to non-inoculated -Ni plants (Fig. 11G and H). For inoculated +Ni plants, APX activity significantly increased by 53, 103, and 63%, respectively, at 8, 12, and 16 dai in comparison to non-inoculated +Ni plants (Fig. 11G and H).

Activities of defense enzymes

There was a significant difference between -Ni and +Ni treatments only for POX, PPO, LOX, and PAL activities (Fig. 12E, H, I, J, and L). For non-inoculated +Ni plants, the activities of POX (58% at 8 dai) (Fig. 12E) and LOX (49, 47, and 29%, respectively, at 8, 12, and 16 dai) (Fig. 12I) significantly increased in comparison to non-inoculated -Ni plants. The PPO (27% at 8 dai) (Fig. 12H) and LOX (86, 35, and 48%, respectively, at 4, 8, and 16 dai) (Fig. 12J) activities significantly increased; however, the PAL activity significantly decreased by 23% at 4 dai (Fig. 12L) for inoculated +Ni plants when compared to inoculated -Ni plants. For inoculated -Ni plants, CHI activity was significantly higher by 42, 141, and 148%, respectively, at 8, 12, and 16 dai in comparison to non-inoculated -Ni plants (Fig. 12A and B). For inoculated +Ni plants, CHI activity significantly increased by 33, 32, 69, and 117%, respectively, at 4, 8,

12, and 16 dai in comparison to non-inoculated +Ni plants (Fig. 12A and B). There GLU (224, 750, 1033, and 1135%), POX (73, 541, 1210, and 1216%), PPO (35, 46, 125, and 145%), and PAL (132, 119, 244, and 722%) activities significantly increased at 4, 8, 12, and 16 dai for inoculated -Ni plants in comparison to non-inoculated -Ni plants (Fig. 12C-H, and K-L). For inoculated +Ni plants, GLU (225, 549, 744, and 1134%), POX (130, 313, 855, and 1039%), PPO (74, 50, 128, and 149%), and PAL (139, 82, 283, and 788%) activities significantly increased at 4, 8, 12, and 16 dai in comparison to non-inoculated +Ni plants (Fig. 12C-H and K-L). For inoculated -Ni plants, LOX activity significantly increased by 34, 151, and 134%, respectively, at 8, 12, and 16 dai in comparison to non-inoculated -Ni plants (Fig. 12I and J). The LOX activity significantly increased by 43, 21, 83, and 168%, respectively, at 4, 8, 12, and 16 dai for inoculated +Ni plants compared to non-inoculated +Ni plants (Fig. 12I and J).

Discussion

Most of the studies related to Ni have been conducted by growing the plants in either soil or nutritive solution containing this micronutrient and in the context of problems related to its toxicity (Hussain et al. 2013; Shahbaz et al. 2018; Freitas et al. 2019; Amjad et al. 2020; Tipu et al. 2020). Interestingly, the foliar application of Ni provides an interesting alternative for the control of many foliar fungal diseases in commercial crops (Wood et al. 2012; Barcelos et al. 2018; Einhardt et al. 2020a,b), and the present study sheds light on the physiological and biochemical aspects of Ni in increasing the resistance of maize plants against NLB.

The mycelia of E. turcicum was inhibited in the in vitro assay by the same Ni concentration used to spray the maize plants. Sharma et al. (2017) reported a decrease in mycelial growth of Colletotrichum gloeosporioides, Dematophora necatrix, and Fusarium oxysporum with the use of Ni nanoparticles. Wiebke-Strohm et al. (2012) suggested that urease, a Ni-dependent metalloenzyme, may indirectly or directly inhibit fungal growth by interfering

with the osmotic balance of mycelia. At the scanning electron microscopy level, it was noticed that mycelia of Penicillium herguei treated with urease obtained from jack bean and soybean seeds caused hyphae plasmolysis and injuries in their cell wall (Becker-Ritt et al. 2007). Moreover, urease from soybean seeds suppressed mycelial growth and/or inhibited conidia germination of Curvularia lunata, Fusarium solani, P. herguei, and three species of Trichoderma (Becker-Ritt et al. 2007). According to Barcelos et al. (2018), urease is regulated by Ni and plays a detrimental role in soybean resistance against powdery mildew by stimulating the antioxidative metabolism of the plants.

The nutritional status of plants affects the infection processes of many of their pathogens (Walters and Bingham 2007). In the plant's tissues, a synergistic relationship of Ni with Cu, Fe, Mn, and Zn occurs (Mizuno et al. 2005). In the present study, the Ni spray resulted in an increase in the foliar concentrations of Mn and Ni for non-inoculated plants and only Ni concentration for inoculated plants. The foliar supply of Ni to pecan trees and barley plants increased the foliar Mn concentration (Ojeda-Barrios et al. 2016; Kumar et al. 2018). High Ni concentration in the leaf tissues of pecan trees and soybean plants was associated with high urease activity (Ojeda-Barrios et al. 2016; Reis et al. 2017). In pecan trees, for instance, urease activity was closely linked to foliar Ni concentration and became a good physiological indicator of the trees' nutritional state (Ojeda-Barrios et al. 2016).

In the present study, NLB symptoms were dramatically reduced in maize plants sprayed with Ni. For the milkwort jewel flower-E. polygoni, -X. campestris pv. campestris and -A. brassicicola, pecan-F. effusum, cucumber-cucumber mosaic virus, and soybean-M. diffusa and -P. pachyrhizi (Boyd et al. 1994; Wood et al. 2004, 2012; Barcelos et al. 2018; Derbalah and Elsharkawy 2019; Einhardt et al. 2020a,b) interactions, the severities of the diseases caused by these pathogens were reduced due to foliar Ni supply. Based on the study carried out by Wiebke-Strohm et al. (2012), the non-expression of the GmEu4 gene coding for a ubiquitous

urease increased the susceptibility of soybean plants against the infection by P. herguei, Phomopsis sp., P. pachyrhizi, and Rhizoctonia solani.

During the infection process of E. turcicum in maize leaves, genes related to ET biosynthesis were expressed (Shi et al. 2018). The negative effect of ET in the resistance of plants against pathogens can be suppressed by Ni due to the inhibition of the enzymatic conversion of 1-aminocyclopropane-1-carboxylic acid (ACC) to ET in the tissues of many plant species (Yang and Hoffman 1984; Pennazio and Roggero 1992; Pantelides et al. 2013). Take this into consideration, the increase of NLB severity for maize plants non-sprayed with Ni can be linked to a great ET production in the leaf tissues.

As the necrotic lesions of NLB expand in maize plants' leaves, there is a decrease in the concentration of photosynthetic pigments and alterations in the values of the leaf gas exchange and Chl a fluorescence parameters (Cuq et al. 1993; Silveira et al. 2019). The values of A, g_s, E, and C_i measured in the leaves of maize plants infected by E. turcicum were lower, starting at 8 dai. The A values, for instance, were lower during the all-time course evaluated, but notably at advanced stages of E. turcicum infection. For some host-pathogen interactions such as rice-Monographella albescens and -Pyricularia oryzae as well as maize-Stenocarpella macrospora and -E. turcicum, fungi infection negatively impacted the values of A, g_s, E, and C_i (Bermúdez-Cardona et al. 2015b; Silveira et al. 2019; Pereira et al. 2020; Dias et al. 2020). In the infected maize leaves, regardless of Ni spray, lower A values were linked to higher and lower C_i and g_s values, respectively, which negatively impacted CO_2 fixation due to stomata closure. In rice leaves with leaf scald lesions, lower A values were associated with roughly proportional decreases in CO_2 diffusion (lower g_s and g_m), impaired photochemistry (lower ETR and J_{max}), and carboxylation efficiency (lower V_{cmax}) (Pereira et al. 2020).

Identifying the photosynthetic limitations imposed on plants is of pivotal importance to better understand their physiology's functionality in response to infection by pathogens.

Accordingly, Chl a fluorescence imaging is a powerful tool to mine the performance of photosynthesis at a cellular, leaf, and whole-plant scale to identify the possible changes at the asymptotic phase of specific stress imposed on the plants (Pérez-Bueno et al. 2019). The F_v/F_m parameter, representing the maximum quantum yield of PSII photochemistry, has been used as a physiological indicator of plant stress (Sharma et al. 2015). Silveira et al. (2019) reported decreases in the F_v/F_m values in maize leaves infected by E. turcicum, starting at 8 dai. Consistent with these authors' findings, in the present study, the F_v/F_m and Y(II) values decreased while the values of Y(NO) increased in the infected leaves of maize plants no sprayed with Ni. By contrast, for Ni-sprayed plants, lower and higher Y(II) and Y(NO) values, respectively, were noticed at the advanced stage of E. turcicum infection. The decrease in F_v/F_m and PSII efficiency demonstrated that the infection by E. turcicum disturbed the photoactivation of PSII that is a clear sign of photoinhibition. According to Yang et al. (2018), under severe stress, tobacco plants infected by Alternaria alternata were affected in the distribution pathway of PSII excitation energy, and the light was dissipated through non-photochemical processes. Chlorophylls are involved in light absorption during photosynthesis (Qiu et al. 2019). The concentration of photosynthetic pigments decreased in the maize leaves infected by E. turcicum and corroborate with the reports for some pathogens infecting maize such as S. macrospora (Bermúdez-Cardona et al. 2015b), Ustilago maydis (Kretschmer et al. 2017), E. turcicum (Silveira et al. 2019), and maize dwarf mosaic virus (Ludmerszki et al. 2015).

As the E. turcicum changes from its biotrophic to a necrotrophic lifestyle with an abundant release of non-host selective toxins and hydrolytic enzymes, there is a rise in the production of reactive oxygen species (ROS) such as H_2O_2 and O_2^- (Kotze et al. 2019; Cuq et al. 1993; Human et al. 2020). High H_2O_2 and O_2^- concentrations resulted in serious perturbations in the cellular networks in the infected maize leaves of plants no sprayed with Ni. By contrast, lower NBL severity in the leaves of Ni-sprayed plants contributed to lower

concentrations of H_2O_2 and MDA. As the levels of free radicals and ROS increase in the leaf tissues of plants, direct damage to lipids, destabilization of cell wall membrane integrity, and functionality and ion balance in the cytoplasm are noticed (de Dios Alché 2019). An increase in MDA concentration and loss of cell membrane integrity has been reported in the maize-E. turcicum (Silveira et al. 2019) and -Fusarium verticillioides (Cacique et al. 2020), wheat-P. oryzae (Aucique-Pérez et al. 2020), and soybean-P. pachyrhizi (Einhardt et al. 2020a,b) interactions. Soybean plants sprayed with Ni showed lower concentrations of MDA, H_2O_2, and O_2^- in response to infection by P. pachyrhizi (Einhardt et al. 2020b).

In the present study, high concentrations of TSP and LTGA derivatives in the leaves of maize plants sprayed with Ni contributed to reducing the NLB symptoms. The lignification of plant tissues helps to limit the colonization by pathogens and the diffusion of their non-host selective toxins and hydrolytic enzymes into plant cells, as well as the use of host' water and nutrients for their nutrition (Pérez et al. 2020; Yadav et al. 2020) besides the fact that fungal mycelia can be impaired when absorbing lignin polymers that interact with chitin, cellulose, and hydroxyproline (Pérez et al. 2020). According to Einhardt et al. (2020a), a high concentration of LTGA derivatives in the leaves of soybean supplied with Ni was of great importance to reduce Asian soybean rust severity.

A rise in the ROS concentration during the infection process of E. turcicum in the maize leaves was maintained and linked to a more robust antioxidative system. The non-enzymatic (e.g., low molecular mass antioxidants such as ascorbic acid (AsA), flavonoids, and glutathione) and enzymatic (e.g., CAT, APX, and SOD) antioxidant systems mounted by plants work synergistically to scavenge the ROS (Huang et al. 2019). In the present study, GR activity was high for non-inoculated +Ni plants, but the contrary was noticed for inoculated +Ni plants. A balance in the biosynthesis, transport, and degradation of glutathione to alleviate the oxidative stress facing by plants is of great importance since GSH, a key molecule in the cellular

defense against oxidative damage caused by ROS is continuously oxidized to GSSG (oxidized glutathione) and then regenerated by GR (Fabiano et al. 2015). It is known that Ni may activate an isoform of glyoxalase I that is involved in the degradation of methylglyoxal (MG) produced by stressed plants, and the GSH is consumed and regenerated in the process of detoxification of MG (Kaur et al. 2013; Mustafiz et al. 2014; Turra et al. 2015). High APX, CAT, GR, and SOD activities in the leaves of maize plants infected by E. turcicum corroborate with the findings of Silveira et al. (2019) and Shi et al. (2018) for the same host-pathogen interaction investigated in the present study.

Plants are prone to defend themselves from the infection of pathogens by activating several biochemical mechanisms of defense (Jain and Khurana 2018). In the present study, upon E. turcicum infection, the activities of several related-defense enzymes such as CHI, GLU, LOX, PAL, POX, and PPO increased in the leaves of maize plants. For infected maize plants sprayed with Ni, high PPO and LOX activities contributed to reducing NLB symptoms. On the other hand, for non-inoculated plants sprayed with Ni, POX activity was high. Einhardt et al. (2020a) reported high POX activity for non-inoculated soybean plants sprayed with Ni. The increased activities of POX and PPO maximize intense oxidation of polyphenols in the infected leaf tissues and produce a biochemical barrier to delay pathogen colonization besides raising the production of some metabolites such as phenols, phytoalexins, and lignin (Patel et al. 2020). Various signaling molecules in plants, such as the oxylipins, are synthesized by LOX, particularly the C6-volatile compounds and jasmonates (Viswanath et al. 2020). The LOX gene was expressed in the leaves of maize plants infected by Cochliobolus carbonum (Park et al. 2010). According to Maschietto et al. (2015), maize resistance against the infection by F. verticillioides is dependent on an earlier activation of LOX genes and those involved in jasmonic acid biosynthesis. Some studies highlighted the importance of LOX expression and LOX activity for the resistance of maize against the infection by F. verticillioides (Maschietto et al.

2015), Peronosclerospora sorghi, Phaeosphaeria maydis, and Sclerophthora macrospora (Kim et al. 2020), rice by Bipolaris oryzae (Debona et al. 2018), finger millet by Magnoporthe grisea (Patil et al. 2020), and wheat by Fusarium poae (Tan et al. 2020).

In conclusion, based on the present study results, the foliar application of Ni played a positive role in the resistance of maize plants against the infection by E. turcicum. As the NBL lesions expanded, the concentration of ROS raised and impaired photosynthesis mainly through biochemical limitations and destruction of pigments. In the leaves of Ni-sprayed plants, the infection by E. turcicum was affected by either a direct effect of this micronutrient against the fungus or indirectly through the potentiation of host defense responses such as higher LOX and PPO activities as well as great production of TSP and lignin.

References

Amjad M, Raza H, Murtaza B, Abbas G, Imran M, Shahid M, Naeem MA, Zakir A, Iqbal MM (2020) Nickel toxicity induced changes in nutrient dynamics and antioxidant profiling in two maize (Zea mays L.) hybrids. Plants 9:5

Aucique-Pérez CE, Resende RS, Martins AO, Silveira PR, Cavalcanti JHF, Vieira NM, Fernie AR, Araújo WL, DaMatta FM, Rodrigues, FA (2020) How do wheat plants cope with Pyricularia oryzae infection? A physiological and metabolic approach. Planta 252:1–17

Barcelos JP, Reis HP, Godoy CV, Gratão PL, Furlani Junior E, Putti FF, Campos M, Reis AR (2018) Impact of foliar nickel application on urease activity, antioxidant metabolism and control of powdery mildew (Microsphaera diffusa) in soybean plants. Plant Pathology 67:1502–1513

Becker-Ritt AB, Martinelli AHS, Mitidieri S, Feder V, Wassermann GE, Santi L, Vainstein MH, Oliveira JTA, Fiuza LM, Pasquali G, Carlini CR (2007) Antifungal activity of plant and bacterial ureases. Toxicon 50:971–983

Bermúdez-Cardona MB, Bispo WMS, Rodrigues FA (2015a) Physiological and biochemical alterations on maize leaves infected by Stenocarpella macrospora. Acta Physiologiae Plantarum 37:158

Bermúdez-Cardona MB, Wordell Filho JA, Rodrigues FA (2015b) Leaf gas exchange and chlorophyll a fluorescence in maize leaves infected with Stenocarpella macrospora. Phytopathology 105:26–34

Boyd RS, Shaw JJ, Martens SN (1994) Nickel hyperaccumulation defends Streptanthus polygaloides (Brassicaceae) against pathogens. American Journal of Botany 81:294–300

Bradford MM (1976) A rapid and sensitive method for the quantitation of microgram quantities of protein utilizing the principle of protein-dye binding. Analytical Biochemistry 72:248–254

Broadley M, Brown P, Cakmak I, Rengel Z, Zhao F (2012) Function of nutrients: micronutrients. In P. Maschner (Ed.). Mineral Nutrition of Higher Plants. 3rd Ed. Elsevier, London. pp. 191–248

Brown PH, Welch RM, Cary EE (1987) Nickel: a micronutrient essential for higher plants. Plant Physiology 85:801–803

Cacique IS, Pinto LF, Aucique-Pérez CE, Wordell Filho JA, Rodrigues FA (2020) Physiological and biochemical insights into the basal level of resistance of two maize hybrids in response to Fusarium verticillioides infection. Plant Physiology and Biochemistry 152:194–210

Carlini CR, Ligabue-Braun R (2016) Ureases as multifunctional toxic proteins: a review. Toxicon 110:90–109

Chaitanya KSK, Naithani SC (1994) Role of superoxide, lipid peroxidation and superoxide dismutase in membrane perturbation during loss of viability in seeds of Shorea robusta Gaertn.f. New Phytologist 126:623–627

Chen H, Xue L, Chintamanani S, Germain H, Lin H, Cui H, Cai R, Zuo J, Tang X, Li X, Guo H, Zhou JM (2009) ETHYLENE INSENSITIVE3 and ETHYLENE INSENSITIVE3-LIKE1 repress SALICYLIC ACID INDUCTION DEFICIENT2 expression to negatively regulate plant innate immunity in Arabidopsis. Plant Cell 21:2527–2540

Cuq F, Petitprez M, Herrmann-Gorline S, Klaebe A, Rossignol M (1993) Monocerin in Exserohilum turcicum isolates from maize and a study of its phytotoxicity. Phytochemistry 34:1265–1270

Datnoff LE, Elmer WH, Huber DM (Eds.) (2007) Mineral Nutrition and Plant Disease. The American Phytopathological Society, Saint Paul

de Dios Alché J (2019) A concise appraisal of lipid oxidation and lipoxidation in higher plants. Redox Biology 23:101136

De Vleesschauwer D, Yang Y, Cruz CV, Höfte M (2010) Abscisic acid-induced resistance against the brown spot pathogen Cochliobolus miyabeanus in rice involves MAP kinase-mediated repression of ethylene signaling. Plant Physiology 152:2036–2052

Debona D, Fortunato AA, Araújo L, Rodrigues ALC, Rodrigues FA (2018) Rice defense responses to Bipolaris oryzae mediated by a strobilurin fungicide. Tropical Plant Pathology 43:389–401

Derbalah ASH, Elsharkawy MM (2019) A new strategy to control Cucumber mosaic virus using fabricated NiO-nanostructures. Journal of Biotechnology 306:134–141

Dias CS, Rios JA, Einhardt AM, Chaves JAA, Rodrigues FA (2020) Effect of glutamate on Pyricularia oryzae infection of rice monitored by changes in photosynthetic parameters and antioxidant metabolism. Physiologia Plantarum 169:179–193

Einhardt AM, Ferreira S, Hawerroth C, Valadares SV, Rodrigues FA (2020a) Nickel potentiates soybean resistance against infection by Phakopsora pachyrhizi. Plant Pathology 69:849–859

Einhardt AM, Ferreira S, Souza GM, Mochko AC, Rodrigues FA (2020b) Cellular oxidative damage and impairment on the photosynthetic apparatus caused by Asian soybean rust on soybeans are alleviated by nickel. Acta Physiologiae Plantarum 42:1–13

Fabiano C, Tezotto T, Favarin JL, Polacco JC, Mazzafera P (2015) Essentiality of nickel in plants: a role in plant stresses. Frontiers in Plant Science 6:754

Fagundes-Nacarath IRF, Debona D, Oliveira ATH, Hawerroth C, Rodrigues FA (2018) Biochemical responses of common bean to white mold potentiated by phosphites. Plant Physiology and Biochemistry 132:308–319

Fortunato AA, Debona D, Bernardeli AMA, Rodrigues FA (2015) Defence-related enzymes in soybean resistance to target spot. Journal of Phytopathology 163:731–742

Freitas DS, Rodak BW, Carneiro MAC, Guilherme LRG (2019) How does Ni fertilization affect a responsive soybean genotype? A dose study. Plant and Soil 441:567–586

Hennessy GG, Demilliano WAJ, Mclaren CG (1990) Influence of primary weather variables on sorghum leaf blight severity in Southern Africa. Phytopathology 80:943–945

Hodges DM, Delong JM, Forney CF, Prange RK (1999) Improving the thiobarbituric acid-reactive-substances assay for estimating lipid peroxidation in plant tissues containing anthocyanin and other interfering compounds. Planta 207:604–611

Hooda KS, Khokhar MK, Shekhar M, Karjagi CG, Kumar B, Mallikarjuna N, Devlash RK, Chandrashekara C, Yadav OP (2017) Turcicum leaf blight-sustainable management of a re-emerging maize disease. Journal of Plant Diseases and Protection 124:101–113

Huang H, Ullah F, Zhou DX, Yi M, Zhao Y (2019) Mechanisms of ROS regulation of plant development and stress responses. Frontiers in Plant Science 10:800

Human, MP, Berger DK, Crampton BG (2020) Time-course RNAseq reveals Exserohilum turcicum effectors and pathogenicity determinants. Frontiers in Microbiology 11:360

Hussain MB, Ali S, Azam A, Hina S, Farooq MA, Ali B, Bharwana SA, Gill MB (2013) Morphological, physiological and biochemical responses of plants to nickel stress: a review. African Journal of Agricultural Research 8:1596–1602

Jain D, Khurana JP (2018) Role of pathogenesis-related (PR) proteins in plant defense mechanism. In: Molecular aspects of plant-pathogen interaction. Springer, Singapore. pp. 265–281

Jondle DJ, Coors JG, Duke SH (1989) Maize leaf β-1,3-glucanase activity in relation to resistance to Exserohilum turcicum. Canadian Journal of Botany 67:263–266

Kaur C, Vishnoi A, Ariyadasa TU, Bhattacharya A, Singla-Pareek SL, Sopory SK (2013) Episodes of horizontal gene-transfer and gene-fusion led to co-existence of different metal-ion specific glyoxalase I. Scientific Reports 3:1–10

Kazemi M, Hajizadeh HS, Gholami M, Asadi M, Aghdasi S (2012) Efficiency of essential oils, citric acid, malic aid and nickel reduced ethylene production and extended vase life of cut Lisianthus flowers. Research Journal of Botany 7:14–18

Kim HC, Kim KH, Song K, Kim JY, Lee BM (2020) Identification and validation of candidate genes conferring resistance to downy mildew in maize (Zea mays L.). Genes 11:191

Kotze RG, Van der Merwe CF, Crampton BG, Kritzinger Q (2019) A histological assessment of the infection strategy of Exserohilum turcicum in maize. Plant Pathology 68:504–512

Kramer DM, Johnson G, Kiirats O, Edwards GE (2004) New fluorescence parameters for the determination of QA redox state and excitation energy fluxes. Photosynthesis Research 79:209–218

Kretschmer M, Croll D, Kronstad JW (2017) Chloroplast-associated metabolic functions influence the susceptibility of maize to Ustilago maydis. Molecular Plant Pathology 18:1210–1221

Kumar O, Singh S K, Latare AM, Yadav SN (2018) Foliar fertilization of nickel affects growth, yield component and micronutrient status of barley (Hordeum vulgare L.) grown on low nickel soil. Archives of Agronomy and Soil Science 64:1407–1418

Leonard KJ, Suggs EG (1974) Setosphaeria prolata, the Ascigerous State of Exserohilum prolatum. Mycologia 66:281

Ludmerszki E, Almási A, Rácz I, Szigeti Z, Solti Á, Oláh C, Rudnóy S (2015) S-methylmethionine contributes to enhanced defense against Maize dwarf mosaic virus infection in maize. Brazilian Journal of Botany 38:771–782

Luttrell ES, Bacon CW (1977) Classification of Myriogenospora in the Clavicipitaceae. Canadian Journal of Botany 55:2090–2097

Malca I, Ullstrup AJ (1962) Effects of carbon and nitrogen nutrition on growth and sporulation of two species of Helminthosporium. Bulletin of the Torrey Botanical Club 89:240–249

Maschietto V, Marocco A, Malachova A, Lanubile A (2015) Resistance to Fusarium verticillioides and fumonisin accumulation in maize inbred lines involves an earlier and enhanced expression of lipoxygenase (LOX) genes. Journal of Plant Physiology 188:9–18

Mizuno T, Usui K, Horie K, Nosaka S, Mizuno N, Obata H (2005) Cloning of three ZIP/Nramp transporter genes from a Ni hyperaccumulator plant Thlaspi japonicum and their Ni^{2+}-transport abilities. Plant Physiology and Biochemistry 43:793–801

Mustafiz A, Ghosh A, Tripathi AK, Kaur C, Ganguly AK, Bhavesh NS, Tripathi JK, Pareek A, Sopory SK, Singla-Pareek SL (2014) A unique Ni^{2+}-dependent and methylglyoxal-inducible rice glyoxalase I possesses a single active site and functions in abiotic stress response. The Plant Journal 78:951–963

Nelson R, Wiesner-Hanks T, Wisser R, Balint-Kurti P (2018) Navigating complexity to breed disease-resistant crops. Nature Reviews Genetics 19:21–33

Ojeda-Barrios DL, Sánchez-Chávez E, Sida-Arreola JP, Valdez-Cepeda R, Balandran-Valladares M (2016) The impact of foliar nickel fertilization on urease activity in pecan trees. Journal of Soil Science and Plant Nutrition 16:237–247

Pant SK, Kumar P, Chauhan VS (2001) Effect of turcicum leaf blight on photosynthesis in maize. Indian Phytopathology 54:251–252

Pantelides IS, Tjamos SE, Pappa S, Kargakis M, Paplomatas EJ (2013) The ethylene receptor ETR1 is required for Fusarium oxysporum pathogenicity. Plant Pathology 62:1302–1309

Park YS, Kunze S, Ni X, Feussner I, Kolomiets MV (2010) Comparative molecular and biochemical characterization of segmentally duplicated 9-lipoxygenase genes ZmLOX4 and ZmLOX5 of maize. Planta 231:1425–1437

Patel ZM, Mahapatra R, Jampala SSM (2020) Role of fungal elicitors in plant defense mechanism. In: Molecular Aspects of Plant Beneficial Microbes in Agriculture. Academic Press, Cambridge. pp. 143–158

Patil SV, Kumudini BS, Pushpalatha HG, De Britto S, Ito SI, Sudheer S, Singh DP, Gupta VK, Jogaiah S (2020) Synchronised regulation of disease resistance in primed finger millet plants against the blast disease. Biotechnology Reports 27:e00484

Pennazio S, Roggero P (1992) Effect of cadmium and nickel on ethylene biosynthesis in soybean. Biologia Plantarum 34:345

Pereira LF, Martins SCV, Aucique-Pérez CE, Silva ET, Ávila RT, DaMatta FM, Rodrigues FA (2020) Silicon alleviates mesophyll limitations of photosynthesis on rice leaves infected by Monographella albescens. Theoretical and Experimental Plant Physiology 32:163–174

Pérez CDP, Pozza EA, Pozza AAA, Elmer WH, Pereira AB, Guimarães DSGG, Monteiro ACA, Rezende MLV (2020) Boron, zinc and manganese suppress rust on coffee plants grown in a nutrient solution. European Journal of Plant Pathology 156:727–738

Pérez-Bueno ML, Pineda M, Barón M (2019) Phenotyping plant responses to biotic stress by chlorophyll fluorescence imaging. Frontiers in Plant Science 10:1135

Polanco LR, Rodrigues FA, Nascimento KJT, Shulman P, Silva LC, Neves FW, Vale FXR (2012) Biochemical aspects of bean resistance to anthracnose mediated by silicon. Annals of Applied Biology 161:140–150

Qiu NW, Jiang DC, Wang XS, Wang BS, Zhou F (2019) Advances in the members and biosynthesis of chlorophyll family. Photosynthetica 57:974–984

Reis AR, Barcelos JPQ, Souza Osório CRW, Santos EF, Lisboa LAM, Santini JMK, Santos MJD, Furlani Junior E, Campos M, Figueiredo PAM, Lavres J, Gratão PL (2017) A glimpse into the physiological, biochemical and nutritional status of soybean plants under Ni-stress conditions. Environmental and Experimental Botany 144:76–87

Rios JA, Aucique-Pérez CE, Debona D, Cruz Neto LBM, Rios VS, Rodrigues FA (2017) Changes in leaf gas exchange, chlorophyll a fluorescence and antioxidant metabolism within wheat leaves infected by Bipolaris sorokiniana. Annals of Applied Biology 170:189–203

Sabir M, Ghafoor A, Zia-ur-Rehman M, AHMAD HR, Aziz T (2011) Growth and metal ionic composition of Zea mays as affected by nickel supplementation in the nutrient solution. International Journal of Agriculture and Biology 13:186–190

Santos RP, Cruz ACF, Iarema L, Kuki KN, Otoni WC (2008) Protocolo para extração de pigmentos foliares em porta-enxertos de videira micropropagados. Ceres 55:356–364

Sarruge JR, Haag HP (1974) Análise química de plantas. Escola Superior de Agricultura Luiz de Queiroz, Piracicaba

Sergiev I, Alexieva V, Karanov E (1997) Effect of spermine, atrazine and combination between them on some endogenous protective systems and stress markers in plants. Comptes Rendus de l'Academie Bulgare des Sciences 51:121–124

Shahbaz AK, Lewińska K, Iqbal J, Ali Q, Mahmood-Ur-Rahman, Iqbal M, Abbas F, Tauqeer HM, Ramzani PMA (2018) Improvement in productivity, nutritional quality, and antioxidative defense mechanisms of sunflower (Helianthus annuus L.) and maize (Zea mays L.) in nickel contaminated soil amended with different biochar and zeolite ratios. Journal of Environmental Management 218:256–270

Shaner G, Finney RE (1977) The effect of nitrogen fertilization on the expression of slow-mildewing resistance in knox wheat. Phytopathology 67:1051–1056

Sharma DK, Andersen SB, Ottosen CO, Rosenqvist E (2015) Wheat cultivars selected for high F_v/F_m under heat stress maintain high photosynthesis, total chlorophyll, stomatal conductance, transpiration and dry matter. Physiologia Plantarum 153:284–298

Sharma P, Sharma A, Sharma M, Bhalla N, Estrela P, Jain A, Thakur P, Thakur A (2017) Nanomaterial fungicides: in vitro and in vivo antimycotic activity of cobalt and nickel nanoferrites on phytopathogenic fungi. Global Challenges 1:1700041

Shi F, Zhang Y, Wang K, Meng Q, Liu X, Ma L, Li Y, Liu J, Ma L (2018) Expression profile analysis of maize in response to Setosphaeria turcica. Gene 659:100–108

Silva PO, Medina EF, Barros RS, Ribeiro DM (2014) Germination of salt-stressed seeds as related to the ethylene biosynthesis ability in three Stylosanthes species. Journal of Plant Physiology 171:14–22

Silveira PR, Milagres PO, Corrêa EF, Aucique-Pérez CE, Wordell Filho JA, Rodrigues FA (2019) Changes in leaf gas exchange, chlorophyll a fluorescence, and antioxidant metabolism within maize leaves infected by Exserohilum turcicum. Biologia Plantarum 63:643–653

Sivanesan A (1984) The bitunicate ascomycetes and their anamorphs. Canadian Journal of Botany 67:1500–1599

Smith NG, Woodburn J (1984) Nickel and ethylene involvement in the senescence of leaves and flowers. Naturwissenschaften 71:210–211

Tan J, Ameye M, Landschoot S, De Zutter N, De Saeger S, De Boevre M, Abdallah MF, Van der Lee T, Waalwijk C, Audenaert, K (2020). At the scene of the crime: New insights into the role of weakly pathogenic members of the fusarium head blight disease complex. Molecular Plant Pathology. In Press

Tatagiba SD, DaMatta FM, Rodrigues FA (2015) Leaf gas exchange and chlorophyll a fluorescence imaging of rice leaves infected with Monographella albescens. Phytopathology 105:180–188

Tipu MI, Ashraf MY, Sarwar N, Akhtar M, Shaheen MR, Ali A, Damalas CA (2020) Growth and physiology of maize (Zea mays L.) in a nickel-contaminated soil and phytoremediation efficiency using EDTA. Journal of Plant Growth Regulation. In Press

Turra GL, Agostini RB, Fauguel CM, Presello DA, Andreo CS, Gonzalez JM, Campos-Bermudez VA (2015) Structure of the novel monomeric glyoxalase I from Zea mays. Acta Crystallographica 71:2009–2020

US EPA. Method 7000B – Flame Atomic Absorption Spectrometry (2007). Available at <https://www.epa.gov/sites/production/files/2015-12/documents/7000b.pdf >. Accessed on October 12, 2020

Vale FXR, Fernandes Filho EI, Liberato JR (2003) QUANT. A software plant disease severity assessment. In: 8th International Congress of Plant Pathology. Christchurch, New Zealand, p. 105

Viswanath KK, Varakumar P, Pamuru RR, Basha SJ, Mehta S, Rao AD (2020) Plant lipoxygenases and their role in plant physiology. Journal of Plant Biology 63:83–95

Walters DR, Bingham IJ (2007) Influence of nutrition on disease development caused by fungal pathogens: implications for plant disease control. Annals of Applied Biology 151:307–324

Weems JD, Bradley CA (2017) Sensitivity of Exserohilum turcicum to demethylation inhibitor fungicides. Crop Protection 99:85–92

Wellburn AR (1994) The spectral determination of chlorophylls a and b, as well as total carotenoids, using various solvents with spectrophotometers of different resolution. Journal of Plant Physiology 144:307–313

Wiebke-Strohm B, Pasquali G, Margis-Pinheiro M, Bencke M, Bücker-Neto L, Becker-Ritt AB, Martinelli AH, Rechenmacher C, Polacco JC, Stolf R, Marcelino FC, Abdelnoor RV, Homrich MS, Del Ponte EM, Carlini CR, Carvalho MC, Bodanese-Zanettini MH (2012) Ubiquitous urease affects soybean susceptibility to fungi. Plant Molecular Biology 79:75–87

Wood BW, Reilly CC, Nyczepir AP (2004) Mouse-ear of pecan: A nickel deficiency. HortScience 39:1238–1242

Wood BW, Reilly CC, Bock CH, Hotchkiss MW (2012) Suppression of pecan scab by nickel. HortScience 47:503–508

Yadav V, Wang Z, Wei C, Amo A, Ahmed B, Yang X, Zhang X (2020) Phenylpropanoid pathway engineering: an emerging approach towards plant defense. Pathogens 9:312

Yang SF, Hoffman NE (1984) Ethylene biosynthesis and its regulation in higher plants. Annual Review of Plant Physiology 35:155–189

Yang Z, Yang Y, Yu S, Wang R, Wang Y, Chen H (2018) Photosynthetic, photochemical and osmotic regulation changes in tobacco resistant and susceptible to Alternaria alternata. Tropical Plant Pathology 43:413–421

Zhang X, Fernandes SB, Kaiser C, Adhikari P, Brown PJ, Mideros SX, Jamann TM (2020) Conserved defense responses between maize and sorghum to Exserohilum turcicum. BMC Plant Biology 20:67

Zheng QL, Nakatsuka A, Matsumoto T, Itamura H (2006) Pre-harvest nickel application to the calyx of 'Saijo'persimmon fruit prolongs postharvest shelf-life. Postharvest Biology and Technology 42:98–103

Table and Figures

Table 1. Analysis of variance for the effects of foliar treatments (T), plant inoculation (PI), and the T × PI interaction for foliar concentrations of copper (Cu), iron (Fe), manganese (Mn), nickel (Ni), and zinc (Zn), severity, area under disease progress curve (AUDPC), ethylene production, leaf gas exchange parameters (net CO_2 assimilation rate (A), stomatal conductance to water vapor (g_s), internal CO_2 concentration (C_i), and transpiration rate (E)), chlorophyll (Chl) a fluorescence parameters (effective PSII quantum yield (Y(II)), quantum yield of regulated energy dissipation (Y(NPQ)), quantum yield of non-regulated energy dissipation (Y(NO)), and maximal photosystem II quantum efficiency (F_v/F_m)), concentrations of chlorophyll (Chl) a, Chl b, carotenoids (CAR), Chl a+b, superoxide anion radical (O_2^-), hydrogen peroxide (H_2O_2), malondialdehyde (MDA), total soluble phenolics (TSP), and lignin-thioglycolic acid (LTGA) derivatives as well as for the activities of antioxidant (superoxide dismutase (SOD), catalase (CAT), glutathione reductase (GR), and ascorbate peroxidase (APX)) and defence-related (chitinase (CHI), β-1,3-glucanase (GLU), peroxidase (POX), polyphenoloxidase (PPO), lipoxygenase (LOX), and phenylalanine ammonia-lyase (PAL)) enzymes.

Variables/Parameters	T	PI	T × PI
Cu	0.466	0.118	0.255
Fe	0.877	0.005	0.158
Mn	0.096	< 0.001	0.035
Ni	< 0.001	< 0.001	0.001
Zn	0.310	0.001	0.050
Severity	0.518	-	-
AUDPC	0.002	-	-
Ethylene production	0.297	< 0.001	0.297
A	0.381	< 0.001	0.562
g_s	0.424	< 0.001	0.667
C_i	0.086	< 0.001	0.635
E	0.211	< 0.001	0.678
Y(II)	0.205	< 0.001	0.618
Y(NPQ)	0.520	0.653	0.206
Y(NO)	0.049	< 0.001	0.262
F_v/F_m	0.890	< 0.001	0.736
Chl a	0.333	< 0.001	0.469
Chl b	0.424	< 0.001	0.872
CAR	0.515	< 0.001	0.357
Chl a+b	0.253	< 0.001	0.486
O_2^-	0.081	< 0.001	0.945
H_2O_2	0.036	< 0.001	0.021
MDA	0.082	< 0.001	0.167
TSP	0.609	< 0.001	0.970
LTGA derivatives	0.726	< 0.001	0.128
SOD	0.566	< 0.001	0.012
CAT	0.398	< 0.001	0.286
GR	0.238	< 0.001	0.023
APX	0.630	< 0.001	0.850
CHI	0.325	< 0.001	0.306
GLU	0.345	< 0.001	0.344
POX	0.862	< 0.001	0.731
PPO	0.364	< 0.001	0.547
LOX	< 0.001	< 0.001	0.167
PAL	0.898	< 0.001	0.979

- = not determined.

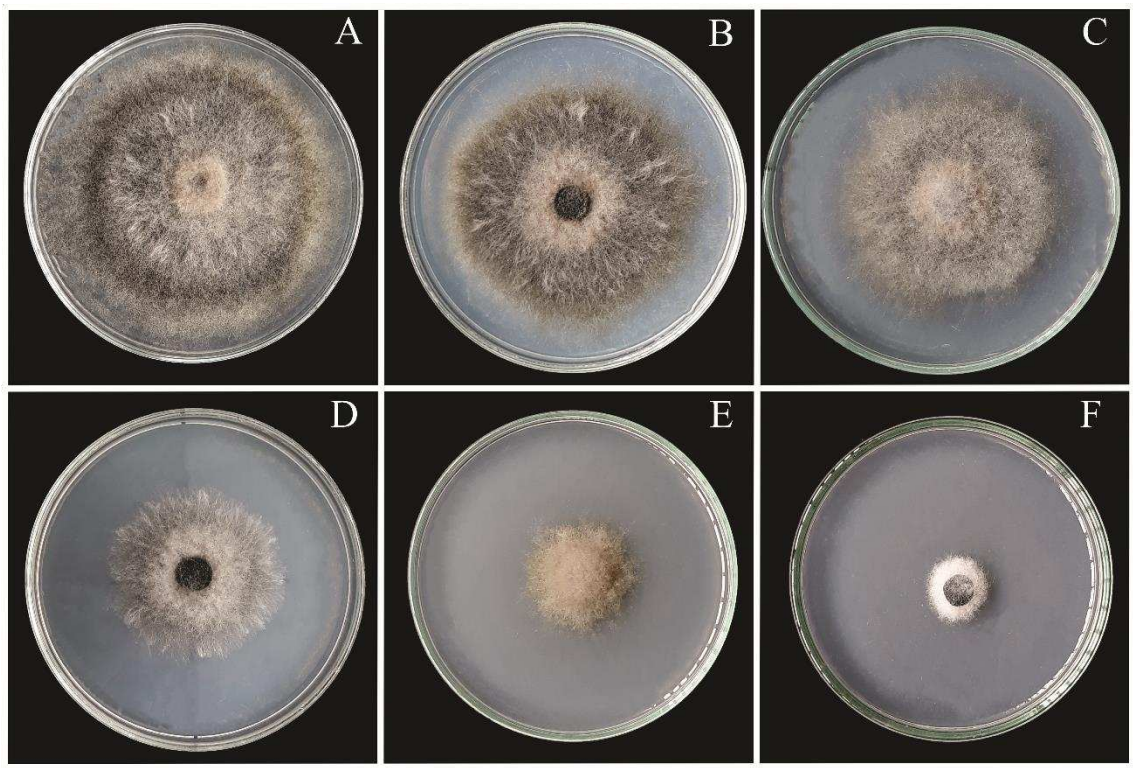

Figure 1. Mycelial growth of Exserohilum turcicum in Petri dishes containing lactose casein hydrolysate medium amended with 0 (A), 0.13 (B), 0.25 (C), 0.38 (D), 0.50 (E), and 1 (F) g of nickel L^{-1}.

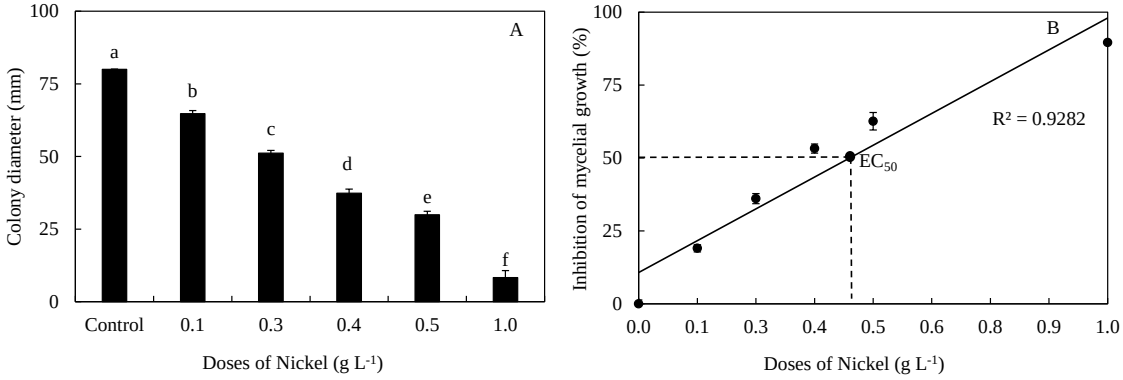

Figure 2. In vitro effect of different nickel (Ni) concentrations on colony diameter (A) of Exserohilum turcicum and effective concentration (EC_{50}) of Ni that inhibited 50% of the mycelial growth of E. turcicum (B). For colony diameter, treatments mean followed by different letters are significantly different ($P \leq 0.05$) according to Tukey's test. Bars represent the standard error of the means. n = 8.

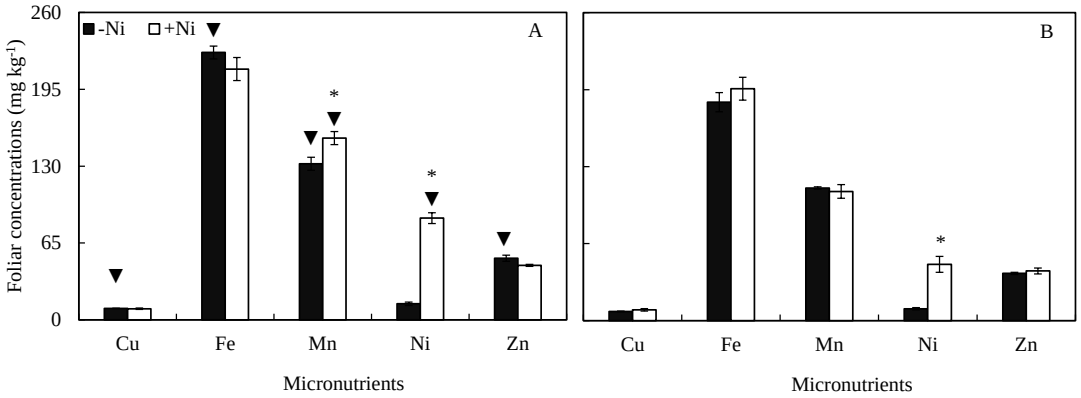

Figure 3. Foliar concentrations of copper (Cu), iron (Fe), manganese (Mn), nickel (Ni), and zinc (Zn) for maize plants sprayed with water (-Ni) or nickel (+Ni) and non-inoculated (NI) (A) or inoculated (I) with Exserohilum turcicum (B). Means followed by an asterisk or by an inverted triangle are significantly different by the F test at 5% of probability. The asterisk compares -Ni and +Ni treatments, and the inverted triangle compares NI and I treatments. Bars represent the standard error of the means. n = 4.

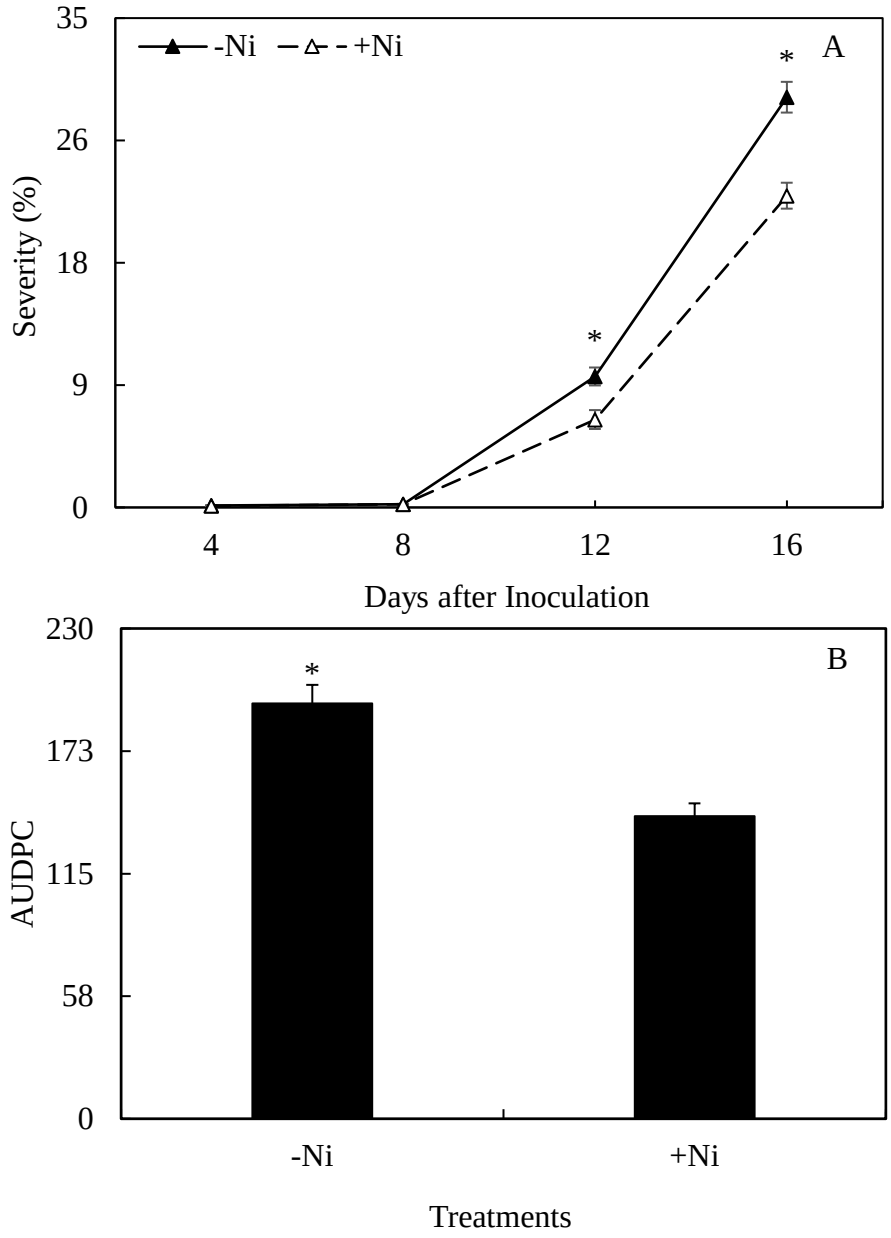

Figure 4. Severity of northern leaf blight (A) and area under disease progress curve (AUDPC) (B) for maize plants sprayed with water (-Ni) or nickel (+Ni). Means for -Ni and +Ni treatments in graphics A (at each evaluation time) and B followed by an asterisk are significantly different by F test at 5% of probability. Bars represent the standard error of the means. n = 4.

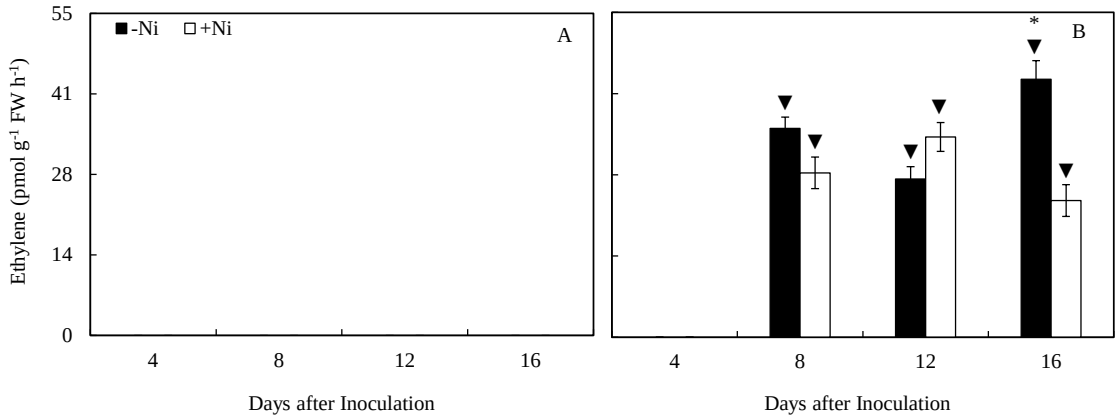

Figure 5. Production of ethylene by maize plants non-inoculated (A) (NI) and inoculated (I) with Exserohilum turcicum (B) that were sprayed with water (-Ni) or nickel (+Ni). For each evaluation time, means followed by an asterisk or by an inverted triangle are significantly different by the F test at 5% of probability. The asterisk compares -Ni and +Ni treatments, and the inverted triangle compares NI and I treatments. Bars represent the standard error of the means. FW = fresh weight. n = 4.

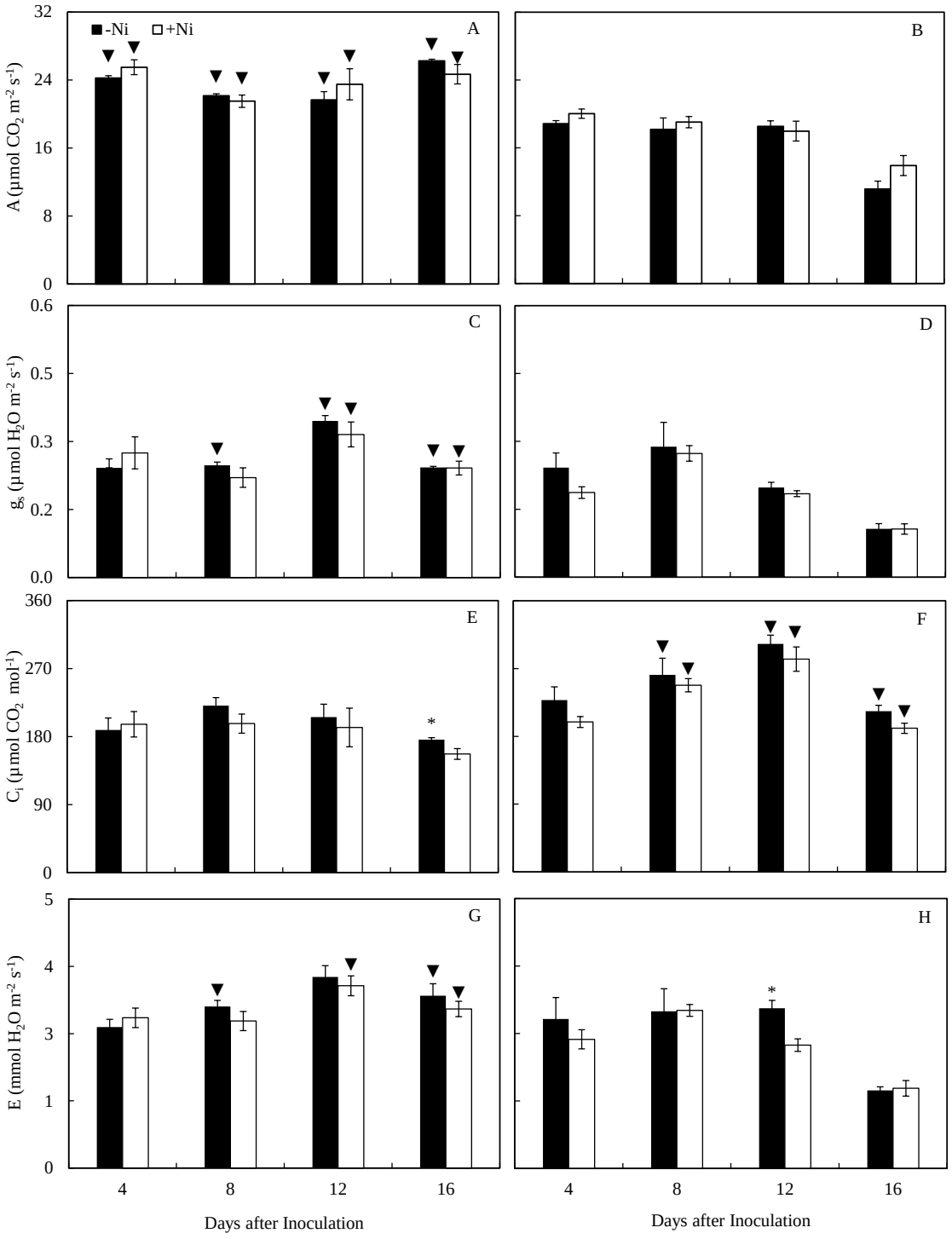

Figure 6. Leaf gas exchange parameters: net carbon assimilation rate (A) (A and B), stomatal conductance to water vapor (g_s) (C and D), internal CO_2 concentration (C_i) (E and F), and transpiration rate (E) (G and H) determined in the leaves of maize plants sprayed with water (-Ni) or nickel (+Ni) and non-inoculated (NI) (A, C, E, and G) or inoculated (I) with Exserohilum

turcicum (B, D, F, and H). For each evaluation time, means followed by an asterisk or by an inverted triangle are significantly different by the F test at 5% of probability. The asterisk compares -Ni and +Ni treatments, and the inverted triangle compares NI and I treatments. Bars represent the standard error of the means. n = 4.

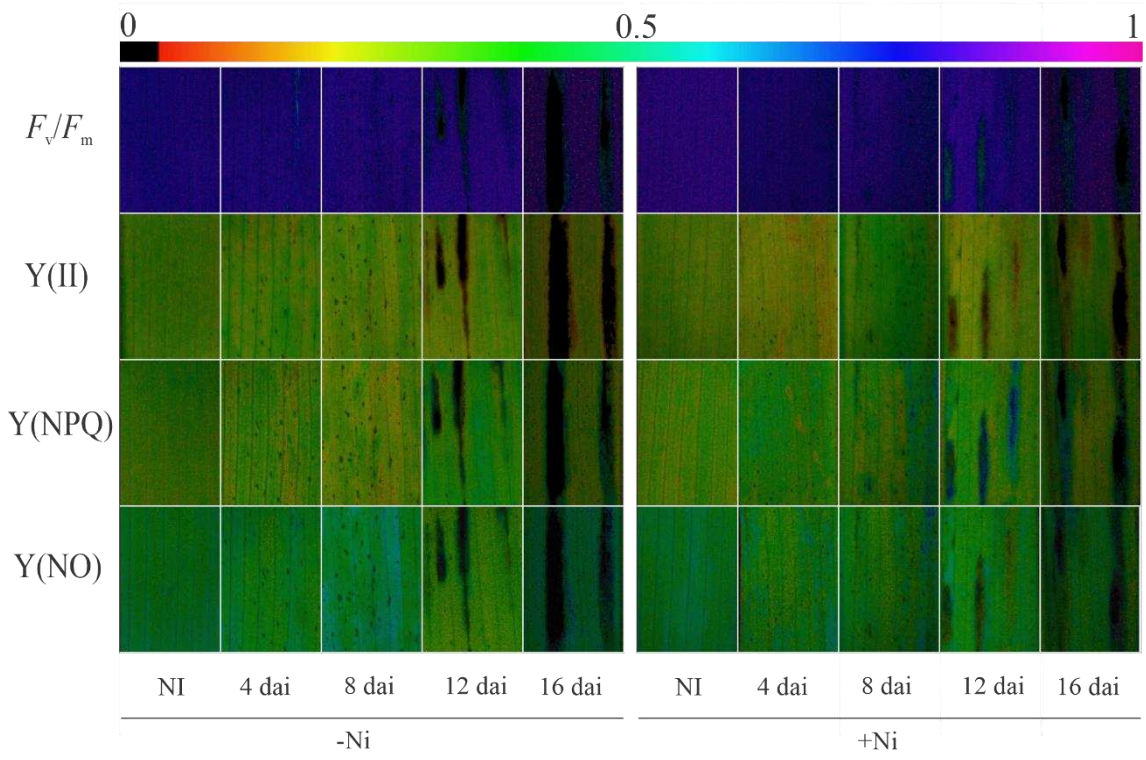

Figure 7. Images of chlorophyll a fluorescence parameters: maximum PSII quantum efficiency (F_v/F_m), photochemical yield (Y(II)), yield for dissipation by down-regulation (Y(NPQ)), and yield for non-regulated dissipation (Y(NO) determined in the leaves of maize plants sprayed with water (-Ni) or nickel (+Ni) and non-inoculated (NI) or from 4 to 16 days after inoculation (dai) with Exserohilum turcicum.

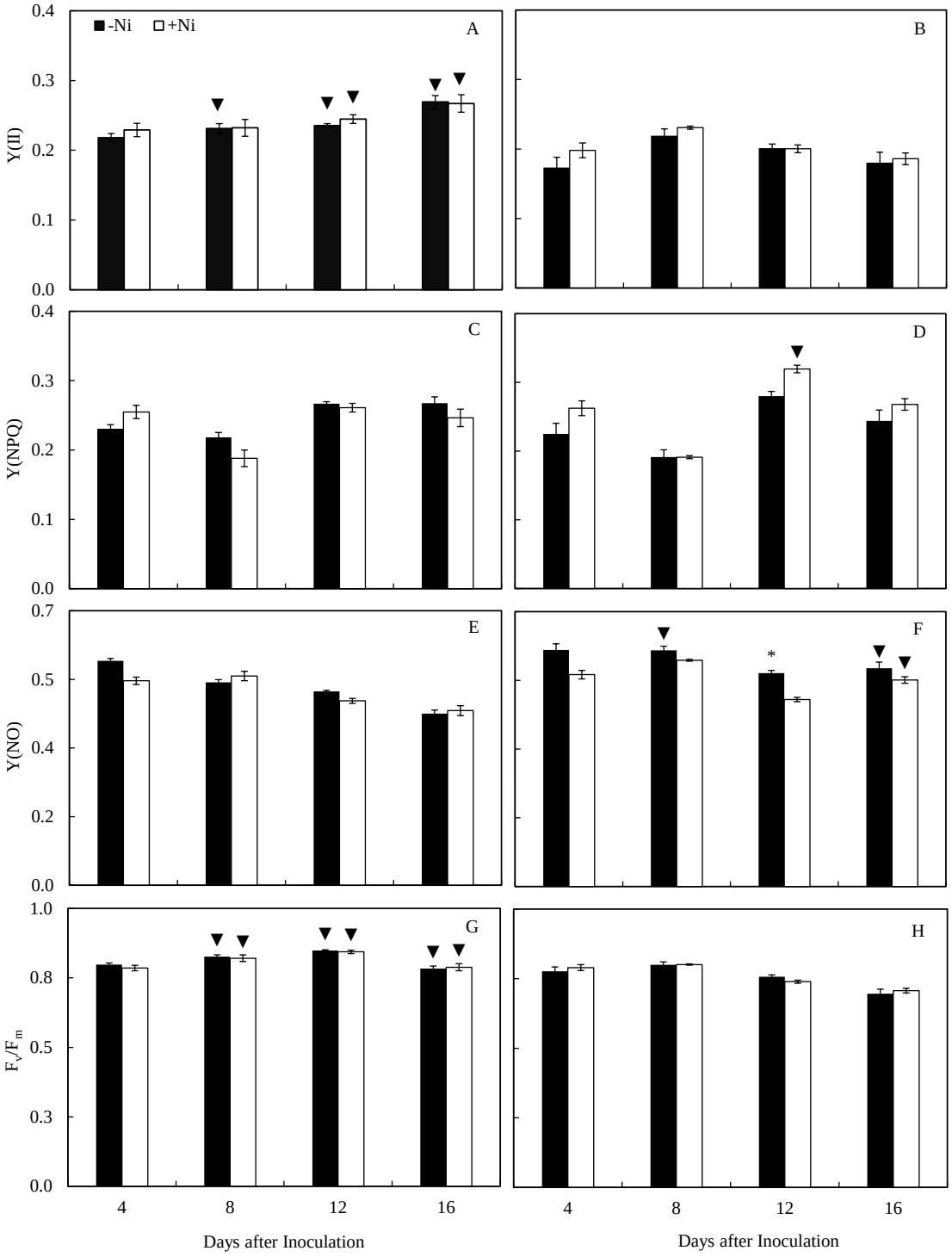

Figure 8. Chlorophyll a parameters: effective PSII quantum yield (Y(II)) (A and B), quantum yield of regulated energy dissipation (Y(NPQ)) (C and D), quantum yield of non-regulated energy dissipation (Y(NO)) (E and F), and variable-to-maximum chlorophyll a fluorescence ratio (F_v/F_m) (G and H) determined in the leaves of maize plants sprayed with water (-Ni) or

nickel (+Ni) and non-inoculated (NI) (A, C, E, and G) or inoculated (I) with Exserohilum turcicum (B, D, F, and H). For each evaluation time, means followed by an asterisk or by an inverted triangle are significantly different by the F test at 5% of probability. The asterisk compares -Ni and +Ni treatments, and the inverted triangle compares NI and I treatments. Bars represent the standard error of the means. n = 4.

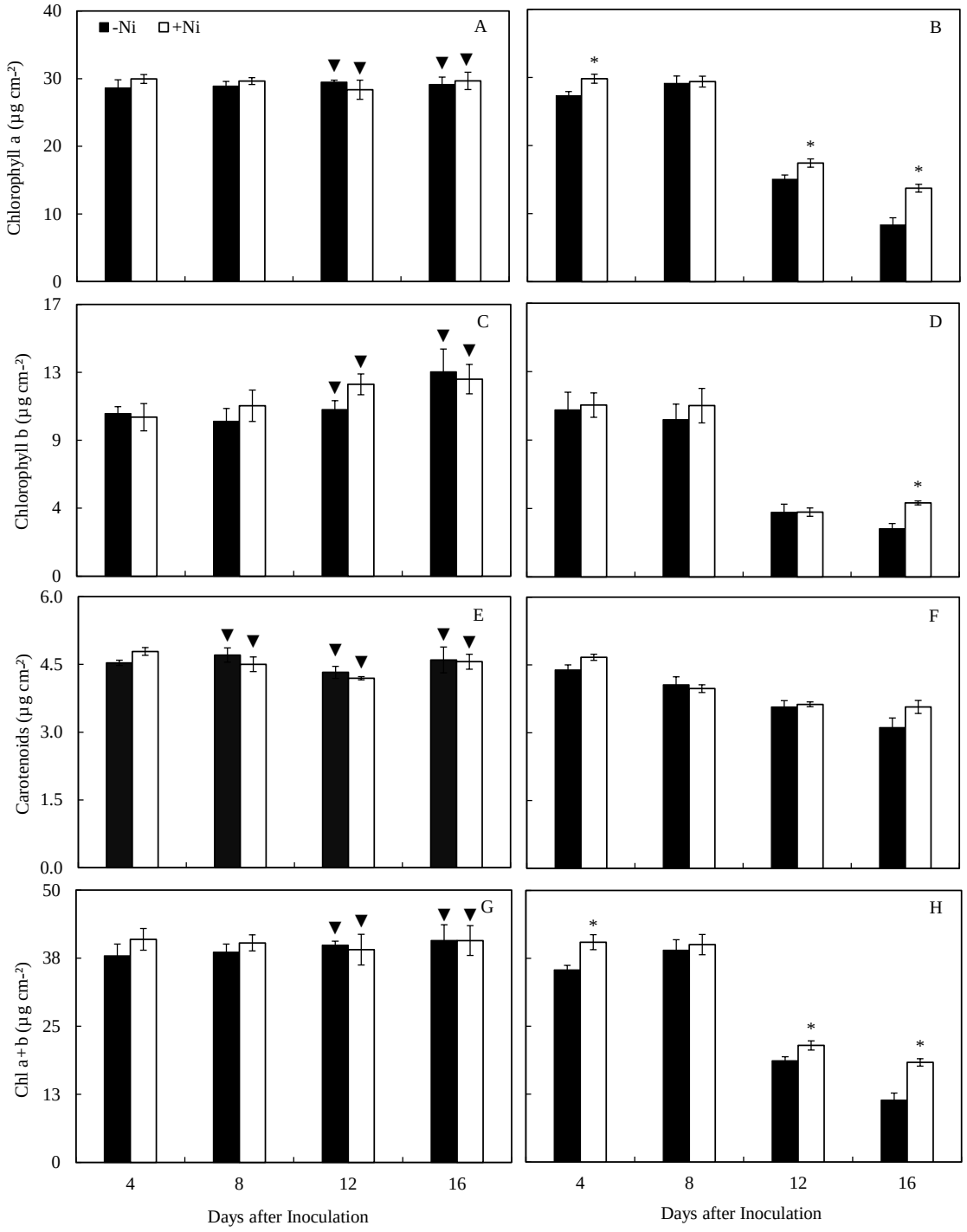

Figure 9. Concentrations of chlorophyll (Chl) a (A and B), Chl b (C and D), carotenoids (E and F), and total Chl (Chl a + b) (c) determined in the leaves of maize plants sprayed with water (-Ni) or nickel (+Ni) and non-inoculated (NI) (A, C, E, and G) or inoculated (I) with Exserohilum turcicum (B, D, F, and H). For each evaluation time, means followed by an asterisk or by an inverted triangle are significantly different by the F test at 5% of probability. The asterisk

compares -Ni and +Ni treatments, and the inverted triangle compares NI and I treatments. Bars represent the standard error of the means. $n = 4$.

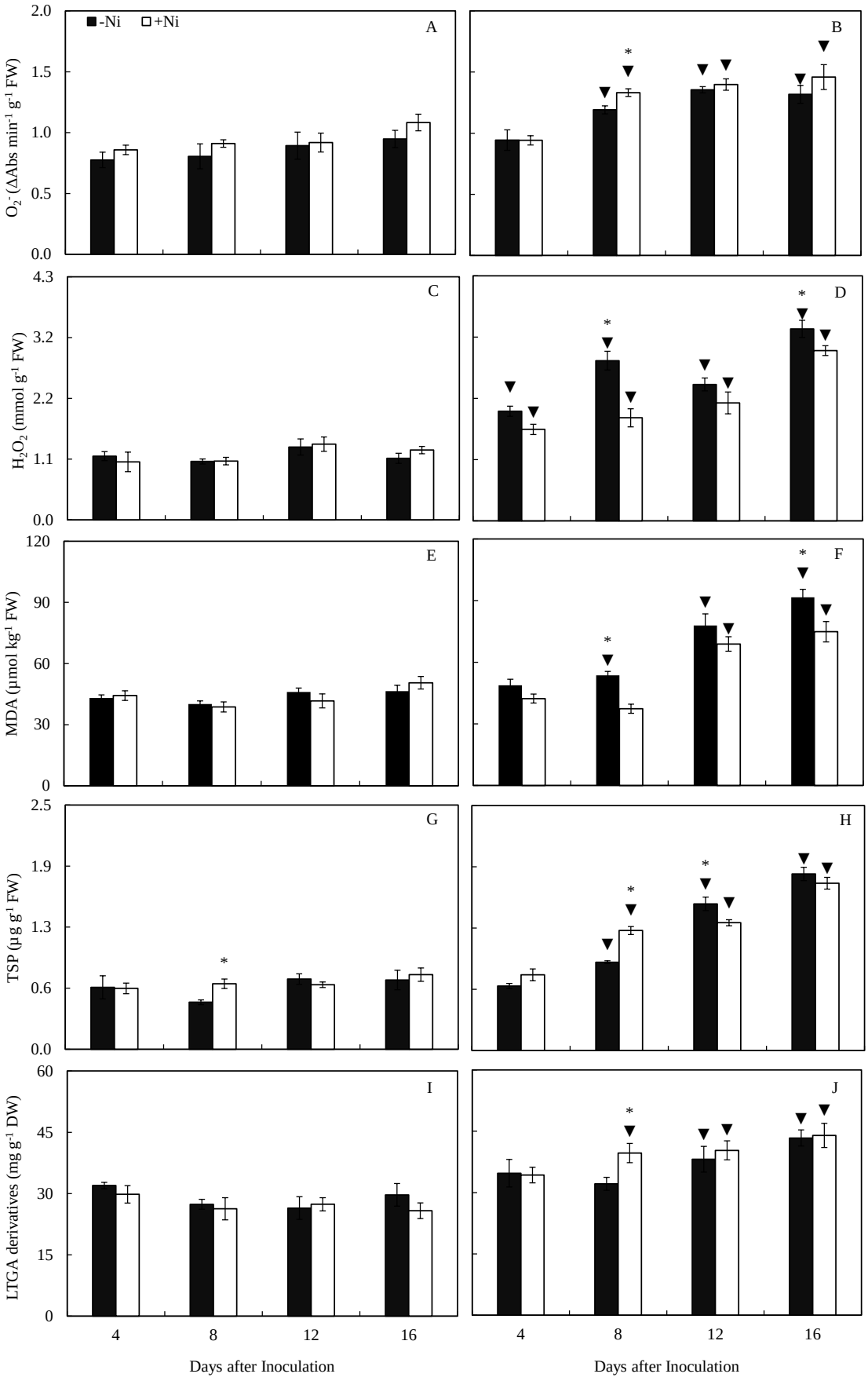
■-Ni □+Ni
A
B
C
D
E
F
G
H
I
J
O_2^- (ΔAbs min^{-1} g^{-1} FW)
H_2O_2 (mmol g^{-1} FW)
MDA (μmol kg^{-1} FW)
TSP (μg g^{-1} FW)
LTGA derivatives (mg g^{-1} DW)
2.0
1.5
1.0
0.5
0.0
4.3
3.2
2.2
1.1
120
90
60
30
2.5
1.9
1.3
0.6
45
15
4
8
12
16
Days after Inoculation
Days after Inoculation

Figure 10. Concentrations of superoxide anion radical (O_2^-) (A and B), hydrogen peroxide (H_2O_2) (C and D), malondialdehyde (MDA) (E and F), total soluble phenolics (TSP) (G and H), and lignin-thioglycolic acid (LTGA) derivatives (I and J) determined in the leaves of maize plants sprayed with water (-Ni) or nickel (+Ni) and non-inoculated (NI) (A, C, E, G, and I) or inoculated (I) with Exserohilum turcicum (B, D, F, H, and J). For each evaluation time, means followed by an asterisk or by an inverted triangle are significantly different by the F test at 5% of probability. The asterisk compares -Ni and +Ni treatments, and the inverted triangle compares NI and I treatments. Bars represent the standard error of the means. FW and DW = fresh and dry weights, respectively. n = 4.

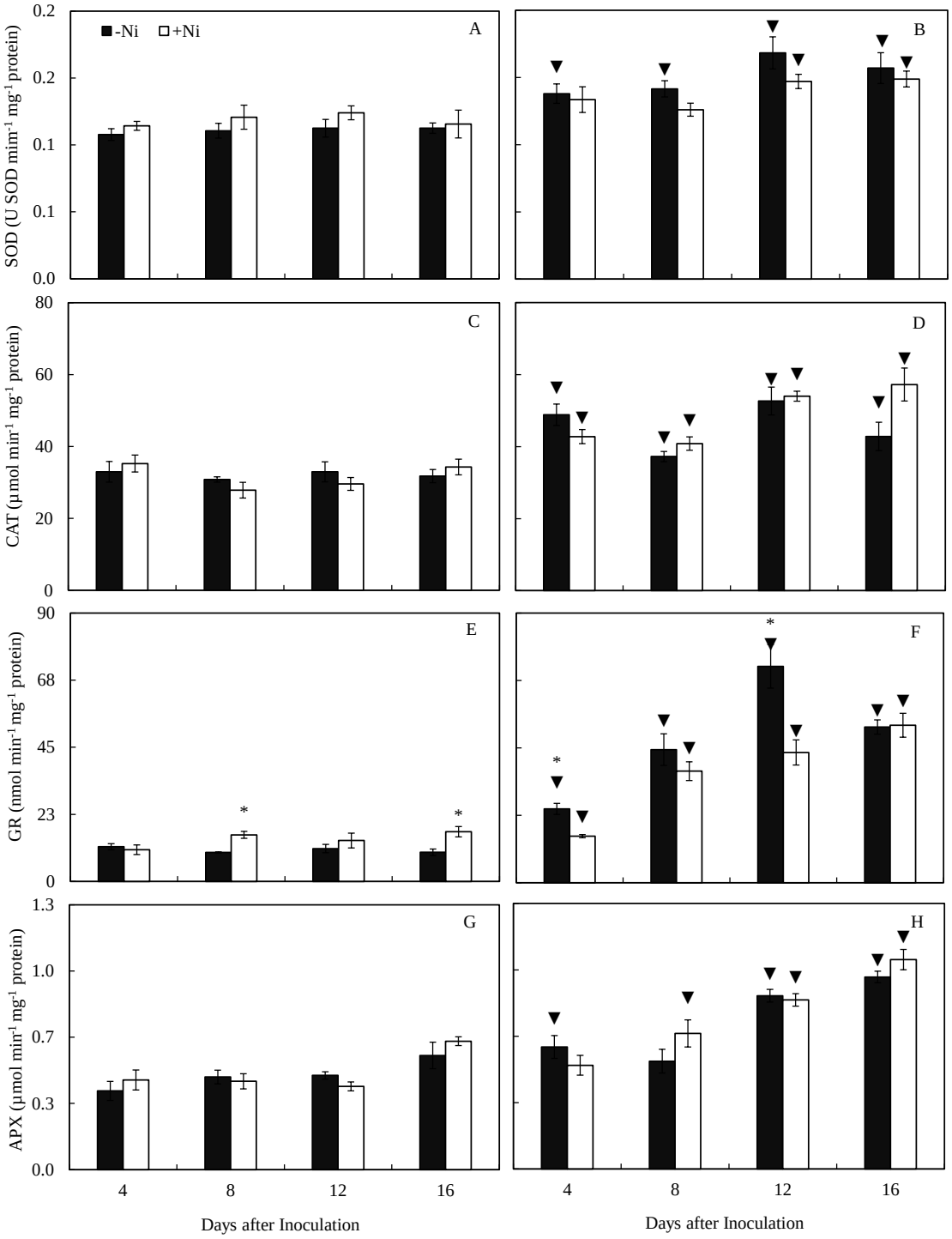

Figure 11. Activities of superoxide dismutase (SOD) (A and B), catalase (CAT) (C and D), glutathione reductase (GR) (E and F), and ascorbate peroxidase (APX) (G and H), determined in the leaves of maize plants sprayed with water (-Ni) or nickel (+Ni) and non-inoculated (NI) (A, C, E, and G) or inoculated (I) with Exserohilum turcicum (B, D, F, and H). For each

evaluation time, means followed by an asterisk or by an inverted triangle are significantly different by the F test at 5% of probability. The asterisk compares -Ni and +Ni treatments, and the inverted triangle compares NI and I treatments. Bars represent the standard error of the means. n = 4.

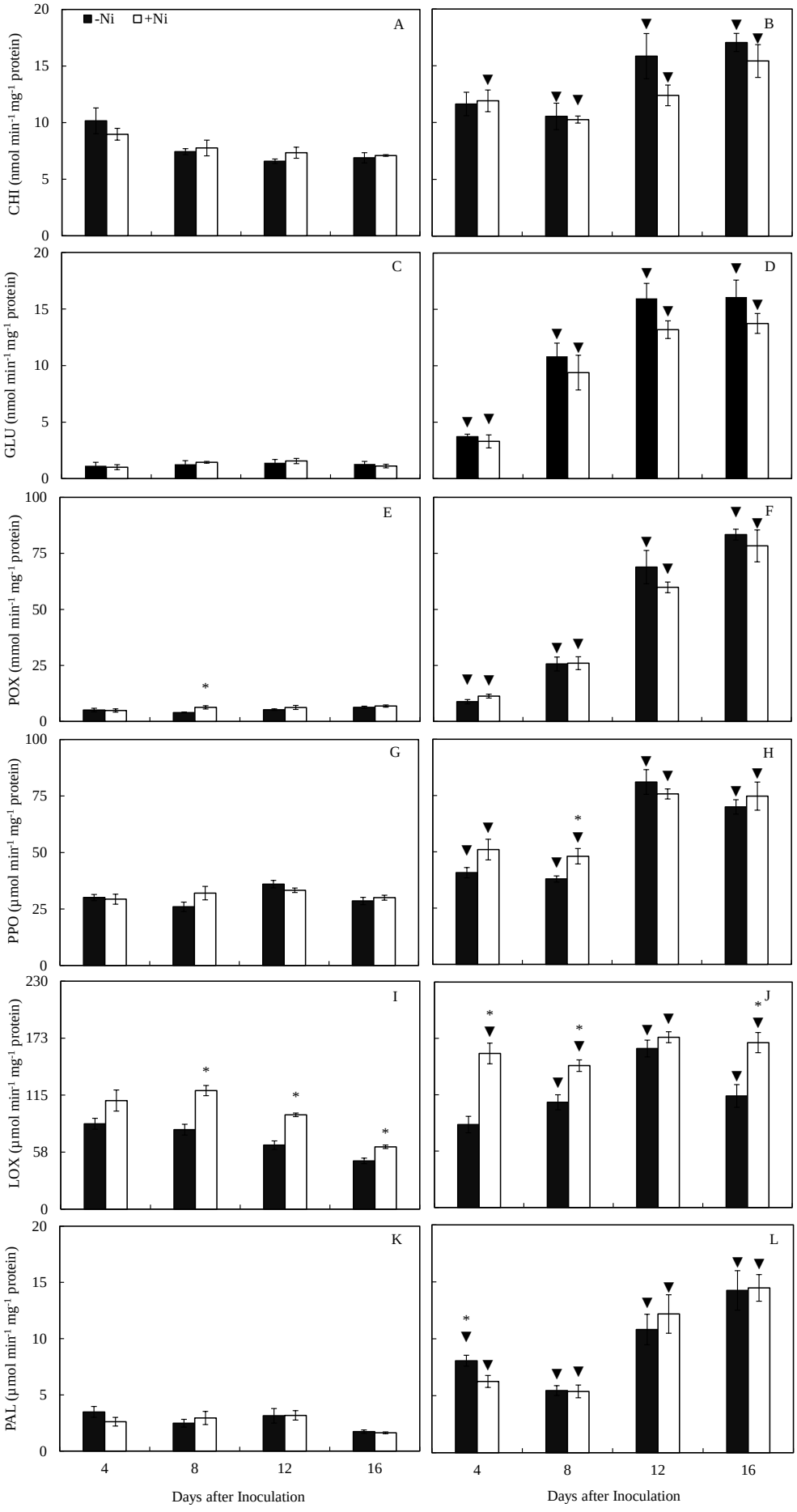
-Ni
+Ni
A
B
C
D
E
F
G
H
I
J
K
L
CHI (nmol min-1 mg-1 protein)
GLU (nmol min-1 mg-1 protein)
POX (mmol min-1 mg-1 protein)
PPO (µmol min-1 mg-1 protein)
LOX (µmol min-1 mg-1 protein)
PAL (µmol min-1 mg-1 protein)
0
5
10
15
20
25
50
75
100
58
115
173
230
4
8
12
16
Days after Inoculation
Days after Inoculation

Figure 12. Activities of chitinase (CHI) (A and B), β-1,3-glucanase (GLU) (C and D), peroxidase (POX) (E and F), polyphenoloxidase (PPO) (G and H), lipoxygenase (LOX) (I and J), and phenylalanine ammonia-lyase (PAL) (K and L) determined in the leaves of maize plants sprayed with water (-Ni) or nickel (+Ni) and non-inoculated (NI) (A, C, E, G, I, and K) or inoculated (I) (B, D, F, H, J, and L) with Exserohilum turcicum. For each evaluation time, means followed by an asterisk or by an inverted triangle are significantly different by the F test at 5% of probability. The asterisk compares -Ni and +Ni treatments, and the inverted triangle compares NI and I treatments. Bars represent the standard error of the means. n = 4.